7.2 Modeling Low-Temperature Geochemical Processes

DK Nordstrom and KM Campbell, US Geological Survey, Boulder, CO, USA

Published by Elsevier Ltd.

This article is a revision of the previous online update by D. K. Nordstrom, volume 5, pp. 1–38, © 2007, Elsevier Ltd.

7.2.1	**Introduction**	27
7.2.1.1	What Is a Model?	28
7.2.2	**Modeling Concepts and Definitions**	29
7.2.2.1	Modeling Concepts	29
7.2.2.2	Modeling Definitions	29
7.2.2.3	Inverse Modeling, Mass Balancing, and Mole Balancing	29
7.2.3	**Solving the Chemical Equilibrium Problem**	31
7.2.4	**Historical Background to Geochemical Modeling**	32
7.2.5	**The Problem of Activity Coefficients**	33
7.2.5.1	Activity Coefficients	33
7.2.5.2	Saturation Indices	34
7.2.6	**Geochemical Databases**	34
7.2.6.1	Thermodynamic Databases	35
7.2.6.2	Kinetic Databases	36
7.2.6.3	Electrolyte Databases	36
7.2.7	**Geochemical Codes**	36
7.2.7.1	USGS Codes	36
7.2.7.2	LLNL/LBNL Codes	37
7.2.7.3	Miami Code	37
7.2.7.4	The Geochemist’s Workbench™	38
7.2.7.5	REDEQL–MINTEQ Codes	38
7.2.7.6	Waterloo Codes	39
7.2.7.7	Harvie–Møller–Weare Code	39
7.2.7.8	FREZCHEM Code	39
7.2.7.9	Windermere Humic Aqueous Model Codes	39
7.2.7.10	Additional Codes	40
7.2.8	**Water–Rock Interactions**	41
7.2.8.1	Aqueous Speciation	41
7.2.8.2	Sorption Reactions	42
7.2.8.3	Aqueous Redox Kinetics and Microbial Growth	42
7.2.8.4	Model Simulations of Mineral Reactions	44
7.2.8.4.1	Which minerals reach solubility equilibrium?	44
7.2.8.4.2	Calcite solubility	46
7.2.8.4.3	Pyrite oxidation	46
7.2.8.4.4	Pyrite oxidation with calcite dissolution and neutralization	48
7.2.8.4.5	Seawater–groundwater mixing	50
7.2.8.4.6	Madison regional limestone aquifer	50
7.2.8.5	Reactive-Transport Modeling in Streams	53
7.2.8.6	Reactive-Transport Modeling in Groundwater	55
7.2.8.7	Geochemical Modeling of Catchments	55
7.2.8.8	Evaporation of Seawater	56
7.2.8.9	Reliability of Geochemical Model Simulations	56
7.2.9	**Final Comments**	58
Acknowledgments		60
References		60

> *A model takes on the quality of theory when it abstracts from raw data the facts that its inventor perceives to be fundamental and controlling, and puts these into relation to each other in ways that were not understood before—thereby generating predictions of surprising new facts.*
>
> H. F. Judson (1980), *The Search for Solutions*

7.2.1 Introduction

Geochemical modeling is widely used for a number of applications from research on the fundamental processes of water–rock interactions to regulatory requirements and policy

Treatise on Geochemistry, Second Edition, (2014), vol. 7, pp. 27-68

decisions regarding permits for industrial and hazardous wastes. In low-temperature environments, generally thought of as those in the temperature range of 0–100 °C and close to atmospheric pressure (1 atm = 1.01325 bar = 101 325 Pa), complex hydrobiogeochemical reactions participate in an array of interconnected processes that affect us, and that, in turn, we affect. Understanding these complex processes often requires tools that are sufficiently sophisticated to portray multicomponent, multiphase chemical reactions yet transparent enough to reveal the main driving forces. Geochemical models are such tools. The major processes that they are required to model include mineral dissolution and precipitation; aqueous inorganic speciation and complexation; solute adsorption and desorption; ion exchange; oxidation–reduction or redox transformations; gas uptake or production; organic matter speciation and complexation; evaporation; dilution; water mixing; reaction during fluid flow; reactions involving microbial activity; and photoactivity. These processes occur in rain, snow, fog, dry atmosphere, soils, bedrock weathering, streams, rivers, lakes, groundwaters, estuaries, brines, and diagenetic environments. Geochemical modeling attempts to understand the redistribution of elements and compounds, through anthropogenic and natural means, for a large range of scale from nanometer to global. 'Aqueous geochemistry' and 'environmental geochemistry' are often used interchangeably with 'low-temperature geochemistry' to emphasize hydrologic or environmental objectives.

Recognition of the strategy or philosophy behind geochemical modeling is not often discussed or explicitly described. Two approaches for modeling groundwater chemistry have been described (i) 'forward modeling,' which predicts water compositions from hypothesized reactions and user assumptions, and (ii) 'inverse modeling,' which uses specific water, mineral, and isotopic compositions to constrain hypothesized reactions (Glynn and Plummer, 2005). These approaches simply reflect the amount of field information that one has available. With minimal information on a site, a modeler is forced to rely on forward modeling and his/her knowledge of hydrogeochemical processes. Optimal information would include detailed mineralogy on drill cores or well cuttings combined with detailed water analyses at varying depths and sufficient spatial distribution to follow geochemical reactions and mixing of waters along defined flow paths. With optimal information, a modeler will depend on inverse modeling.

This chapter outlines the main concepts and key developments in the field of geochemical modeling for low-temperature environments and illustrates their use with examples. It proceeds with a short discussion of what modeling is, continues with concepts and definitions commonly used, and follows with a short history of geochemical models, a discussion of databases, the codes that embody models, and recent examples of how these codes have been used in water–rock interactions. An important new stage of development has been reached in this field with questions of reliability and validity of models. Future work will be obligated to document ranges of certainty and sources of uncertainty, sensitivity of models and codes to parameter errors and assumptions, propagation of errors, and delineation of the range of applicability.

7.2.1.1 What Is a Model?

A 'model' has a relation to 'reality,' but reality is experiential, and the moment we attempt to convey the experience, we are seriously constrained by three limitations: our own ability to communicate, the capability of the communication medium to portray the experience, and the ability of the person receiving the communication to understand it. Communication requires the use of language and the use of percepts and concepts, and the process of perceiving, conceiving, and communicating is an abstracting process that removes us from the immediate experience. Any attempt to transform an experience into language suffers from this abstraction process so that we lose the immediate experience to gain some understanding of it. The problem is to transform existential knowledge to communicated or processed knowledge. To communicate knowledge, we must use a simplified and abstract symbolism (words, mathematics, pictures, diagrams, analogues, allegories, three-dimensional physical constructs, etc.) to describe a material object or phenomenon, that is, a model. Models take on many forms, but they are all characterized by being a simplification or idealization of reality. "… models include only properties and relationships that are needed to understand those aspects of the real system that we are interested in …" (Derry, 1999). Assumptions, both explicit and implicit, are made in model construction, because either we do not know all the necessary properties or we do not need to know them. Hopefully, models have caught the essential properties of that which they are attempting to portray so that they are useful and lead to new insights and to better answers for existing questions and problems.

Scientific models begin as ideas and opinions that are formalized into a language, often, but not necessarily, mathematical language. Furthermore, they must have testable consequences. The emphasis on testability, or falsifiability, is a fundamental attribute (Popper, 1934). Greenwood (1989) stated that the word model should be reserved "… for well-constrained logical propositions, not necessarily mathematical, that have necessary and testable consequences, and avoid the use of the word if we are merely constructing a scenario of possibilities." A scientific model is a testable idea, hypothesis, theory, or combination of theories that provides new insight or a new interpretation of an existing problem. An additional quality often attributed to a model or theory is its ability to explain a large number of observations while maintaining simplicity (Occam's razor). The simplest model that explains the most observations is the one that will have the most appeal and applicability.

Models are applied to a 'system' or a portion of the observable universe separated by well-defined boundaries for the purpose of investigation. A chemical model is a theoretical construct that permits the calculation of chemical properties and processes, such as the thermodynamic, kinetic, or quantum mechanical properties of a system. A geochemical model is a chemical model developed for geologic systems. Geochemical models often incorporate chemical models, such as ion association (IA) and aqueous speciation, together with mineralogical data and assumptions about mass transfer to study water–rock interactions.

A computer code is obviously not a model. It is unfortunate that one commonly finds, in the literature, reference to the

MINTEQ model, the PHREEQC model, or the EQ3/6 model when these are not models but computer codes. Some of the models used by these codes are the same so that a different code name does not necessarily mean a different model is being used. Even within a single code, different models coexist. A computer code that incorporates a geochemical model is one of several possible tools for interpreting water–rock interactions in low-temperature geochemistry. Although low-temperature geochemical processes and their models will be the main focus of this chapter, computer codes in common use and examples of their application are also covered.

7.2.2 Modeling Concepts and Definitions

7.2.2.1 Modeling Concepts

Many different forms of models are utilized, usually dictated by the objectives of research. *Conceptual models* are the most fundamental (Bredehoeft, 2003, 2005). The success or failure of a model depends on the robustness of the conceptual model, not the code. It also depends on the creativity of the modeler (Adams, 1974) and whether Chamberlin's method of 'multiple working hypotheses' has been followed (Chamberlin, 1897). All of us have some kind of concept of water–rock interactions. For a groundwater interacting with aquifer minerals, one might conceive that most minerals would be undersaturated in the area of recharge but that some minerals (those that dissolve fastest) would become saturated at some point downgradient, having reached their equilibrium solubility (a state of *partial equilibrium*). The conceptual model can be formalized into a set of mathematical equations using chemical principles, the *mathematical model*, entered into a computer program, or *code*; predictions can be made to test assumptions and databases against results from real field data. This exercise helps to quantify and constrain the possible reactions that might occur in the subsurface. Mathematical equations for complex interacting variables are not always solved exactly, and therefore, systems of numerical approximations, or *numerical models*, have been developed. Alternatively, an experiment could be set up in the laboratory with columns made of aquifer material with groundwater flowing through to simulate the reactions, the *experimental model* or *scale model*. Having obtained results from a mathematical or scale model, some unexpected results often occur, which force us to change our original conceptual model. This example demonstrates how science works; it is an ongoing process of approximation that iterates between idea, theory, observational testing of theory, and back to modifications of theory or development of new theories.

7.2.2.2 Modeling Definitions

In low-temperature geochemistry and geochemical modeling, it is helpful to define several words and phrases in common use.

Aqueous speciation. The distribution of dissolved components among free ions, ion pairs, and complexes. For example, dissolved iron in acid mine drainage (AMD) can be present as $Fe_{(aq)}^{2+}$ (free ferrous iron), $FeSO_{4(aq)}^{0}$ (ion pair), $Fe_{(aq)}^{3+}$ (free ferric iron), $Fe(OH)_{(aq)}^{2+}$, and $FeSO_{4(aq)}^{+}$ species. These species are present in a single phase, an aqueous solution. Aqueous speciation is not uniquely defined but depends on the theoretical formulation of mass-action equilibria and activity coefficients; that is, it is model-dependent. Some aqueous speciation can be determined analytically, but operational definitions and assumptions are still unavoidable.

Phase. Commonly defined as a uniform, homogeneous, physically distinct, and mechanically separable part of a system. Unfortunately, mineral phases are often not uniform, homogeneous, or mechanically separable except in theory. Sophisticated microscopic and spectroscopic techniques and operational definitions are needed to define some mineral phases.

Phase speciation. The distribution of components among two or more phases. In a wet soil, iron can be present in at least three phases: as the x-ray amorphous oxyhydroxide, ferrihydrite; as goethite; and as dissolved aqueous iron.

Mass transfer. The transfer of mass between two or more phases, for example, the precipitation and dissolution of minerals in a groundwater.

Reaction-path calculation. A sequence of mass-transfer calculations that follows defined phase (or reaction) boundaries during incremental steps of reaction progress.

Mass transport. Solute movement by mass flow of a fluid (could be liquid, gas, or a mixture of solid and liquid and/or gas).

Reactive transport. Mass transfer combined with mass transport; commonly refers to geochemical reactions during stream flow or groundwater flow.

Forward geochemical modeling. Given an initial water of known composition and a rock of known mineralogy and composition, the rock and water are computationally reacted under a given set of conditions (constant or variable temperature, pressure, and water composition) to produce rock and water (or set of rocks and waters). In forward modeling, the products are inferred from an assumed set of conditions (equilibrium or not, phases allowed to precipitate or not, etc.) and thermodynamic and/or kinetic data are necessary.

Inverse geochemical modeling. Given a set of two or more actual water analyses along a flow path that have already reacted with a rock of known mineralogy, the reactions are inferred. In inverse modeling, the reactions are computed from the known field conditions (known water-chemistry evolution and known mineralogy) and assumed mineral reactivity. Inverse modeling is based on mass or mole balancing, and thermodynamic and kinetic data are not necessary, although saturation indices provide useful constraints. Relativistic kinetics (i.e., relative mineral reaction rates) are deduced as part of the results.

7.2.2.3 Inverse Modeling, Mass Balancing, and Mole Balancing

A key concept to interpreting water–rock interactions is mass balancing between water-chemistry data, mineral/gas transformations, and biologic uptake or release. The mass-balance concept is a means of keeping track of reacting phases that transfer mass during fluid flow. It is an integral part of the continuity equation for steady-state and transient-state flow conditions. Formalizing mass balances for solutes during fluid flow is simple if the solutes are conservative but more complex when reactions take place. For applications to the environment, different types of mass balances have been used and these require some explanation.

Three closely related types of mass-balance approaches will be discussed. In its simplest form, mass balancing is an expression of the law of conservation of mass; that is, any partitioning of mass through a system must equal the total sum. The first type of mass-balance approach, catchment mass balances (or mass fluxes), use 'input–output' accounting methods to identify overall gains and losses of solutes during the flow of water from meteoric inputs to stream outflow at a specified point (Bormann and Likens, 1967; Likens et al., 1977). Pačes (1983, 1984) called this the integral mass-balance approach:

$$\begin{aligned}&[\text{Mass rate}_{\text{in}} - \text{Mass rate}_{\text{out}}] \pm \text{Mass rate}_{\text{internal}}\\&\quad = \text{Rate of accumulation/depletion}\end{aligned} \qquad [1]$$

In difference form,

$$\frac{\Delta m_{\text{trans}}}{\Delta t} + \frac{\Delta m_{\text{int}}}{\Delta t} = \frac{\Delta m_{\text{tot}}}{\Delta t} \qquad [2]$$

where $\Delta m_{\text{trans}}/\Delta t$ is the difference in rate of mass (of some component) transported into and out of the system via fluid flow, $\Delta m_{\text{int}}/\Delta t$ is the rate of mass produced or removed from the fluid by internal chemical reaction, and $\Delta m_{\text{tot}}/\Delta t$ is the total rate of change in mass for a component in the fluid. Steady-state conditions are often assumed so that the accumulation/depletion rate becomes zero and the difference between input and output for a component becomes equal to the internal processes that produce or remove that component. These mass rates of change are usually obtained as integral mass fluxes (computed as discharge times concentration).

For catchments in which input from precipitation and dry deposition can be measured and the output through a weir or similar confining outflow can be measured, the difference in solute flow averaged over an appropriate period of time provides an accounting of solutes gained or lost. Overviews and summaries of essential concepts of catchment mass balances have been presented by Drever (1997a,b), Bassett (1997), and Bricker et al. (2003). The input–output mass-balance treats the catchment as a black box, but knowledge of biogeochemical processes, use of lab experiments, additional field data, and well-controlled small-scale field-plot studies can help to identify the dominant processes causing the gain or loss of a particular solute. Load (or mass flux) calculations for a river or stream use the same type of accounting procedure.

A second type of mass-balance approach is quantitative incorporation of mass balances within a reactive-transport model and can be applied to groundwaters, surface waters, and surface water–groundwater interactions. Pačes (1983, 1984) called this the local mass-balance approach. There are numerous examples and explanations of this approach (e.g., Domenico and Schwartz, 1990; Freeze and Cherry, 1979; Steefel et al., 2005; Zhu and Anderson, 2002). It is also based on eqn [2] but uses a partial differential equation with terms for advection, reaction, and dispersion, respectively:

$$\left(\frac{\partial c_i}{\partial t}\right) = -v\left(\frac{\partial c_i}{\partial x}\right) - \sum_k^n R_i + D\left(\frac{\partial^2 c_i}{\partial x^2}\right) \qquad [3]$$

where c_i is the concentration of component i, t is time, v is the linear velocity along a flow line, $\sum_k^n R_i$ is the sum of all chemical reaction rates involving component i from n to k, and D is the dispersion coefficient. Thermal effects, variably saturated flow, and sedimentation can also be modeled by incorporating the appropriate terms.

A third type of mass-balance approach is to leave the physical flow conditions implicit, assume steady-state flow along a flow line in an aquifer, and account for observed chemical changes that occur as the groundwater flows from recharge to discharge (Plummer, 1977; Plummer and Back, 1980). This approach was introduced formally by the classic publications of Garrels (1967) and Garrels and Mackenzie (1967), who calculated mass balances derived from springwater data in the Sierra Nevada Mountains of California. The modeler begins with aqueous chemical data along a flow path in an aquifer (or catchment) of known mineralogy and accounts for changes in solute concentrations by specified reaction sources and sinks. The analytical solution is achieved by solving a set of simultaneous linear equations known as mole balancing:

$$\sum_{j=1}^{j} b_p \alpha_p^i = \Delta m_i = m_{i(\text{final})} - m_{i(\text{initial})} \qquad [4]$$

in which m_i is the number of moles of element/component i per kilogram of water, α_p^i is the stoichiometric coefficient of element i in phase p, b_p is the mass-transfer coefficient of the pth phase, and j is the number of phases (Plummer et al., 1983). Because groundwaters are frequently mixtures of different water-quality types, mixing fractions can also be employed in the matrix array. Redox chemistry can be included through conservation of electrons, and water balance can be used to simulate evaporation. Plummer (1984) has called this type of modeling the inverse method, because it proceeds in a reverse manner to that of forward modeling; that is, it backs out the probable reactions from known data on water chemistry, isotopes, and mineralogy. Parkhurst (1997) simply referred to it as mole balancing. Semantics aside, this model is developed for water–rock interactions from "a set of mixing fractions of initial aqueous solutions and mole transfers of minerals and gases that quantitatively account for the chemical composition of the final solution" (Parkhurst, 1997). This third type of mass balancing has been developed in more detail by Bricker et al. (2003) and Bowser and Jones (2002).

Three papers are worth mentioning to demonstrate the fundamental nature of mole balancing for interpreting groundwater chemistry. Plummer (1984) described attempts to model the Madison Limestone aquifer, in parts of South Dakota, Wyoming, and Montana, by both forward and inverse methods. Two valuable conclusions from this paper were that information gained from mole balancing was needed to provide relativistic reaction rates for forward modeling and that even with these rates, the well-water compositions could not be closely matched, whereas they can be exactly matched with inverse modeling. Furthermore, forward modeling required much more effort and contained more uncertainty. Similar conclusions were reached by Glynn and Brown (1996, 2012) in their detailed study of the acidic plume moving in the Pinal Creek Basin in Arizona. They found that the best approach was to pursue a series of mole-balance calculations, improving their modeling with each reexamination of the phases and reactions considered. Then they took their refined mole-balance results and made further improvements by forward modeling. Inverse modeling, however, was a key to their successful interpretation. The complex nature of interpreting a dispersed contaminant plume and the associated mineral dissolution front required the use of reactive-transport modeling. The reactive-transport modeling, however, would have been much more uncertain without the inverse modeling at the front end.

The inverse or mass-balance modeling approach provides additional constraints on reactant and product mineral phases when the mineral mass transfers are plotted as a function of the range of solid-solution compositions. Bowser and Jones (2002) discovered this application when investigating the effect of compositional ranges of feldspars, phyllosilicates, and amphiboles on mass balances for catchments and groundwaters dominated by silicate hydrolysis.

It has been pointed out that inverse modeling assumes advective, steady-state flow and that ‘reaction inversion’ does not occur (Steefel and Van Cappellen, 1998). Although these are important issues, they are often not serious limitations. These assumptions are not a firm requirement for the system being studied; it is only essential that the consequences of assuming them for non-steady-state flow (with or without dispersion) do not have a significant effect on the results of the calculation. For example, it can be argued that over a long enough period of time or for a large enough aquifer, steady-state conditions never truly apply. Indeed, steady state is an approximation of the physical and chemical state of an aquifer system that works well for many, if not most, aquifers. As Zhu and Anderson (2002) stated, the most important criterion is that the same parcel of water has traveled from point A to point B. They also stated that chemical steady state is sufficient but not necessary “because the underlying mathematical equations to be solved... are the integrated forms of mass conservation (Lichtner, 1996).” At the Iron Mountain Mines, northern California (Alpers et al., 1992), high concentrations of sulfate (tens of grams per liter) and metals (grams per liter) discharge from two major portals. The groundwater movement is complex because it has advective and nonadvective (dispersive and convective) properties. There are substantial thermal and chemical gradients that affect flow regime in addition to head distribution. The variable effluent flows would indicate transient-state conditions. The chemistry, however, is still dominated by oxidation of sulfide minerals and acid dissolution of aluminosilicate minerals, and a mass-balance calculation will still reflect these geochemical processes. A mass balance going from rainwater to portal effluent will delineate the key minerals that dissolve and precipitate along the flow path. Steefel and Van Cappellen (1998) correctly stated that inverse modeling cannot be applied to contaminant plumes or reaction fronts unless the spatial delineation of the reaction front is clearly defined. ‘Reaction inversion,’ such as the dissolution of a particular mineral changing to precipitation between two points along a flow path such that no overall reaction appears to have taken place, is an interesting problem. Without additional information, it would not be possible to distinguish between no reaction and reaction inversion. In such instances, it makes no difference to the modeling or the conclusions, because the net result is the same. It is as if the element of concern was conserved in the solid phase during that increment of fluid flow, a safe assumption for silica in quartz but not for silica from weathering feldspars. It might only matter if these small-scale processes affect other processes such as the unidirectional release or attenuation of trace elements (released upon mineral dissolution but not coprecipitated or adsorbed upon mineral precipitation or vice versa) or similar irreversible processes involving nutrients. Further discussion of inverse modeling is found in **Sections 7.2.7.1** and 7.2.8.4.6.

7.2.3 Solving the Chemical Equilibrium Problem

Although both kinetic and equilibrium expressions can be used in geochemical modeling computations, the ‘equilibrium problem’ is the foundation of most calculations of this type. Simply stated, the chemical equilibrium problem is the determination of the most stable state of a system for a given set of pressure (P), temperature (T), and compositional constraints (X_i). These variables, P, T, and X_i, need not be fixed, but they must be defined for the given system. The chemical state of a system is given by the total Gibbs free energy, G, and its differential change with the extent of reaction or progress variable, ξ (De Donder, 1920), denotes the state of the system in mathematical terms. For a system at equilibrium,

$$\left(\frac{\partial G}{\partial \xi}\right)_{P,T} = 0 \qquad [5]$$

and any perturbation from equilibrium will cause this differential to be other than 0. The progress variable is a singular quantity that expresses the extent to which a reaction has taken place. It is equal to the change in the number of moles, n_i, of a reactant (or product) normalized to the stoichiometric coefficient, v_i, for that component, element, or species. In differential form,

$$\partial \xi = \frac{\partial n_i}{v_i} \qquad [6]$$

Solving the equilibrium problem means finding the minimum in the free energy surface for the defined system. Two general approaches have been used: the equilibrium constant approach and the free energy minimization approach. As the names suggest, they primarily use equilibrium constants to solve the problem or they use free energies. Of course, the approaches are basically the same because they are related by $\Delta_r G^\circ = -RT \ln K$, where R is the universal gas constant, T is the absolute temperature in Kelvin, and K is the equilibrium constant, but the logarithmic conversion leads to different numerical techniques. Both approaches have to employ mass-balance and mass-action equations. Upon substitution of mass-action into mass-balance expressions (or vice versa), a set of nonlinear equations is derived that are readily solved by a numerical method coded for a computer. The mathematical formulation of the chemical equilibrium problem is explained in Zeleznik and Gordon (1968), Van Zeggeren and Storey (1970), Wolery (1979), and Smith and Missen (1982). Harvie and Weare (1980) and Harvie et al. (1987) have improved the free energy minimization algorithm for solving the general chemical equilibrium problem and applied it to finding parameters for the

Pitzer method of calculating equilibria in brines. Rubin (1983, 1990) provided more formalism for dealing with reactive-transport and nonequilibrium conditions. Further discussion of the numerical techniques can be found in the books by Smith and Missen (1982), Nordstrom and Munoz (1994), Appelo and Postma (2005), Bethke (2008), and Bundschuh and Zilberbrand (2012). A simple problem involving speciation of an aqueous solution at equilibrium with gypsum is solved by both the Newton–Raphson method and the 'continued fraction' method in Nordstrom and Munoz (1994).

7.2.4 Historical Background to Geochemical Modeling

The founders of geochemistry, F. W. Clarke, G. M. Goldschmidt, V. I. Vernadsky, and A. E. Fersman, clearly made major contributions to our 'models' of geochemical processes. Today, however, we think of geochemical models in terms of high-speed quantitative computations of water–rock interactions made possible with fast processors and disks with large memories. This direction of research began with the principles of physical chemistry adapted for solving aqueous low-temperature geochemical problems by Hem (1959), Garrels (1960), Sillén (1961), Garrels and Christ (1965), and Krauskopf (1967). The scholarly structures that these authors built would not have been possible without the foundations laid by those who came before and developed the science of physical chemistry: Wilhelm Ostwald, Jacobus Henricus van't Hoff, and Svante Arrhenius (Servos, 1990). These chemists, along with numerous others they influenced, established the principles upon which aqueous low-temperature geochemistry and geochemical modeling is based. van't Hoff himself was an early developer of geochemical models in his efforts to apply physical chemistry to the interpretation of the equilibrium factors determining the stability of gypsum and anhydrite (van't Hoff et al., 1903) and the equilibrium interpretation of the Permian Zechstein evaporite deposits (Eugster, 1971; van't Hoff, 1905, 1909, 1912).

Probably the earliest paper to apply a speciation calculation to natural water was Goldberg's (1954) estimate of the different forms of dissolved copper in seawater based on Niels Bjerrum's theory of ion-pair formation and Jannik Bjerrum's data (see Bjerrum, 1950). He found that 65% was in the free ion (Cu^{2+}) form and another 33% was present as either a cation or neutral species form (copper–chloride complexes). This calculation, however, did not take into account simultaneous competitive complexing from all the other ions and organic matter in seawater. The free copper ion is estimated to be $\leq$0.012% of the total dissolved copper (Donat and Bruland, 1995). Speciation was central to Krauskopf's (1951) study on gold solubility, his discussion of trace-metal enrichment in sedimentary deposits (Krauskopf, 1955), and his examination of the factors controlling trace-metal concentrations in seawater (Krauskopf, 1956). In the US Geological Survey (USGS), Hem and Cropper (1959) and Hem (1961) were estimating distribution of ionic species and activities of ions at chemical equilibrium in natural waters. Sillén's (1961) first paper on seawater considered hydrolysis and complex formation. At this time, he and his colleagues were pioneering the application of computers to solve complex aqueous solution equilibria (Dyrssen et al., 1968; Ingri and Sillén, 1962; Ingri et al., 1967; Sillén, 1962). The classic paper that applied aqueous speciation to natural water was that of Garrels and Thompson (1962) in their 'Chemical Model of Seawater.' This model contained unique features such as the mean-salt method for estimating activity coefficients and was the first to calculate simultaneously the major aqueous seawater species.

The adaptation of water–rock geochemical modeling to computers was pioneered by Helgeson and his colleagues, who focused on ore deposits and high-temperature, high-pressure reactions (Helgeson, 1964, 1967, 1969) but also considered low-temperature processes (Helgeson et al., 1969, 1970). Helgeson's (1971) research continued with the application of computers to the calculation of geochemical kinetics. Theoretical approaches were developed for geochemical kinetics (Aagard and Helgeson, 1982; Helgeson and Murphy, 1983) and computations compared to measured reaction rates (Helgeson et al., 1984; Murphy and Helgeson, 1987) and coupled with diffusion (Murphy et al., 1989). These approaches provide insight to the mechanisms of controlled laboratory studies on mineral dissolution rates, but difficulties are encountered when applications are made to the complex conditions of the natural environment. Experimental and theoretical approaches to mineral dissolution fail to predict the actual dissolution rates in catchments, because experiments do not reproduce the composition and structure of natural mineral surfaces, they do not account for adsorbed inhibitors, they do not consider the effect of variable climate and hydrologic flow rates, and they do not account for biologic activity (Brantley and Olsen, **Chapter 7.3**). These factors may have taken anywhere from decades to millennia to develop, and they can change over short periods of time. Computer codes that incorporate reaction kinetics into groundwater or catchment codes usually do so with some type of generalized first-order rate law.

Beginning in the 1960s and expanding considerably during the 1970s, a series of computer codes were developed that could perform a wide variety of aqueous geochemical calculations (Bassett and Melchior, 1990; Mangold and Tsang, 1991), and these evolved considerably during the 1980s and 1990s to include simulation of more processes, coupling of processes (especially reaction with transport), and the availability of more options (Alpers and Nordstrom, 1999). The advances in geochemical modeling are apparent in the evolution of Barnes' *Geochemistry of Hydrothermal Ore Deposits* from first edition (Barnes, 1967) to third edition (Barnes, 1997), in the American Chemical Society (ACS) books *Chemical Modeling in Aqueous Systems* that have shown significant advances from the first (Jenne, 1979) to the second (Melchior and Bassett, 1990), and in the plethora of papers on this subject since the 1980s. Nevertheless, advanced sophistication for geochemical codes does not imply a parallel advance in our understanding of geochemical processes. The sophistication of software has outdistanced our capacity to evaluate the software over a range of conditions, and it has outdistanced our ability to obtain the field data to constrain and test the software.

7.2.5 The Problem of Activity Coefficients

7.2.5.1 Activity Coefficients

Aqueous electrolytes and the equilibrium constants that define various reactions in low-temperature geochemistry are inexorably linked with the problem of activity coefficients or the problem of nonideality for aqueous electrolyte solutions. Thermodynamic equilibrium constants, defined by an extrapolation to infinite dilution for the standard-state condition (not the only possible standard state), require the use of activity coefficients. Unfortunately, there is neither a simple nor universal nonideality method that works for all electrolytes under all conditions. This section provides a brief overview of a major subject still undergoing research and development but for which several satisfactory approaches are available.

If the activity of a solute or ion was ideal, it could be taken as equivalent to the molal concentration, m_i, of the i ion or solute. However, interactions with other ions and with the solvent water are strong enough to cause nonideal behavior, and the characteristic variable relating concentration to chemical potential is the activity coefficient, γ_i,

$$a_i = \gamma_i m_i \qquad [7]$$

With the accumulation of activity coefficient measurements and the search for a theoretical expression, it was discovered that in dilute solutions, the logarithm of the activity coefficient was an approximate function of the square root of the molality:

$$\ln \gamma_i = -\alpha_i m_i^{1/2} \qquad [8]$$

where α_i was simply a constant. Brønsted (1922) introduced a linear term to eqn [8] in which the coefficient, β, is a 'specific-ion interaction parameter,'

$$\ln \gamma_i = -\alpha_i m_i^{1/2} - \beta m_i \qquad [9]$$

Later modifications of this general approach became known as the specific-ion interaction theory (SIT) because of the explicit dependence on the solute or ions being considered.

An important concept that aided in the development of electrolyte theory was the ionic strength, I, introduced by Lewis and Randall (1921):

$$I = \frac{1}{2}\sum m_i z_i^2 \qquad [10]$$

where z_i is the ionic charge. Thereafter, the ionic strength was used as a parameter in activity coefficient equations. Debye and Hückel (1923) derived an equation from electrostatic theory, which, in the limit of infinite dilution (hence, the Debye–Hückel limiting law), becomes

$$\log \gamma_i = -A z_i^2 I^{1/2} \qquad [11]$$

where A is a Debye–Hückel solvent parameter (dependent on the properties of the solvent).

Their extended Debye–Hückel equation is

$$\log \gamma_i = -\frac{A z_i^2 I^{1/2}}{1 + B a_i I^{1/2}} \qquad [12]$$

where B is another Debye–Hückel solvent parameter and a_i is an ion-size diameter derived by empirical fit but approximates the hydrated ion diameter. This equation is applicable up to about 0.1 molal. The use of the extended Debye–Hückel equation with the appropriate equilibrium constants for mass-action expressions to solve a complex chemical equilibrium problem is known as the IA method. The method uses the concept of attraction between ions of opposite charge bonding to make an ion pair or triplet that reduces the concentration of charged ions. Hence, the *total ionic strength* would be without any ion-pair association, and the *effective ionic strength* would be less because it would include IA.

Hückel (1925) demonstrated that by adding the linear term with a fitted coefficient to the extended Debye–Hückel equation (eqn [12]), activity coefficients for ionic strengths up to a few molal for simple single electrolytes could be reliably fit:

$$\log \gamma_i = -\frac{A z_i^2 I^{1/2}}{1 + B a_i I^{1/2}} + b_i I \qquad [13]$$

Eqn [13] was adopted in the original aqueous model developed by Helgeson and colleagues (Helgeson, 1969; Helgeson et al., 1981) and by Truesdell and Jones (1974). The IA method using eqn [13] for major ions (mixed electrolytes) in natural water compares well with other more precise methods (see the succeeding text) up to an effective ionic strength of seawater (0.7 m, whereas the total ionic strength is nearly 1 molal) but not much higher.

Further modifications of these equations were tried over the next several decades. The next better approximation is to allow the linear coefficient to be a function of the ionic strength (Pitzer and Brewer, 1961), and it was utilized by Helgeson and Kirkham (1974a,b, 1976), Helgeson et al. (1981), and Tanger and Helgeson (1988) in the development of the Helgeson–Kirkham–Flowers (HKF) equations, which is based on the Born function (using the dielectric constant of the solvent) and ion hydration.

Contributions by Guggenheim (1935) and Scatchard (1936) and the KTH Swedish group (Grenthe et al., 1992, 1997) became the Brønsted–Guggenheim–Scatchard or SIT (specific-ion interaction theory) method:

$$\log \gamma_i = -\frac{A z_i^2 I^{1/2}}{1 + 1.5 I^{1/2}} + \sum_k \varepsilon(i,k,I) m_k \qquad [14]$$

in which the linear term is a function of molality summed for all the other ions in solutions, k, and $\varepsilon(i, k, I)$ tends to be constant at higher molalities but solute- or ion-specific. The last term in eqn [14] represents the deviation of the experimentally measured activity coefficient from the prediction of the simplified Debye–Hückel equation.

Pitzer (1973) reexamined the statistical mechanics of aqueous electrolytes in water and derived a different semiempirical method for activity coefficients, commonly termed the Pitzer specific-ion-interaction model. He fitted a slightly different function for behavior at low concentrations and used a virial coefficient formulation for high concentrations. The results have proved extremely fruitful for modeling activity coefficients over a very large range of molality. The general equation limited to the second-order term is

$$\begin{aligned} \ln \gamma_{\pm} = {} & -\frac{A}{3}|z_+ z_-| f(I) + \frac{2\nu_+\nu_-}{\nu} B(I) m \\ & + \frac{2(\nu_+\nu_-)^{3/2}}{\nu} C m^2 \end{aligned} \qquad [15]$$

where

$$f(I) = \frac{I^{1/2}}{1 + 1.2I^{1/2}} + 1.67\ln\left(1 + 1.2I^{1/2}\right)$$

and

$$B(I) = 2\beta^{\circ} + \frac{2\beta'}{\alpha^2 I}\left[1 - \left(1 + \alpha I^{1/2} - \frac{1}{2}\alpha^2 I\right)e^{-\alpha I^{1/2}}\right]$$

and where β° and β' are specific-ion parameters, α is a constant for a similarly charged class of electrolytes, and C is a specific-ion parameter independent of ionic strength. The B and C parameters are second and third virial coefficients. The parameter $\nu = \nu_+ + \nu_-$ is the sum of the stoichiometric coefficients for the cation, ν_+, and the anion, ν_-, of the solute. The Pitzer parameters have been fitted for a wide range of solutes and have been used for mixed electrolyte solutions to model the mineral solubility behavior in brines (Harvie and Weare, 1980; Harvie et al., 1980). Grenthe et al. (1997) made an extensive comparison of the SIT method with the Pitzer method in detail and came to the following conclusions: (i) the more extensively parameterized Pitzer model allows the most precise and accurate modeling of activity coefficients and equilibrium constants, provided that all the interaction coefficients are known; (ii) when Pitzer parameters are missing (not available from experimental data), they must be estimated and the precision and accuracy of the activity coefficients can be significantly compromised; (iii) the parameters in the SIT model can be related to those in the Pitzer model and provide another means of estimating Pitzer parameters; (iv) the SIT model is in good agreement with the Pitzer model for the range $m = 0.1$–4 mol kg^{-1}; and (v) the Pitzer model is the preferred formalism for solutions or brines of high ionic strength. An extensive discussion of the development of the Pitzer model and several hybrid approaches can be found in Pitzer (1991a) and Millero (2001). It appears that hybrid approaches provide the best promise in the future, because they combine the extensive data available on equilibrium constants with a better formulation of activity coefficients.

The difference between the extended Debye–Hückel equation and the Pitzer equations has to do with how much of the nonideality of electrostatic interactions is incorporated into mass-action expressions and how much into the activity coefficient expression. It is important to remember that the expression for activity coefficients is inexorably bound up with equilibrium constants and they must be consistent with each other in a chemical model. Ion-pair interactions can be quantified in two ways, explicitly through stability constants (IA method) or implicitly through empirical fits with activity coefficient parameters (Pitzer method). Both approaches can be successful with enough effort to achieve consistency. At the present, the Pitzer method works much better for brines, and the IA method works better for dilute waters because of the greater number of components and species for which basic data exist. When the effort is made to compare both approaches for the same set of high-quality data and the ionic strengths are not too high, they appear to be comparable (Felmy et al., 1990). The primary challenge for the future will be to ensure that consistency is maintained between the thermodynamic data, the expressions for nonideality, and the mass-action expressions in geochemical modeling codes and to incorporate more trace elements and redox species within the same formulation.

7.2.5.2 Saturation Indices

After speciation and activities have been calculated for all the free ions, ion pairs, triplets, etc., a mineral saturation index can be computed. The saturation index, SI, is defined as the logarithm of the ratio of the ion-activity product, IAP, to the solubility product constant, K_{sp},

$$\mathrm{SI} = \log\left[\frac{\mathrm{IAP}}{K_{\mathrm{sp}}}\right] \qquad [16]$$

If the solution is at equilibrium, the $\mathrm{IAP} = K_{\mathrm{sp}}$ and the $\mathrm{SI} = 0$. If the $\mathrm{SI} > 0$, then the solution is supersaturated and the mineral would tend to precipitate; if the $\mathrm{SI} < 0$, the solution is undersaturated and the mineral would tend to dissolve, if present. Because the SI is affected by the stoichiometry of the mineral formula, it is best to normalize the SI to the total mineral stoichiometry, as pointed out by Zhang and Nancollas (1990):

$$\mathrm{SI} = \log\left[\frac{\mathrm{IAP}}{K_{\mathrm{sp}}}\right]^{1/\nu} \qquad [17]$$

where $\nu = \nu_+ + \nu_-$, the sum of the stoichiometries of the positive and negative components in the mineral formula. For the saturation index of calcite, the IAP is $\left(a_{\mathrm{Ca}^{2+}}\right)\left(a_{\mathrm{CO_3}^{2-}}\right)$ and the K_{sp} is the same product at solubility equilibrium and $\nu = 2$. Including the stoichiometric coefficient makes comparisons between different mineral saturation indices on the same basis for the same water sample.

Saturation index computations describe the 'tendency' of a water sample to be saturated, but they do not necessarily demonstrate whether mineral dissolution or precipitation actually happens. For dissolution to occur, the mineral must be present and it must dissolve at a rate that is fast enough relative to the flow rate of the water to affect the water chemistry (Berner, 1978). Likewise for a mineral to precipitate, it must precipitate at a rate fast enough to affect the water chemistry. The kinetics of precipitation and dissolution reactions must be applied to get a realistic interpretation of water–rock interactions.

7.2.6 Geochemical Databases

Input for aqueous geochemical codes consists of field data (geology, petrology, mineralogy, and water analyses), thermodynamic and aqueous electrolyte data, and kinetic and sorption data if the code includes these processes. Thermodynamic data are fundamental to most geochemical computations, and several major compilations are available. Although the guidelines and necessary relations for thermodynamic consistency are well established (Haas and Fisher, 1976; Helgeson, 1968, 1969; Nordstrom and Munoz, 1994; Nordstrom et al., 1990; Rossini et al., 1952; Wagman et al., 1982), it has been difficult to employ them in the development of databases. Two general approaches have been recognized: serial networks and simultaneous regression. With serial networks, an evaluator begins with a single starting point, such as the standard-state properties for an element (or all elements) and gradually builds in the properties of compounds through the appropriate reaction combinations. Serial networks, such as that developed by the former National Bureau of Standards (National Institute of Standards and Technology) database (Wagman et al., 1982), achieved continuity for a large data set but lost some thermodynamic constraints, whereas simultaneous regression, which preserves thermodynamic relationships, can only be done on a limited subset of data, and the weighting of the regression fit depends on the judgment of the evaluator (Archer and Nordstrom, 2003). Computer codes have been developed for the purpose of correlating and evaluating a diversity of thermodynamic data (Ball et al., 1988; Haas, 1974, 1989), but they have not been widely used and have now been replaced by spreadsheet computations. Serious discrepancies in thermodynamic properties do appear among these compilations, and some of the discrepancies have been incorporated into the databases of geochemical codes. Many users of these codes are not familiar with these databases, and the possible uncertainties propagated through the computations from thermodynamic errors. Such error propagation may or may not be important, depending on the specific objectives of the geochemical problem being addressed. Users must be aware of the errors associated with thermodynamic data when making these computations.

7.2.6.1 Thermodynamic Databases

Since the early compilations of thermodynamic data (e.g., Lewis and Randall, 1923), numerous measurements were made during the twentieth century leading to the well-known compilations of Latimer (1952) and Rossini et al. (1952). Measurements and compilations continued to expand through the latter part of the twentieth century, and comprehensive inventories, such as Sillén and Martell (1964, 1971), Martell and Smith (1974–1976), Perrin (1979, 1982), Serjeant and Dempsey (1979), Wagman et al. (1982), Högfeldt (1982), Gurvich et al. (1989a,b, 1993), Robie and Hemingway (1995), and Chase (1998), summarized and organized a considerable amount of data. Unfortunately, these were primarily compilations and not evaluations, with the exception of Wagman et al. (1982) in which references were not reported and Gurvich et al. (1993), Chase (1998), and Robie and Hemingway (1995). Notable evaluations were the publication of the CODATA tables (Cox et al., 1989; Garvin et al., 1987), the Organisation Economic Co-operation and Development/Nuclear Energy Agency Thermochemical Database (OECD/NEA TDB) publications (Brown et al., 2005; Bruno et al., 2007; Gamsjäger et al. 2005; Grenthe et al., 1992; Guillamont et al., 2003; Hummel et al., 2005; Lemire et al., 2001; Olin et al. 2005; Rand et al., 2009; Rard et al., 1999; Silva et al., 1995), the Swiss radioactive waste management agency Nagra/PSI publication on evaluating data for nuclear waste objectives (Hummel et al., 2002; Thoenen et al., 2004), and the International Union of Pure and Applied Chemistry (IUPAC) solubility data series compilations (e.g., Dirkse, 1986; Lambert and Clever, 1992; Scharlin, 1996). The OECD/NEA TDB, although focusing on radionuclides of most concern to safe disposal of high-level radioactive wastes and military wastes, contains a considerable amount of auxiliary data on other common aqueous and solid species that had to be evaluated along with the actinides.

Additional work on compilation and evaluation of thermodynamic databases within the chemical community has progressed in recent years (Voigt et al., 2007). A commercial database known as DDB (Dortmund Data Bank) has been underway in Germany since 1973, begun at the University of Dortmund and now located at the University of Oldenburg (http://www.ddbst.de; last accessed 3 May 2012). They store original data (>50 000 references) and derived thermodynamic data. The Paris School of Mines launched a database project, CDT (Common Thermodynamic Database) to coordinate geochemical data and to have a common review platform. Storage, traceability, and internal consistency are all part of the objectives. Geoscience Australia has a thermodynamic database project called FreeGs that has freely accessible standard-state data for minerals and reactions over a wide range of temperature and pressure (http://dbforms.ga.gov.au/www/thermo.thermo_reports_pkg.reports_exec; last accessed 3 May 2012 and not the website found in Voigt et al., 2007). The THEREDA (Thermodynamic Reference Database) is supported by the German Nuclear Safety and Reactor Safety federal agencies and Freiberg Technical University so that it, such as the NEA TDB and LLNL databases, is focused on radionuclide- and groundwater-related data that might affect near-field and far-field processes. It is in the early stages of development, and in their third release (21 February 2012), they have parameters for Na, Mg, Ca, K, Cl, SO_4, $HCO_3/CO_{2(g)}$, and H_2O (https://www.thereda.de/; last accessed 4 May 2012).

For aqueous geochemical modeling, the equilibrium constant tables of Nordstrom et al. (1990) have proven useful and are found in USGS and US Environmental Protection Agency (USEPA) codes described in the succeeding text and in popular water-chemistry/aqueous-geochemistry textbooks (Appelo and Postma, 2005; Drever, 1997a; Langmuir, 1997; Stumm and Morgan, 1996). These tables have been recompiled, expanded, and tabulated in terms of thermodynamic properties (G, H, S, C_P, and log K for reaction and individual species, Nordstrom and Munoz, 1994). The tabulation of Nordstrom and Munoz (1994) was organized in such a way that individual species can be compared with reactions measured independently to demonstrate consistency. Consequently, it is easy to check thermodynamic relations to see if the properties for individual species are consistent with tabulated reaction equilibria. Only values that agreed within a close range of the stated uncertainties were included in the tables.

Internally consistent data, primarily for high-temperature mineral phases, have been developed by Berman (1988), Holland and Powell (1998), and Gottschalk (1997). Application of the HKF model for water–mineral equilibria has led to extensive tables of thermodynamic data for a wide range of temperature and pressure (up to 5 kbar and 1000 °C, Shock and Helgeson, 1988, 1990; Oelkers et al., 1995). These tables were compiled with the aid of the SUPCRT92 code (Johnson et al., 1992). An online updated data listing and free interactive support for SUPCRT92 are maintained at Arizona State University at http://geopig3.la.asu.edu:8080/GEOPIG/ (last accessed 4 May 2012). A number of US Department of Energy thermodynamic data qualification reports, known as the Yucca Mountain database, were issued beginning in 2000, which led to the major evaluation and update of the SUPCRT92 database incorporating many new measurements (Apps and Spycher, 2004; Wolery and Jove-Colon, 2004, 2007).

Another database that has focused on internal consistency can be found online under Thermo-Calc (Andersson et al., 2002; Lukas et al., 2007), and it is closely tied into equilibrium phase diagrams because it is designed primarily for alloys and metallurgical objectives. The National Institute for Standards and Technology (NIST) maintains thermodynamic properties on a website (http://webbook.nist.gov/; last accessed 4 May 2012) and published an extensive list of thermophysical and thermochemical properties (Lide and Kehiaian, 1994). Additional pre-1993 compilations and sources of specific thermodynamic data can be found in Nordstrom and Munoz (1994).

As mentioned in the review of thermodynamic databases by Oelkers et al. (2009), a convergence of thermodynamic properties of the same minerals from many different sources is a hopeful sign that consistency is improving over time.

7.2.6.2 Kinetic Databases

There are limited kinetic databases for aquatic geochemistry, partly because of the enormous range of conditions that need to be measured and normalized. Another approach would be to compile relative reaction rates for minerals based on both lab studies and field studies that could be a guide for modelers. White and Buss (**Chapter 7.4**) have compiled data for dissolution rates of common silicate minerals and discussed their relation to solute fluxes from drainage basins. Brantley and Olsen (**Chapter 7.3**) have compiled more data on dissolution rates for calcite, silicates, and oxides and outlined the basic kinetic equations, temperature dependence, and effects of organic and inorganic ligands. Rate coefficients for an even larger group of silicates, oxides, hydroxides, carbonates, sulfates, sulfides, phosphates, and halides have been compiled by Palandri and Kharaka (2004).

7.2.6.3 Electrolyte Databases

The classic books by Harned and Owen (1958) and Robinson and Stokes (1959) put electrolyte theory on a firm basis and provided important tabulations of electrolyte data for calculations of activity coefficients and related properties. A comprehensive compilation of electrolyte data (activity and diffusion coefficients, viscosity, density, and conductance) can be found in Lobo and Quaresma (1989).

Advances in electrolyte theory, especially the use of the Pitzer method (Pitzer, 1973, 1979), led to alternate methods of calculating activities and speciation. The books edited first by Pytkowicz (1979) and later by Pitzer (1991b) provided a general overview of the different approaches and hybrid approaches to these computations. A more recent reference providing a thorough overview of the subject with tables of molal properties, activity coefficients and parameters, and dissociation/association constants is Millero (2001). These references explain the general use of the IA method with extended forms of Debye–Hückel equations, the Pitzer specific-ion interaction method, and hybrid approaches that take advantage of the best aspects of both approaches.

7.2.7 Geochemical Codes

This listing and description of geochemical codes is not meant to be either exhaustive or complete. It is meant to be a brief overview of several codes in current and common use. Earlier reviews by Yeh and Tripathi (1989a), Mangold and Tsang (1991), Parkhurst and Plummer (1993), and Alpers and Nordstrom (1999) provide information on more codes, their evolution, and references to earlier reviews on codes and geochemical modeling. More recently, Bethke (2008), Oelkers et al. (2009), and Zilberbrand (2012) provided lists of recent codes in common use. Loeppert et al. (1995) also contains useful information on geochemical codes and modeling, especially for soil interactions. It is important to remember that most codes in active use often undergo enhancements, database updates, and other improvements. The descriptions given in this section may not apply to some of these same codes a few years from now.

7.2.7.1 USGS Codes

The USGS has developed several codes that are useful for the interpretation of water-chemistry data and for simulating water–rock interactions. Two similar aqueous speciation codes were developed in parallel, WATEQ (Truesdell and Jones, 1974) and SOLMNEQ (Kharaka and Barnes, 1973). The primary aim of these programs was to aid in the interpretation of water-quality data. SOLMNEQ, however, had a different subroutine for calculating temperature and pressure dependence and could calculate reaction equilibria above 100 °C. WATEQ was intended for temperatures of 0–100 °C. Both of these programs have been updated. WATEQ4F v.2 (Ball and Nordstrom, 1991, with database updates to 2012) uses the IA method with an expanded form of the extended Debye–Hückel equation for major ions (Hückel, 1925; Nordstrom and Munoz 1994; Truesdell and Jones, 1974), includes independent redox speciation computations that assume redox disequilibrium, and has database updates for uranium (Grenthe et al., 1992), chromium (Ball and Nordstrom, 1998), arsenic redox species (Archer and Nordstrom, 2003; Nordstrom and Archer, 2003), and conductivity calculations (McCleskey et al., 2012). SOLMINEQ.88 (Kharaka et al., 1988; Perkins et al., 1990) covers the temperature range of 0–350 °C and 1–1000 bar pressure, includes both the IA method and the Pitzer method, and has mass-transfer options such as boiling, fluid mixing, gas partitioning, mineral precipitation, mineral dissolution, ion exchange, and sorption. It has been found to be particularly applicable to deep sedimentary basins, especially those containing oil and gas deposits. The latest version, SOLMINEQ.GW, is explained in an introductory text on groundwater geochemistry (Hitchon et al., 1996).

Parkhurst et al. (1980) developed the PHREEQE code to compute, in addition to aqueous speciation, mass transfer and reaction paths. A separate but similar code, PHRQPITZ, uses the Pitzer method for brine calculations (Plummer and Parkhurst, 1990; Plummer et al., 1988). The PHREEQE code has been regularly upgraded, and the recent version, PHREEQC version 2, includes ion exchange, evaporation, fluid mixing, sorption, solid-solution equilibria, kinetics, one-dimensional transport (advection, dispersion, and diffusion into stagnant zones or dual porosity), and inverse modeling (Parkhurst and Appelo, 1999). An interface (PHREEQCI) was developed for interactive modification of the input files by Charlton et al. (1997). The latest development in this series is PHAST, which includes three-dimensional transport (Parkhurst et al., 2004) and several enhancements and new features found in version 2 (Parkhurst et al., 2010). The program PHAST uses the solute-transport simulator HST3D (Kipp, 1987, 1998) and iterates at every time step with PHREEQC. Thorstenson and Parkhurst (2002) have developed the theory needed to calculate individual isotope equilibrium constants for use in geochemical models and utilized them in PHREEQC to calculate carbon-isotope compositions in unsaturated zone with seasonally varying CO_2 production (Parkhurst et al., 2001). Appelo and Postma (2005) have published a textbook on groundwater geochemistry that uses PHREEQC in many of its examples, and Merkel and Planer-Friedrich (2008) have published a practical guide to modeling aquatic systems using PHREEQC extensively with numerous examples for the beginning user. Charlton and Parkhurst (2011) have developed a set of modules that allows easy integration of PHREEQC into other software.

Geochemical modeling of reactants in flowing mountainous stream systems can be done with the USGS codes OTIS (Runkel, 1998) and OTEQ (Runkel, 2010; Runkel et al., 1996a, b, 1999) that model solute transport and reactive transport, respectively. OTIS, or one-dimensional transport with inflow and storage, is based on the earlier work of Bencala (1983) and Bencala and Walters (1983). The OTEQ code combines the OTIS code with MINTEQA2 for chemical reaction at each incremental step of transport. These codes are calibrated with constant-flow tracer-injection studies and testable assumptions regarding the solubility product constant of the precipitating phases (Kimball et al., 2003). They have been tested in numerous settings, primarily with the objective of quantifying and predicting the sources, transport, and fate of acid drainage from mined environments in the Western United States, including the evaluation of remedial alternatives (Ball et al., 2004; Broshears et al., 1996; Kimball and Runkel, 2010; Kimball et al., 2010; Runkel and Kimball, 2002; Runkel et al., 1996a,b, 1999, 2007, 2012).

Codes for inverse modeling began with the program BALANCE (Parkhurst et al., 1982) from which the interactive code NETPATH (Plummer et al., 1991) evolved. NETPATH, in addition to mass balancing, allows database management for a suite of wells and can compute speciation and saturation indices with WATEQ. Inverse modeling has now been programmed into PHREEQC along with uncertainty propagation (Parkhurst, 1997). Bowser and Jones (1990, 2002) have incorporated the mass-balance approach into a spreadsheet format that allows graphical output and a quick reconnaissance of ranges of mineral compositions that are permissible models for silicate solid-solution series. USGS codes and manuals can be downloaded free. The current version and additional bibliographic and information files for PHREEQC are available at http://wwwbrr.cr.usgs.gov/projects/GWC_coupled/ (last accessed 19 June 2012).

7.2.7.2 LLNL/LBNL Codes

A set of computer codes known as EQ3/6 was originally developed by Wolery (1979) to model rock–water interactions in hydrothermal systems for the temperature range of 0–300 °C. Software development was later sponsored by the US Department of Energy at Lawrence Livermore National Laboratories (LLNL) to model geochemical processes anticipated in high-level nuclear waste repositories. This geochemical code has become one of the most sophisticated and most applicable for a wide range of conditions and processes. In addition to speciation and mass-transfer computations, it allows for equilibrium and nonequilibrium reactions, solid–solution reactions, kinetics, IA and Pitzer methods, and both inorganic and organic species. The program has been used for several municipal and industrial waste situations to assess natural and engineered remediation processes, to model geologic CO_2 sequestration (Johnson et al., 2005), to model mineral precipitation at high ionic strengths (Brown and Ebinger, 1998), and to model evaporative evolution of a Yucca Mountain brine (Alai et al., 2005). It has five supporting thermodynamic data files, and the thermodynamic data are evaluated and updated with the SUPCRT92 software (Johnson et al., 1992), based on Helgeson's formulation for activity coefficients and aqueous thermodynamic properties over a wide range of temperature and pressure (Helgeson and Kirkham, 1974a,b, 1976; Helgeson et al., 1981) and solid-phase thermodynamic properties (Helgeson et al., 1978). Thermodynamic data are updated with the availability of published research (e.g., Shock and Helgeson, 1988, 1990; Shock et al., 1989; Wolery and Jove-Colon, 2007).

Pruess (1991, 2004) developed the TOUGH code for multiphase fluid and heat flow at Lawrence Berkeley National Laboratory (LBNL), which was expanded and modified to include chemical reaction (TOUGHREACT, Xu et al., 1997, 2008, 2009; Xu and Pruess, 1998, 2001). It has been applied to a wide range of geochemical processes, including pyrite oxidation (Xu et al., 2000), CO_2 sequestration (Xu et al., 2003, 2004, 2006), supercritical water conditions (Croucher and O'Sullivan, 2008), supergene copper enrichment (Xu et al., 2001), and water–rock interactions in geothermal systems (Dobson et al., 2004). Thermodynamic data are largely based on SUPCRT92 with appropriate updates from more recent literature sources.

7.2.7.3 Miami Code

It would be difficult to find more comprehensive or more detailed studies on the physical chemistry of seawater than those done at the University of Miami (Millero, 2001). Several codes were developed for calculation of activity coefficients and speciation of both major ions and trace elements in seawater. The activity coefficient models have been influenced strongly by the Pitzer method but are best described as hybrid because of the use of ion-pair formation constants (Millero and Schreiber, 1982). The current code uses QBASIC to compute activity coefficients for 12 major cations and anions, seven neutral solutes, and more than 36 minor or trace ions. At 25 °C, the ionic strength range is 0–6 m. For major components, the temperature range has been extended to 0–50 °C, and in many cases, the temperature dependence is reasonably estimated to 75 °C. Details of the model and the parameters and their sources can be found in Millero and Roy (1997) and Millero and Pierrot (1998). Comparison of some computed (with the Miami code) and measured individual-ion-activity coefficients for seawater is shown in **Section 7.2.8.8** on model reliability.

7.2.7.4 The Geochemist's Workbench™

A set of five programs known as The Geochemist's Workbench™ or GWB was developed by Bethke (1994) with a wide range of capabilities similar to EQ3/6 and PHREEQC v.2. The GWB performs speciation, mass transfer, reaction-path calculations, isotopic calculations, temperature dependence for 0–300 °C, independent redox calculations, and sorption calculations. Several electrolyte databases are available including IA with Debye–Hückel activity coefficients, the Pitzer formulation, the Harvie–Møller–Weare formulation, and a PHRQPITZ-compatible formulation. The default database is that of LLNL, but any database in GWB format can be used, such as those from PHREEQC, Visual MINTEQ, WATEQ4F, and Dzombak and Morel (1990) for sorption on hydrous ferric oxides. The program X2t allows the coupling of two-dimensional transport with geochemical reaction. Basin3 is a basin-modeling program that can be linked to GWB. Another advantageous feature is the plotting capability that can produce pε–pH or activity–activity or fugacity–fugacity diagrams from GWB output. Bethke (2008) has published a textbook on *Geochemical and Biogeochemical Reaction Modeling* that guides the reader through a variety of geochemical computations using GWB and provides the basis for a course in geochemical modeling. The most recent release at the time of publication is GWB 9.0, which incorporates a new user interface and new kinetic options (http://www.gwb.com/gwb.htm; last accessed 30 April 2012). Applications include CO_2 sequestration (Moore et al., 2005; Nondorf et al., 2011; Parry et al., 2007; Rosenqvist et al., 2012), AMD (Berger et al., 2000), and microbial respiration (Bethke et al., 2011; Jin and Bethke, 2005, 2007).

7.2.7.5 REDEQL–MINTEQ Codes

One of the first speciation programs that included mass-transfer reactions at equilibrium was REDEQL (Morel and Morgan, 1972). The primary aim of this set of codes was to compute the equilibrium chemistry of dilute aqueous solutions in the laboratory and was among the first to include sorption. It also has been widely used to interpret water quality in environmental systems. This FORTRAN code has evolved through several versions, parallel with advances in computer hardware and software. Incorporation of the WATEQ3 database (Ball et al., 1981) with the MINEQL program (Westall et al., 1976) produced MINTEQ (Felmy et al., 1984), which became the USEPA-supported code, MINTEQA2 (Allison et al., 1991). The more recent upgrade is MINTEQA2/PRODEFA2 v. 4 (USEPA, 1998, 1999 (revised)) and contains code revisions, updates in thermodynamic data, and modifications to minimize nonconvergence problems to improve titration modeling, to minimize phase rule violations, to enhance execution speed, and to allow output of selected results to spreadsheets. PRODEFA2 is an ancillary program that produces MINTEQA2 input files using an interactive preprocessor. Thermodynamic data and computational abilities for Be, Co(II/III), Mo(IV), and Sn(II, IV) species have been added to the program. Numerous researchers have made their own modifications to the program so that several versions exist that differ in their databases and reliability. Examples of test cases to demonstrate the input setup, capabilities of the code, and comparisons of standard test cases have not been included in the documentation, as has been done for other programs.

Perhaps the most noteworthy aspect of the upgraded MINTEQA2 code is the Gaussian model for interactions of dissolved organic matter with cations. The model formulation is based on the statistical treatment of proton binding (Posner, 1964) that was developed by Perdue and Lytle (1983), Perdue et al. (1984), and Dobbs et al. (1989). This approach uses a continuous distribution of sites as opposed to discrete site binding. It is equivalent to a collection of monoprotic ligands, each able to bind protons and metal cations, with the variations in log K described by a single Gaussian distribution for each class of sites. Another code, MODELm (Huber et al., 2002), uses a linear differential equilibrium function to account for trace-metal complexation with natural organic matter and was compared to those done by MINTEQA2. MODELm predicted greater amounts of metal–organic complexing than MINTEQA2, but no conclusions were drawn as to the cause of this difference. MODELm can be used in MINTEQA2 instead of the Gaussian distribution model. Although cation–organic binding in natural waters is a highly complex and challenging subject to quantify for modeling purposes, advances since the early 1990s are leading us much closer to practical approaches that can be incorporated into computerized equilibrium and nonequilibrium chemical codes. Geochemistry will benefit from continued research in this area because organic matter exerts such a strong control on the behavior of trace elements in most aquatic systems. More testing and evaluation of a range of natural waters with different trace-element concentration and organic matter types is needed in the future. Evaluation should be accomplished by comparing analytical speciation with computed speciation.

A Windows version of MINTEQA2 v. 4.0, known as Visual MINTEQ, is available at no cost from http://www2.lwr.kth.se/English/OurSoftware/vminteq/ at The Royal Institute of Technology, Sweden (last accessed 14 April 2012). It is supported by two Swedish research councils, VR and MISTRA. The code includes the NIST database, adsorption with five surface-complexation models, ion exchange, and metal–humate complexation with either the Gaussian DOM Model or the Stockholm Humic Model. Input data are accepted from Excel spreadsheets, and output is exported to Excel. A major update was completed in January 2011 (version 3.0). The Royal Institute of Technology also has produced HYDRA and MEDUSA for creating a database for a given system and creating activity–activity and pε–pH diagrams. Links to other similar programs can be found online.

A Windows version of MINTEQA2, known as MINEQL+ v. 4.6, has several enhancements that make it an attractive alternative to other versions. The user interface with a relational database technique for scanning thermodynamic data, a utility for creating a personal database, a relational spreadsheet editor for modifying chemical species, a multirun manager, special reports for convenient data extraction or additional calculations, and a tutorial with several examples provides a much more flexible and practical code for modelers. It also provides graphic output for log *C*–pH plots, ion-fraction diagrams, solubility plots, titration curves, and sensitivity plots. It is limited in temperature to 0–50 °C and ionic strength <0.5 M. The program is available through Environmental Research Software (http://www.mineql.com/; last accessed 14 April 2012).

7.2.7.6 Waterloo Codes

A considerable history of hydrogeochemical modeling and its application has evolved at the University of Waterloo, Ontario, Canada, and a series of reactive-transport codes have evolved with it. These codes have been primarily applied to mine tailings piles. A finite element transport module, PLUME2D, was utilized with the MINTEQA2 module in an efficient two-step sequential solution algorithm to produce MINTRAN (Walter et al., 1994). Leachates from heterogeneous mine overburden spoil piles that made a contaminant front were modeled with MINTRAN and other codes at open-pit lignite mines in Germany (Gerke et al., 1998). When a numerical model that coupled oxygen diffusion and sulfide-mineral oxidation, PYROX, was added to MINTRAN, it became MINTOX (Wunderly et al., 1996). MINTOX proved to be capable of simulating 35 years of contaminant transport at the Nickel Rim mine tailings impoundment (Bain et al., 2000). The more recent version is MIN3P (Mayer et al., 1999), which is a general reactive-transport code for variably saturated media. It has been applied to the Nickel Rim impoundment and to the contaminated groundwater downgradient of the Königstein uranium mine in Saxony, Germany (Bain et al., 2001). At Königstein, reactions involving iron, uranium, sulfate, cadmium, chromium, nickel, lead, and zinc were all modeled. A short review of similar codes and an update on those codes can be found in Mayer et al. (2003).

7.2.7.7 Harvie–Møller–Weare Code

With the arrival of the Pitzer method for calculating activity coefficients at high ionic strengths (≥ 1 m), research by Harvie and Weare (1980) led to computations of equilibrium mineral solubilities for brines. They could calculate solubility data from gypsum ($I < 0.06$ m) to bischofite saturation (>20 m). This capability made it possible to more accurately calculate the mineral sequences during seawater evaporation and quantitatively solve a problem that had puzzled van't Hoff (Harvie et al., 1980). The original model included the components Na, K, Mg, Ca, Cl, SO_4, and H_2O and was applied to the simpler salt systems and to mineral equilibria in seawater (Eugster et al., 1980). With further revision of the parameters, the model was expanded to include more complex electrolyte mixtures and their salts for seawater evaporation (Harvie et al., 1982). Later, the number of components was expanded to include H, OH, HCO_3, CO_3, and CO_2 (Harvie et al., 1984). Incorporating the temperature dependence to allow calculations from 25 to 250 °C was achieved by Møller (1988) and for lower temperatures (0–250 °C) by Greenberg and Møller (1989) and Spencer et al. (1990). Marion and Farren (1999) extended the model of Spencer et al. (1990) for more sulfate minerals during evaporation and freezing of seawater down to temperatures of −37 °C. Pressure dependence for aqueous solutes and minerals in the Na–Ca–Cl–SO_4–H_2O system to 200 °C and 1 kbar was obtained by Monnin (1990) and applied to deep Red Sea brines and sediment pore waters (Monnin and Ramboz, 1996). Møller et al. (1998) developed the TEQUIL code for geothermal brines. Ptacek and Blowes (2000) and Ptacek and Blowes (2003) have reviewed the status of the Pitzer method applications for sulfate mineral solubilities and demonstrated the applicability of a modified Harvie–Møller–Weare (HMW) to mineral solubilities in mine tailings piles. Numerous publications have expanded the Pitzer parameter database, such as Christov (2004), Tosca et al. (2007), and Marion et al. (2008) for Fe(II/III) species and Christov (2001, 2003) and Christov et al. (2007) for aluminum species. Christov and Møller (2004a,b) have expanded the range of temperature up to 250 °C and high concentration for acidic and basic alkali and calcium chloride and sulfate systems.

7.2.7.8 FREZCHEM Code

Version 1 of FREZCHEM (Marion and Grant, 1994) extended the Spencer–Møller–Weare model (Spencer et al., 1990) so that it could compute equilibria at subzero temperatures (currently to −70 and to −113 °C for some limited systems). Later versions added more components and species and improved the algorithm. Important additions include carbonate chemistry (Marion, 2001), strong acids (Marion, 2002), ferrous iron (Marion et al., 2003), ferrous and ferric iron (Marion et al., 2008), pressure dependence up to 1 kbar and calculation of density (Marion, 2007; Marion et al., 2005), gas hydrates (Marion et al., 2006), and aluminum–silicon chemistry in acid playa lakes (Marion et al., 2009). More recently, the temperature range has been extended upward to 100 °C and applied to hot spring chemistry (Marion et al., 2011). This extended code has been named CHEMCHAU (FREZCHEM Version 14.2). Two publications describe the code and its database and capabilities (Marion and Kargel, 2008; Marion et al., 2010), and a user-friendly online access offers modelers the opportunity of making computations (http://frezchem.dri.edu/Archive/Release_Notes_142.pdf; last accessed 15 April 2012).

7.2.7.9 Windermere Humic Aqueous Model Codes

Tipping (1994) proposed an alternative and practical model for humic acid–metal binding embodied in the speciation code Windermere Humic Aqueous Model (WHAM) that has two versions, one for water and one for soils (Tipping, 1998). This aqueous metal–organic model is based on the concept of electrostatic interactions at discrete sites. Hence, it is readily amenable to use with inorganic chemical speciation programs for aqueous solutions and includes ionic strength and temperature effects. Tipping et al. (2002) provide a thorough evaluation of humic substance binding with aluminum and iron in freshwaters. They demonstrate that 60–70% of the dissolved organic carbon (DOC) in their samples was humic substances involved in metal complexation: after accounting for organic complexation, the inorganic speciation is consistent with control of dissolved aluminum and iron concentration by their hydrous oxides. A full explanation of the developments that led up to the WHAM model and descriptions of many other models (multiple versus single discrete models, continuous models, competitive versus noncompetitive models, empirical models, site heterogeneity/polyelectrolyte models, and Gaussian distribution models) can be found in Tipping (2002). The WHAM model has been used for additional aluminum speciation studies (De Wit et al., 1999, 2001; Jansen et al., 2005; Lofts et al., 2001; Tipping and Carter, 2011), for mercury–humic interactions (Tipping, 2007), and most importantly, for comparisons with trace-metal speciation determined analytically (Guthrie et al., 2005; Jansen et al., 2003; Lofts and Tipping, 2011) and modeling trace-metal speciation in seawater (Stockdale et al. 2011). The latest WHAM code, version 7, which now includes rare earth elements (REE), silver, uncertainty calculations, and precipitation of iron and aluminum hydroxides, is available at http://www.ife.ac.uk/aquatic_processes/wham/WHAMtitlebar.htm (Tipping et al., 2011; last accessed 17 April 2012). The WHAM-F_{tox} code uses the WHAM code along with the assumption that cation binding to organic matter will be similar to cation binding onto macroinvertebrates to model toxicity (Stockdale et al., 2010). An example of a continuous distribution for binding sites can be found in the development of the Natural Organic Anion Equilibrium Model, or NOAEM (Gryzb, 1995), which also can be used in conjunction with ionic components and electrostatic theory.

7.2.7.10 Additional Codes

The coupled code developed by Steefel and Lasaga (1994) for multicomponent reactive transport with kinetics of precipitation and dissolution of minerals has been developed further into the OS3D/GIMRT code (Steefel and Yabusaki, 1996). This model has been applied to reaction fronts in fracture-dominated flow systems (Steefel and Lichtner, 1998). Further developments for nonuniform velocity fields by Yabusaki et al. (1998) required the use of massively parallel processing computers, although "... the accuracy of the numerical formulation coupling the nonlinear processes becomes difficult to verify." Steefel (2007) has continued to develop reactive-transport modeling with the CrunchFlow code and modeled biostimulation of a uranium-contaminated aquifer to reduce and precipitate uranium (Li et al., 2011) and to reduce sulfate (Druhan et al., 2012).

The code BIOKEMOD has been developed to simulate geochemical and microbiological reactions in batch aqueous solutions (Salvage and Yeh, 1998). It has been tested and found to simulate a range of processes that include complexation, adsorption, ion exchange, precipitation/dissolution, biomass growth, degradation of chemicals by metabolism of substrates, metabolism of nutrients, and redox. The code has been coupled to HYDROGEOCHEM (Yeh and Cheng, 1999; Yeh and Tripathi, 1989b) for simulation of reactive-transport modeling with biogeochemical transformation of pollutants in groundwaters. HYDROGEOCHEM simulates transient and steady-state density-dependent conditions with transient or steady-state distribution of reactive species for saturated or unsaturated media. Recent versions of HYDROGEOCHEM (1 and 2) can be obtained from Scientific Software Group (http://www.scisoftware.com/products/hydrogeochem_overview/hydrogeochem_overview.html; last accessed 1 June 2006).

The code FEREACT was developed for two-dimensional steady-state flow with equilibrium and kinetically controlled reactions (Tebes-Stevens et al., 1998). Another code, which was developed for biogeochemical transport and interactions of oxidative decay of organics with oxygen, iron, manganese, and sulfur redox species, has been introduced by Hunter et al. (1998).

Lichtner (2001) developed the computer code FLOTRAN, with coupled thermal–hydrologic–chemical (THC) processes in variably saturated, nonisothermal, porous media in one, two, or three spatial dimensions. Chemical reactions included in FLOTRAN consist of homogeneous gaseous reactions, mineral precipitation/dissolution, ion exchange, and adsorption. Kinetic rate laws and redox disequilibrium are allowed with this code. Debye–Hückel and Pitzer options are both available for computing activity coefficients, and thermodynamic data are based on the EQ3/6 database or user-defined databases. Several options are available in FLOTRAN for representing fractured media. The equivalent continuum model formulation represents fracture and matrix continua as an equivalent single continuum. Two distinct forms of dual continuum models also are available, defined in terms of connectivity of the matrix. These models are the dual continuum connected matrix and the dual continuum disconnected matrix options. A parallel version of the code, PFLOTRAN, has been developed based on the PETSC parallel library at Argonne National Laboratory.

Park and Ortoleva (2003) have developed WRIS.TEQ, a comprehensive reaction–transport–mechanical simulator that includes kinetic and thermodynamic properties with mass transport (advection and diffusion). A unique property of this code is a dynamic compositional and textural model specifically designed for sediment alteration during diagenesis.

The RATAP program was developed by Scharer et al. (1994) to predict acid generation in sulfide tailings piles. It includes sulfide-mineral oxidation kinetics, oxygen diffusion, temperature effects, and fluid transport. It was reviewed as part of the MEND program (Mine Environment Neutral Drainage) in a 1990 report. Another program that serves a similar purpose is SULFIDOX (Pantelis et al., 2002; Ritchie, 2003). The geochemistry module in SULFIDOX is based on PHREEQE, and the program has been developed from considerations of oxygen transport and temperature gradients developed within waste-rock piles.

Two other programs designed to simulate reactive transport include CHEMFRONTS (Bäverman et al., 1999) and RETRASO (Saaltink et al., 2004).

The CHESS code, originally developed for coupling to transport codes at the School of Mines in Paris (Van der Lee, 1998; Van der Lee and De Windt, 2001), computes a wide variety of useful processes including speciation, sorption, ion exchange, mass-transfer equilibria and kinetics, colloid formation, redox reactions, temperature dependence (0–300 °C), titrations, mixing, and with JCHESS, the ability to plot activity diagrams and Piper diagrams. Available for downloads on Windows, Mac OS, Linux, and Solaris systems and with the possibility of using PHREEQC, EQ3/6, MINTEQ, and NEA databases in addition to its own database; it can be accessed at http://chess.geosciences.ensmp.fr/ (last accessed 30 April 2012).

Further research on reactive-transport theory, modeling, and codes can be found in the *Reviews in Mineralogy* volume edited by Lichtner et al. (1996), the *Reviews* volume edited by Oelkers and Schott (2009), and the special issue of *Journal of Hydrology*, vol. 209 (1998).

7.2.8 Water–Rock Interactions

About a dozen or so major hydrogeochemical processes dominate the compositions of most surface and groundwaters. These processes include calcite dissolution and precipitation, gypsum dissolution and precipitation, pyrite oxidation and formation of hydrous ferric oxides, silicate mineral dissolution (feldspars, micas, chlorites, amphiboles, olivines, and pyroxenes) and clay mineral formation (kaolinitization, saprolitization, laterization, and illitization), dolomite dissolution and calcite precipitation (dedolomitization), dolomite formation (dolomitization), sulfate reduction and pyrite formation, silica precipitation, evaporation, and cation exchange. They are explained in several available textbooks (e.g., Appelo and Postma, 2005; Bethke, 2008; Drever, 1997a; Langmuir, 1997), and only a few examples are given here to demonstrate how complex geochemistry can be simulated with available codes. Aqueous speciation is discussed first, because it is required for more complex computations. For geochemical modeling, aqueous speciation usually occurs so quickly that it can safely be assumed to be at equilibrium. This assumption is valid for the vast majority of aqueous reactions but not for redox reactions and some reactions involving complex stoichiometry or organics. Because of the importance of redox reactions, a section follows on modeling aqueous redox kinetics and microbial growth kinetics. In this section, water–mineral reaction modeling includes calcite dissolution/precipitation, pyrite oxidation, pyrite oxidation in the presence of calcite both with and without oxygen, seawater–groundwater mixing, dedolomitization based on modeling of the Madison Limestone aquifer, and evaporation of seawater.

7.2.8.1 Aqueous Speciation

Some brief examples of aqueous speciation are given here to demonstrate the large decreases in free ion concentration or activity that occur as a result of ion-pair formation or complexation. Dissolved aqueous ions can have negative or positive charges, and ion-pair formation arises when two ions of opposite charge are attracted to each other and become bonded. Polyvalent ions have a greater tendency to associate with other ions of opposite charge, and among polyvalent cations that are found commonly in waters, iron and aluminum are prime examples. Alpers and Nordstrom (1999) tabulated analyses of four acid mine waters with pH in the range 4.9–0.48 and showed the effects of speciation for copper, sulfate, aluminum, and iron using the WATEQ4F code. Table 1 shows the total dissolved concentrations and the main species for aluminum and sulfate. Several conclusions are readily apparent. First, to approximate the free ion concentrations by the total dissolved concentrations is fair, as for sulfate in AMD-A (83%), to poor, as for aluminum in AMD-D (4.1%). Furthermore, for a wide range of total dissolved sulfate concentration, the $AlSO_4^+$ ion pair is always important (50–70% of the dissolved aluminum), but with increasing sulfate concentration and decreasing pH, the $Al(SO_4)_2^-$ ion triplet becomes increasingly important. This ion triplet has an association constant that is not well established, and some codes might not include it in their database.

Table 1 Example of aqueous aluminum and sulfate speciation for acid mine waters covering a range of pH and composition

Sample	*AMD-A*	*AMD-B*	*AMD-C*	*AMD-D*
Temperature (°C)	16.0	19.5	24.0	34.8
pH	4.9	3.25	1.10	0.48
Total dissolved Al (mg l^{-1})	5.06	19.8	1410	2210
% as Al^{3+}	29	26	10	4.1
% as $AlSO_4^+$	51	66	57	61
% as $Al(SO_4)_2^-$	2	4.5	32	32
Total dissolved SO_4 (mg l^{-1})	206	483	50 000	118 000
% as SO_4^{2-}	83	71	18	8
% as HSO_4^-	0	2	32	53
% as $AlSO_4^+$ and $Al(SO_4)_2^-$	4.5	11	12	8
% as Fe(II/III)–SO_4 ions	0	2	29	26

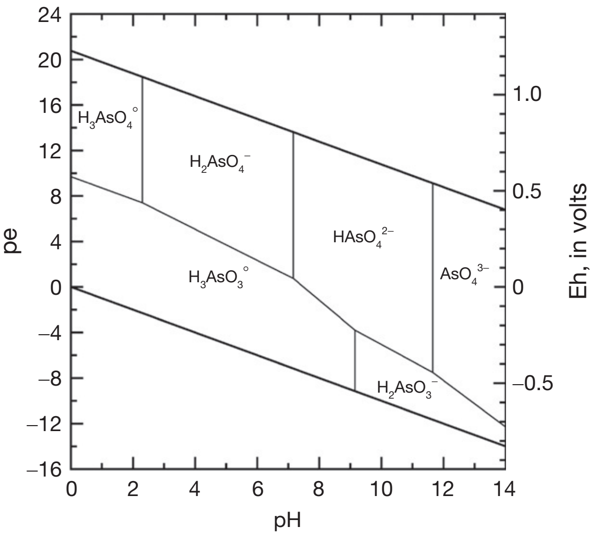

Figure 1 Species predominance diagram for dissolved arsenic at 25 °C and 1 bar. Reproduced from Nordstrom DK and Archer DG (2003) Arsenic thermodynamic data and environmental geochemistry. In: Welch AH and Stollenwerk KG (eds) *Arsenic in Ground Water*, pp. 1–25. Boston, MA: Kluwer.

Another example of aqueous speciation that includes redox can be shown with the arsenic pε–pH diagram shown in Figure 1. Arsenic can exist in several oxidation states, including As(−III) as in arsine gas (AsH_3), As(0) as in elemental arsenic, As(II) as in realgar (AsS), As(III) as in orpiment (As_2S_3) and dissolved arsenite, and As(V) as in dissolved arsenate. **Figure 1** shows the dominant dissolved species, arsenate and arsenite, and their hydrolysis products as a function of redox potential and pH based on the thermodynamic evaluation of Nordstrom and Archer (2003). These results show the dominance of hydrolysis for arsenate species, but it is of minor consequence for the arsenite species. Hydrolysis is of major importance in understanding mineral reactions, kinetics of reactions, and sorption behavior. At neutral to high pH, the adsorption of arsenate onto hydrous ferric oxides is weaker, and the high anionic charge on the dissolved arsenate developed through hydrolysis combined with negatively charged surfaces helps to account for this lack of adsorption. The lack of significant arsenite hydrolysis helps explain the more competitive adsorption of arsenate relative to arsenite.

7.2.8.2 Sorption Reactions

Although sorption modeling should be included in our discussion, this extensively researched area warrants an entirely separate chapter. Several books cover the subject well, including Dzombak and Morel (1990), Davis and Hayes (1986), Stumm (1987), Hochella and White (1990), a new volume from OECD/NEA (2012), and the chapters by Kulik (2009) and Sherman (2009).

7.2.8.3 Aqueous Redox Kinetics and Microbial Growth

Equilibrium thermodynamics describes the energetics of reactions and provides a quantitative answer to what reactions are possible. Kinetics describes the rates and mechanisms of reactions. Kinetics and thermodynamics are linked because the inherent energy driving a reaction will affect its rate. Also, it can be shown that when the forward rate of a reaction is equal to the reverse rate, then the ratio of the rates can be directly related to the equilibrium constant (Boudart, 1976; van't Hoff, 1898). Microbial kinetics complicates interpretations because of the numerous factors that affect microbial metabolism, such as temperature, nutrient concentrations, carbon source, redox conditions, and enzyme inhibitors. Interpreting environmental aqueous kinetics adds another layer of complexity because of additional factors such as discerning biotic from abiotic rates, microbial competition, symbiosis, predator-prey dynamics, and dynamic changes in water saturation.

The basic concepts of chemical kinetics are described extensively in a number of publications (e.g., Benson, 1960; Laidler, 1987; Langmuir, 1997; Morel and Hering, 1993; Nordstrom 1999; Stone and Morgan, 1990; Stumm and Morgan 1996) but will be discussed briefly here as an overview. The rate of reaction is defined as the time rate of formation of products or consumption of reactants. It is the differential change in the number of moles of reactant or product (proportional to the stoichiometric coefficient) with a differential change in time

$$r = \frac{\partial M_i}{v_i \partial t} = \frac{\partial n_i}{v_i \partial t} = \frac{\partial \xi}{\partial t} \qquad [18]$$

which we recognize as the differential change in the progress variable with time (eqn [6]), v_i is the stoichiometric coefficient of component or species i, n_i is the number of moles, and M_i is molar concentration. Equation [18] is written such that the rate is independent of which reactant or product species is chosen, and it is assumed to be at constant volume.

The rate law is the empirical equation that links the rate of reaction to the concentrations of species. For an elementary reaction (single reaction step),

$$a\mathrm{A} + b\mathrm{B} \rightarrow c\mathrm{C} \qquad [19]$$

where lowercase letters are the stoichiometric coefficients of the reaction, the reaction rate law can be written

$$r \equiv \frac{\partial M_\mathrm{C}}{c \partial t} \equiv -\frac{\partial M_\mathrm{A}}{a \partial t} \equiv -\frac{\partial M_\mathrm{B}}{b \partial t} \qquad [20]$$

Reaction rates are usually dependent on the concentrations of the reactants, and the general rate equation can be derived from the equilibrium constant expression (van't Hoff, 1898). Many (but not all) reaction rates take the general form

$$r = k M_\mathrm{A}^{\alpha} M_\mathrm{B}^{\beta} \cdots M_\mathrm{Z}^{\omega} \qquad [21]$$

where k is the empirically determined rate constant. For reaction [19], we have

$$r = k M_\mathrm{A}^{a} M_\mathrm{B}^{b} \qquad [22]$$

Rate constants only apply to elementary reactions; when several steps are involved, the composite proportionality constant is a rate coefficient (Laidler and Meiser, 1982). The order of the reaction with respect to a reactant is defined by the stoichiometric coefficient (e.g., the order of the reaction with respect to 'A' species is 'a'), and the overall reaction order is defined as the sum of exponents ($a+b$). Rates can be of a fractional order, depending on the stoichiometric coefficients. Rates are rarely more than second order. The rate constant often increases as temperature (T in Kelvin) increases, and the dependence of k on T can be expressed with the Arrhenius equation (Arrhenius, 1889):

$$k = A e^{-E/RT} \qquad [23]$$

where A is a constant, E is the energy of activation, and R is the gas constant. The rate can also be dependent on ionic strength such that increasing ionic strength usually increases reaction rates between anions and cations, usually decreases the rate between like-charged species, and has no effect when species are uncharged (Stone and Morgan, 1990).

When reactions exhibit reversibility (i.e., reactions near equilibrium), the forward and backward reactions must be incorporated through the mathematical relation between the equilibrium constant, K, and the forward and reverse rate constants (k_fd and k_bk, respectively):

$$K = \frac{k_\mathrm{fd}}{k_\mathrm{bk}} \qquad [24]$$

For a simple first-order reaction such as

$$\mathrm{A} \rightarrow \mathrm{B} \qquad [25]$$

the reaction rate can be written

$$\frac{\mathrm{d}M_\mathrm{A}}{\mathrm{d}t} = -k_\mathrm{fd} M_\mathrm{A} + k_\mathrm{bk} M_\mathrm{B} = -k_\mathrm{fd}\left(M_\mathrm{A} - \frac{1}{K} M_\mathrm{B}\right) \qquad [26]$$

Additional examples of reaction rates near equilibrium can be found in Atkins (1998).

An example of chemical kinetics applied to a common geochemical reaction is abiotic Fe^{2+} oxidation under acidic conditions ($2.2 < pH < 3.5$) (Langmuir, 1997; Morel and Hering, 1993 and references therein). Ferrous iron is oxidized to Fe(III) according to

$$Fe^{2+} + {}^{1}\!/_{4}O_2 + {}^{1}\!/_{2}H_2O \rightarrow FeOH^{2+} \qquad [27]$$

Assuming water is in excess and does not change enough to contribute to the rate, the rate law can be expressed as

$$\frac{dM_{Fe^{2+}}}{dt} = -kM_{(Fe^{2+})}P_{O_2} \qquad [28]$$

where $k = 10^{-3.2}\ bar^{-1}\ day^{-1}$ at 20 °C (Langmuir, 1997). Based on this rate, the half-life of Fe^{2+} is on the order of years. However, the actual rate of Fe(II) oxidation in the environment has been observed to be five to six orders of magnitude faster due to the presence of acidophilic iron-oxidizing microorganisms (Nordstrom, 1985, 2003; Singer and Stumm, 1970). Abiotic rates under circumneutral conditions are more complicated and may depend on total iron concentration and solution composition and speciation (e.g., Santana-Casiano et al., 2006).

As illustrated by this example, microorganisms can profoundly affect the geochemical conditions in numerous environments, from extremes of acidic conditions in acid rock drainage to highly contaminated aquifers. Many redox reactions are controlled by activity of microorganisms; where there is thermodynamically available energy for metabolism (chemical disequilibrium), there is often an organism that will catalyze the redox process. In some cases, these processes have been harnessed in engineered treatment or remediation. One example is the use of chemolithoautotrophs in heap bioleaching of metal ores, allowing more efficient extraction of metals than traditional chemical and mechanical separation procedures (Johnson, 2001). In both engineered and natural systems, it is often necessary or desirable to quantitatively understand the biogeochemical processes controlling important redox processes, generally accomplished through incorporation of microbial growth kinetics into a model.

Microbial growth kinetics constitute a particular set of mathematical expressions due to the nature of microbial metabolism and exponential growth (cell division). A simplified scheme of microbial growth follows a general pattern shown in **Figure 2**. The lag phase is often a physiological adaptation to conditions, requiring production or activation of important enzymes. Growth rate becomes nonzero during the acceleration and exponential growth phases, where cell division is occurring. Upon exhaustion of nutrients, accumulation of toxic by-products, or significant changes in geochemistry (e.g., pH), the cells are no longer able to grow, constituting the stationary phase, ultimately ending in cell death (Monod, 1949). During acceleration and growth phases, redox reactions are driven by substrate concentrations and enzyme activity.

Zero- or first-order kinetics are sometimes used to approximate microbially driven reactions, but chemical kinetics are applicable only under very specific circumstances, such as during the linear portion of exponential growth when the growth rate is constant. However, without confirmation of this assumption, chemical kinetics are limited in their applicability to geobiological systems. This problem was demonstrated in a study of a benzene-, toluene-, and xylene-contaminated aquifer in California, where geochemical reactive-transport modeling was being used to evaluate potential application of monitored natural attenuation (MNA, Bekins et al., 1998). Despite the common use of first-order expressions to describe field data, the ability of the first-order model to extrapolate was severely limited because it substantially underpredicted substrate consumption at longer times, which had implications for evaluating possible efficacy of MNA at the site.

Microbial kinetics have been successfully modeled in many environmental systems (e.g., Bekins et al., 1998) using the Monod expression. Monod kinetics is mathematically similar to Michaelis–Menten enzyme kinetics (Michaelis and Menten, 1913), because redox reactions are the bulk manifestation of one or more enzymatically driven processes. The general form for a process that involves a substrate (S) concentration and a terminal electron acceptor (TEA) concentration (A) is given as the dual Monod expression:

$$r = r_{\max}\left(\frac{S}{K_s + S}\right)\left(\frac{A}{K_A + A}\right) \qquad [29]$$

where r is the specific growth rate, $r_{\max}$ is the maximum growth rate, and K_s and K_A are the affinity constants (based on Monod 1949). The specific growth rate is further defined as

$$r = \frac{dX}{dt}X \qquad [30]$$

where X is the cell concentration in solution. Successful microbial rate laws need to explicitly account for abundance of microorganisms (Thullner et al., 2007) and reflect the behavior of the growth curve (**Figure 2**).

There are alternative approaches to the Monod expression that have been discussed in the literature. One method, called the partial equilibrium approach, assumes the rates are controlled by the available ΔG for the reaction (e.g., Curtis, 2003). This method has the advantage of directly incorporating thermodynamic considerations into the kinetics but has some limitations in capturing microbial community effects (e.g., competition for substrates) and during rapidly changing

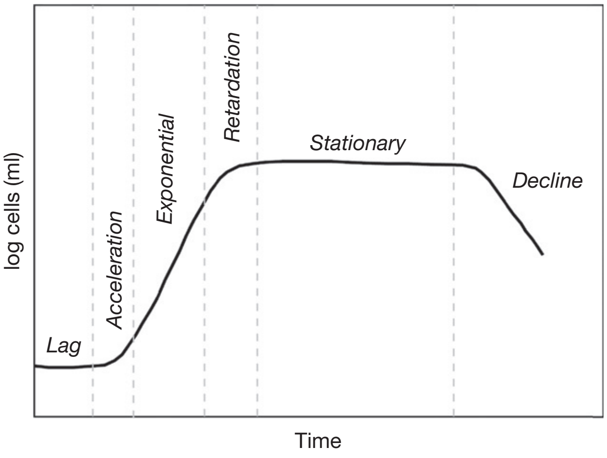

Figure 2 Phases of microbial growth, based on Monod (1949).

geochemical conditions (Thullner et al., 2007). Another method that has been used is the Pirt equation, which is based on defining a minimum maintenance energy that the cell needs to survive. A parameter is adjusted based on whether the conditions are energy-sufficient or energy-limited compared to the maintenance energy (Pirt, 1982).

The Monod expression has been modified in many ways to adjust to particular environmental, experimental, or biochemical considerations. Factors that affect the microbial kinetics include inhibition (metabolic by-products, changes in pH, and release of toxic trace elements), temperature, bioavailability of substrate or TEA, or changes in community dynamics with multiple species (predation and competition for substrates). One example of a modified Monod expression is Fe(II) oxidation coupled to O_2 by the acidophilic chemolithoautotroph *Acidithiobacillus ferrooxidans* at low pH (<3). Because this organism grows in acid rock drainage, the conditions are considered an open system with respect to oxygen, and the simplified Monod expression is

$$r = r_{\max}\left(\frac{S}{K_s + S}\right) \qquad [31]$$

where S is the Fe(II) concentration and K_s is the substrate affinity constant. Using this equation, the authors were able to model batch experiments of Fe(II) oxidation by a pure strain of *A. ferrooxidans* isolated from acid rock drainage using the simplified Monod expression (eqn [30]) in the geochemical code PHREEQC (**Figure 3**). In the experiments, bacteria were grown in a '9 K' medium (based on Silverman and Lundgren 1959; initial Fe(II) = 159 mM, initial pH = 2). Dissolved (<0.22 μm) Fe(II), Fe(T), and pH were monitored over the course of the experiment. The constants, $r_{\max}$ and K_s, were optimized using UCODE, a least squares fitting routine, coupled to PHREEQC (Campbell et al., 2011). The Monod expression successfully described the experimental Fe(II) concentration over the entire time course as shown in **Figure 3**.

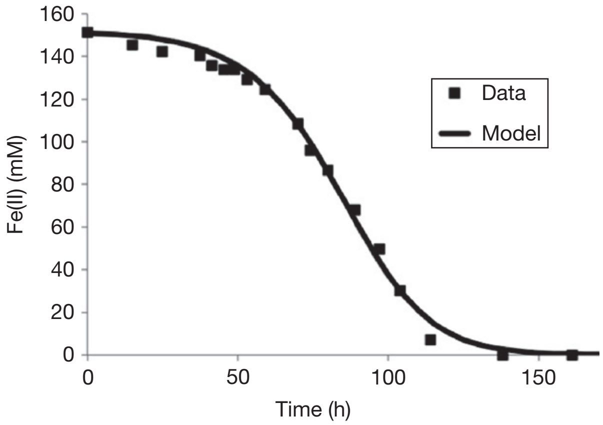

Figure 3 Experimental and PHREEQC model results for microbial Fe(II) oxidation. The code included a simple Monod expression for microbial kinetics.

In some batch conditions, the accumulation of Fe(III) slows the rate of Fe(II) oxidation, and a product inhibition term can be added:

$$r = r_{\max}\left(\frac{S}{K_s\left(1 + \frac{I}{K_p}\right) + S}\right) \qquad [32]$$

where I is the inhibitor concentration (in this example, Fe(III)) and K_p is the inhibition constant. Alternatively, a generalized microbial rate law that accounts for multiple enzyme reactions and multiple inhibiting reactions has been proposed (Thullner et al., 2007):

$$r = \kappa X\left(\prod_i \frac{c_i}{K_{m,i} + c_i}\right)\left(\prod_j \frac{I_j}{I_j + c_j}\right) \qquad [33]$$

in which κ is the reaction rate coefficient, X is the biomass concentration, $K_{m,i}$ is the Monod half-saturation constant, and the inhibition function is a separate Monod term where I_j is an inhibition constant for the jth inhibitor.

In a series of papers (referenced in Bethke, 2008), a three-term generalized rate expression for microbial respiration and fermentation that included a thermodynamic driving factor was formulated:

$$r = kXF_D F_A F_T \qquad [34]$$

in which k is the rate coefficient, X is the biomass concentration, F_D is the Monod function for electron donors, F_A is the Monod function for electron acceptors, and F_T is the thermodynamic potential factor, $(1 - Q/K)$, where Q is the ion-activity product and K is the equilibrium constant. There are other expressions for inhibitory effects and are described in detail in several reviews of microbial Fe(II) oxidation (Molchanov et al., 2007, Nemati et al., 1998, Ojumu et al., 2006). Our example demonstrates the versatility in the Monod expression for including feedbacks for various geochemical effects that may affect the rate of microbial redox processes and may be extended to include additional biogeochemical interactions. Incorporation of thermodynamic properties has been attempted as well, to include minimum requirements for ATP production and account for multiple microbial populations competing for substrate (e.g., Yabusaki et al., 2007). However, it is important to note that each additional factor included in the expression is accompanied by at least one empirical constant; there must be a balance between number of fitted parameters and model reliability and uniqueness (Thullner et al., 2007). Furthermore, we cannot know adequately all the dominant microorganisms in any given environment and their nutrient growth rates and their inhibitors as function of time and space. Hence, we must make crude assumptions, which can be tested by application of these equations. Whether or not these equations are still applicable to macroscale or regional field situations has yet to be determined.

7.2.8.4 Model Simulations of Mineral Reactions

7.2.8.4.1 Which minerals reach solubility equilibrium?

A great many mass transfer and redox reactions can be calculated with several available codes, but the user must decide whether or not it is reasonable to assume equilibrium. It usually takes a considerable amount of experience to develop the knowledge of which minerals typically reach equilibrium solubility and which ones should not. However, a few guidelines can help with this issue. If common minerals such as feldspars, quartz, calcite, gypsum, and halite are considered, their solubility and their dissolution rates differ substantially (Brantley and Olsen, Chapter 7.3). Well-crystallized quartz is quite insoluble and has one of the lowest dissolution rates (Lasaga, 1984). Feldspars dissolve more quickly but incongruently. Calcite dissolves more rapidly than feldspar and less rapidly than gypsum and halite, which are more soluble. Halite is the most soluble and dissolves the most quickly. Precipitation kinetics follows similar trends. Halite and gypsum precipitate more quickly than calcite, which precipitates more quickly than quartz or feldspar. Neglecting grain size effects on solubility and the effects of solution composition on precipitation rates, the reason for these differences has to do with chemical bonding within the lattice. The stronger and more covalent the bonds (quartz and feldspar), the less soluble is the compound and the more difficulty it would have reaching equilibrium solubility at ambient temperatures. The more ionic the bonding, the more affinity it would have for the polar molecules of water and the greater its solubility. Furthermore, if a mineral has a complex stoichiometry like a mica or amphibole, it is likely to be more difficult to precipitate from solution at ambient temperatures than a mineral having a simple stoichiometry like halite. Using these rough guidelines, the chart shown in Figure 4 divides up common minerals into those that are 'reactive' (the more ionically bonded minerals) and those that are 'nonreactive.' The quotation marks are there to emphasize that all minerals can be said to be reactive to some extent, but those that are so slow to react relative to the flow rate of the water dissolving them (under ambient temperature and pressure conditions) are nonreactive for most practical purposes. Then those that are 'reactive' can be further divided into those that are of simple or complex stoichiometry. Those minerals that occur in the 'reactive' group of simple stoichiometry are most likely to reach solubility equilibrium at or near ambient conditions.

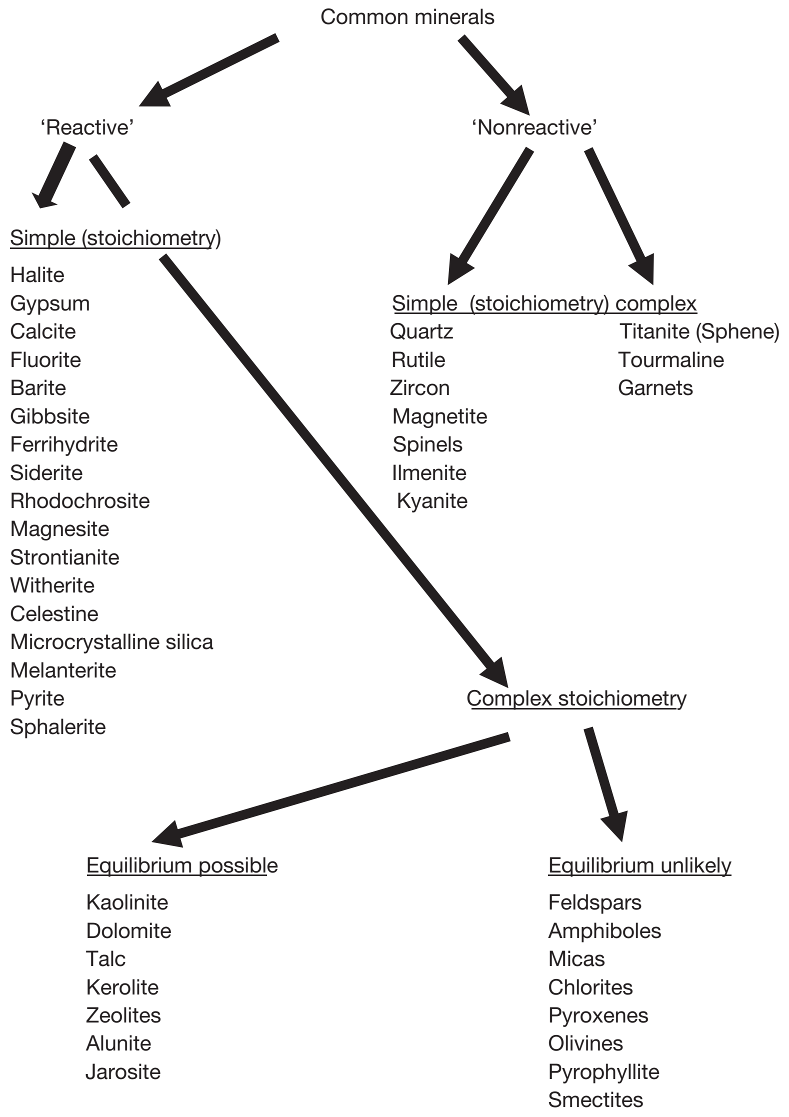

Figure 4 Classification of common minerals into 'reactive' and 'nonreactive' and those with simple or complex stoichiometry. Reproduced from Nordstrom DK (2009) Pitfalls and limitations of mineral equilibrium assumptions for geochemical modeling of water–rock interactions at mine sites. *8th Int. Conf. Acid Rock Drainage*, Skellefteå, Sweden, 23–26 June, pp. 362–372.

7.2.8.4.2 Calcite solubility

One of the most ubiquitous geochemical reactions is the dissolution and precipitation of calcite because of its common occurrence, relative stability, and abundant sources of dissolved inorganic carbon (DIC) and calcium. Furthermore, it is important for pH buffering of natural waters and in the CO_2 cycle (Butler, 1982, the definitive presentation of CO_2 equilibria and their applications). Dissolution of calcite in the environment can be the dominant source of dissolved calcium in many waters, but DIC can have at least two significant sources: calcite dissolution and CO_2 produced from organic decay. Calcite dissolution has been simulated using PHREEQCI for a range of carbon dioxide partial pressure, P_{CO_2}. **Figure 5(a)** is a plot of calcite dissolution in terms of calcium and DIC concentrations at P_{CO_2} values ranging from atmospheric ($10^{-3.5}$) to those typical of high-CO_2 groundwaters (10^{-1}). Computationally, increments of calcite were dissolved in water at fixed partial pressure until solubility equilibrium was reached. The solid line represents the equilibrium solubility of calcite for this range of carbon dioxide partial pressure, and the equilibrium pH values at each P_{CO_2} from 8.3 to 6.7 are shown in parentheses.

Many shallow groundwaters reflect calcite dissolution/precipitation as the dominant control on water quality. Groundwaters incorporate higher P_{CO_2} than that of the atmosphere because of carbon dioxide production in the soil zone from organic matter decomposition. A range of P_{CO_2} from 10^{-2} to 10^{-1} and pH values from 7 to 8 are common for most groundwaters. Groundwater analyses in a limestone terrain of Pennsylvania (Langmuir, 1971) are compared in **Figure 5(b)** to the predictions in **Figure 5(a)**. Although this plot simplifies the water chemistry and does not take into account dissolution of other minerals, it does show the dominant control by a relatively simple reaction. The P_{CO_2} values fall within the expected range, and calcite solubility equilibrium provides an upper boundary. The saturation index plot in **Figure 6** for the same samples takes into account temperature and ionic strength effects on the activities and also shows that saturation with respect to calcite is reached and provides an upper limit to calcium and DIC concentrations. As the pH increases, there is a greater proportion of carbonate ions relative to bicarbonate that increases the saturation with respect to calcite. At pH values below ~7, waters are nearly always undersaturated with respect to calcite (and most other carbonate minerals).

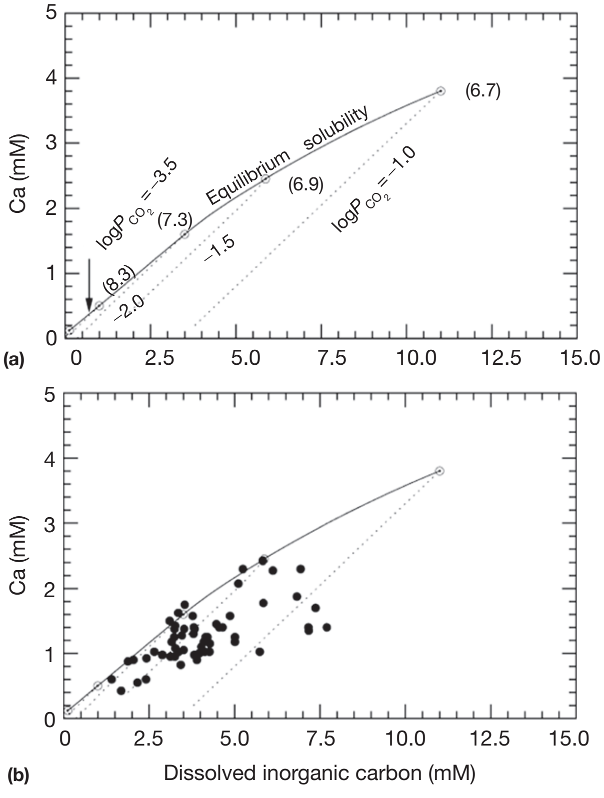

Figure 5 (a) Calcium and DIC concentrations plotted for calcite dissolution at $\log P_{CO_2} = -3.5, -2, -1.5$, and -1 (dotted lines) up to equilibrium calcite solubility (solid line). The pH values for each equilibrium solubility at the specified $\log P_{CO_2}$ are shown in parentheses. Plot was computed with PHREEQCI for 25 °C and 1 bar. (b) Calcium and DIC concentrations plotted from data of Langmuir (1971) for groundwaters taken from a limestone aquifer in Pennsylvania. Dotted and dashed lines are the same as those in (a).

7.2.8.4.3 Pyrite oxidation

Pyrite oxidation is a complex hydrobiogeochemical process that accounts for about 11% of the sulfate found in river drainages (Berner and Berner, 1996), although these estimates do not include large flows of AMD from Rio Tinto and Odiel Basins to the ocean (Nieto et al., 2007). Mining activities have increased the rate of pyrite oxidation and caused severe contamination of many waterways with acid and metals. When pyrite oxidizes, the sulfur rapidly converts to sulfate but the oxidation of the iron proceeds more slowly, depending on pH. Simulating the oxidation of pyrite is instructive in summarizing the chemistry of this complex process (Nordstrom, 2000, 2011). In **Figure 7**, PHREEQCI was used to simulate pyrite oxidation by adding increments of oxygen to pyrite in water. The reaction also could be simulated by adding increments of pyrite to an excess of oxygen. The results vary with the amount of oxidation allowed in the resultant solution and are represented in the figure by solution pH as a function of the amount of pyrite oxidized.

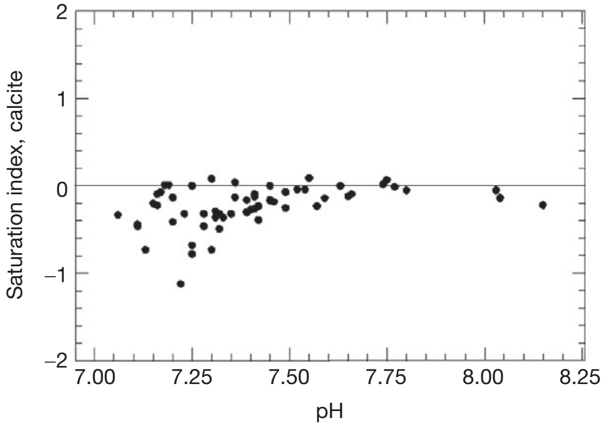

Figure 6 Saturation indices for calcite from the same groundwaters as in **Figure 5** plotted as a function of pH.

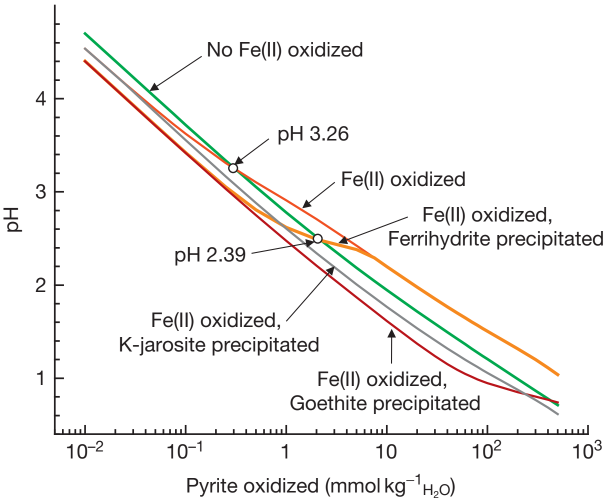

Figure 7 Change in pH as a function of the amount of pyrite oxidized under five scenarios: (i) Pyrite oxidizes to an acid ferrous sulfate solution without any further oxidation (solid green line); (ii) pyrite oxidizes, and the resultant ferrous sulfate solution is allowed to oxidize, but no precipitation is allowed (upper red line); (iii) pyrite oxidizes, the ferrous sulfate solution oxidizes and precipitates ferrihydrite (pK_{sp}=4.89, orange line); (iv) pyrite oxidizes, ferrous iron oxidizes, and jarosite precipitates (solid black line), and (v) pyrite oxidizes, ferrous iron oxidizes, and goethite precipitates (magenta line). Computed with PHREEQCI at 25 °C and 1 bar, thermodynamic data from Nordstrom et al. (1990).

First, pyrite oxidation to an acid ferrous sulfate solution only is shown by the green line labeled no Fe(II) oxidized in Figure 7 and the stoichiometric eqn [35]:

$$\mathrm{FeS}_{2(s)} + \frac{7}{2}\mathrm{O}_{2(g)} + \mathrm{H_2O}_{(l)} \rightarrow \mathrm{Fe}^{2+}_{(aq)} + 2\mathrm{SO}^{2-}_{4(aq)} + 2\mathrm{H}^{+}_{(aq)} \qquad [35]$$

Second, the same reaction is simulated, but the ferrous iron is allowed to oxidize without forming a precipitate, shown by the red line with a crossover pH of 3.26. Third, a precipitate, such as ferrihydrite, is allowed to form, which lowers the crossover pH to 2.39 as shown by the orange line. If the K_{sp} of the precipitating phase is lower, such as that for crystalline goethite, the crossover pH is much lower, as shown by the magenta line. However, crystalline goethite is not stable at pH values below about 2, and jarosite would precipitate instead. The reason for showing the goethite curve is to demonstrate the effect of lowering the K_{sp} for a precipitating phase of the same stoichiometry. The black line shows the pH evolution with jarosite as the precipitating phase (using the K_{sp} value from Baron and Palmer, 1996). The jarosite line is never seen to cross over because there are so many protons formed in the formation of jarosite that the proton consumption from aqueous iron oxidation is overwhelmed:

$$\begin{aligned} &3\mathrm{FeS_2} + \mathrm{K}^+ + \frac{15}{2}\mathrm{H_2O} + \frac{45}{4}\mathrm{O_2} \\ &\rightarrow \mathrm{KFe_3(SO_4)_2(OH)_6} + 9\mathrm{H}^+ + 4\mathrm{SO}_4^{2-} \end{aligned} \qquad [36]$$

All lines, except the jarosite line, cross over the original solid black line, because the oxidation of ferrous iron involves both proton-consuming and proton-producing reactions. The oxidation of Fe^{2+} to Fe^{3+} consumes protons:

$$\mathrm{Fe}^{2+} + \frac{1}{4}\mathrm{O_2} + \mathrm{H}^+ \rightarrow \mathrm{Fe}^{3+} + \frac{1}{2}\mathrm{H_2O} \qquad [37]$$

which happens at all pH values. The hydrolysis and precipitation of a ferric hydroxide phase produces protons:

$$\mathrm{Fe}^{3+} + \mathrm{H_2O} \rightarrow \mathrm{Fe(OH)}^{2+} + \mathrm{H}^+ \qquad [38]$$

$$\mathrm{Fe}^{3+} + 3\mathrm{H_2O} \rightarrow \mathrm{Fe(OH)}_{3(S)} + 3\mathrm{H}^+ \qquad [39]$$

which only happens if the pH has reached the point of hydrolysis, that is, near or above a pH = pK_1 = 2.2 for Fe^{3+} hydrolysis. Consequently, at lower pH values, there is no hydrolysis and the pH can only increase on oxidation. The crossover pH reflects the balance between the proton-consuming and the proton-producing reactions, a small buffering process represented by the small plateau in the curves. This diagram, although explaining some of the complexities of the chemistry of acid rock drainage, does not include the consequences of acid dissolution involving calcite and aluminosilicate minerals.

Nevertheless, some water analyses are available from mine sites that are predominantly affected by pyrite oxidation and little else. These samples, collected from the Leviathan Mine area, California, and Iron Mountain, California (Ball and Nordstrom, 1989; Nordstrom, 1977), include a pH measured *in situ* and a pH measured some weeks later after the ferrous iron had oxidized and precipitated. Figure 8 reproduces Figure 7 with only the two lines shown for pyrite oxidation, no ferrous iron oxidation (green line), and pyrite oxidation with precipitation of ferrihydrite (or the most soluble hydrous ferric oxide, as a orange line). Because there are low concentrations of cations in these samples, the initial pH values (open circles) can be assumed to be caused by pyrite oxidation. The final pH after oxidation and precipitation is shown by the closed circles. The final pH can be seen to closely approximate the dashed line in agreement with the simulation. In this comparison of a simulation with actual field data, two aspects are noteworthy. First is the good agreement, but since this simulation is sensitive to the chosen K_{sp} of the precipitating phase, the agreement indicates that the solubility product constant for freshly precipitating hydrous ferric oxide is a reasonable model choice.

Aqueous speciation related to Figure 7 is shown in Figure 9(a)–9(c) for the conditions of (a) no Fe(II) oxidation; (b) with Fe(II) oxidation, but no precipitation; and (c) with Fe(II)

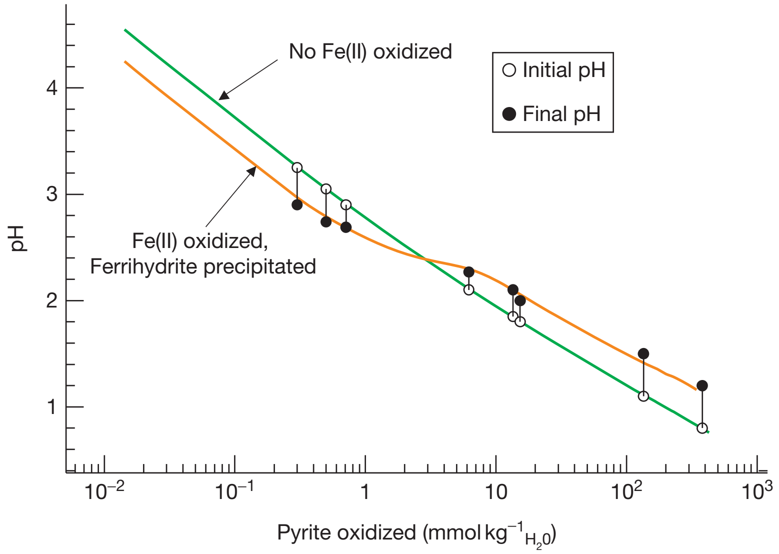

Figure 8 Change in pH as a function of the amount of pyrite oxidized under scenarios (i) and (iii) from **Figure 7**. Points are actual values measured from acid mine waters. Initial pH is based on field measurements taken on-site, and the amount of pyrite oxidized is derived from stoichiometry assuming that all dissolved sulfate is from pyrite oxidation. Final pH was measured after the sample had been allowed to oxidize for at least 2 weeks in an unfiltered, unpreserved bottle.

oxidation and jarosite precipitation. In contrast to Figures 7 and 8, Figure 9 was plotted as a linear axis for pyrite oxidized because of the merging of all the lines at low concentration. In Figure 9(a), HSO_4^- predominates over SO_4^{2-} because the pH is less than 2 (for H_2SO_4, pK_2 is 1.98) and the $FeHSO_4^+$ becomes increasingly predominant over any other Fe(II) species with increasing oxidation. With iron oxidation (Figure 9 (b)), HSO_4^- and $FeSO_4^+$ equally predominate, but this trend changes with jarosite precipitation (Figure 9(c)). The change in the total dissolved iron concentration is shown in Figure 9 (c), which allows one to estimate how much jarosite precipitated. Removal of dissolved iron by jarosite precipitation decreases the amount of all aqueous iron species so that the HSO_4^- species is still predominant.

7.2.8.4.4 Pyrite oxidation with calcite dissolution and neutralization

Calcite is often found with pyrite in mineralized areas. Limestone is also used to neutralize AMD. For these reasons, the next set of reactions worth modeling would be a mixture of pyrite and calcite, but decisions have to be made about the proportion of these minerals and what minerals should be allowed to precipitate as secondary phases. The simplest case would be under anoxic conditions so the Fe(II) does not oxidize, an excess of calcite, would allow precipitation of gypsum and siderite. This simulation is shown in Figure 10, with and without precipitation of secondary minerals and always under open system conditions. Although pH declines without formation of secondary minerals, it is primarily due to the relative proportions of calcite and pyrite that dissolve. In contrast allowing gypsum to precipitate has the effect of increasing the pH because for equilibrium to be maintained, greater amounts of calcite have to dissolve to replace the calcium removed by gypsum precipitation. With siderite and gypsum precipitation, the pH is buffered because no protons are formed or consumed in the equilibrium reaction:

$$
\begin{aligned}
&0.5FeS_2 + 1.75O_2 + CaCO_3 + 1.97H_2O \\
&\quad \rightarrow 0.985CaSO_4{\cdot}2H_2O + 0.5FeCO_3 + 0.015SO_4^{2-} \\
&\qquad + 0.5CO_2 + 0.015Ca^{2+}
\end{aligned}
\qquad [40]
$$

Furthermore, the onset of both gypsum and siderite precipitation occurs near the same conditions, after about 10 mmol $kg^{-1}_{H_2O}$ of pyrite has oxidized (or nearly 550 mg l^{-1} dissolved iron and 2000 mg l^{-1} dissolved sulfate). Under oxic conditions, a similar trend is observed with pH at about 7.72 with both gypsum and ferrihydrite precipitation.

Changing the proportions of calcite to pyrite is considered next (Figure 11(a)) for conditions where pyrite is oxidized to ferrous iron only and gypsum and siderite are allowed to precipitate when their solubility equilibria are reached. Figure 11(b) shows the same processes but with oxic conditions allowing gypsum and ferrihydrite to precipitate when their solubility equilibria are reached. When the mole ratio of calcite to pyrite is 0.5, there is negligible amelioration of the acid formed compared to the pH trend without any calcite present. Under anoxic conditions, the pH is buffered at about 5.7 when the mole ratio of calcite to pyrite is unity. Higher ratios bring the pH up above 7. These simulations indicate that the number of moles of calcite needed to neutralize the water should be twice that for pyrite assuming reactions reach equilibrium (i.e., no armoring effects of iron precipitates on the calcite to change its dissolution rate, calcite and pyrite dissolve at similar rates, and siderite and gypsum precipitate at similar rates). This reaction changes markedly with iron oxidation, as shown in Figure 11(b). Again for a calcite/pyrite mole ratio of 0.5, calcite dissolution has little effect until the highest amounts are dissolved and then some leveling off of the pH is seen. This plateau reflects a buffering effect. For a mole ratio of 1:1, the pH actually increases when more than 1 mmol $kg^{-1}_{H_2O}$ pyrite oxidized, which is caused by enough CO_2 being produced to begin buffering the solution. Between 1 and 500 mmol $kg^{-1}_{H_2O}$ pyrite oxidized, there is an order of magnitude increase in the HCO_3/H_2CO_3 ratio for the 1:1 mole ratio example.

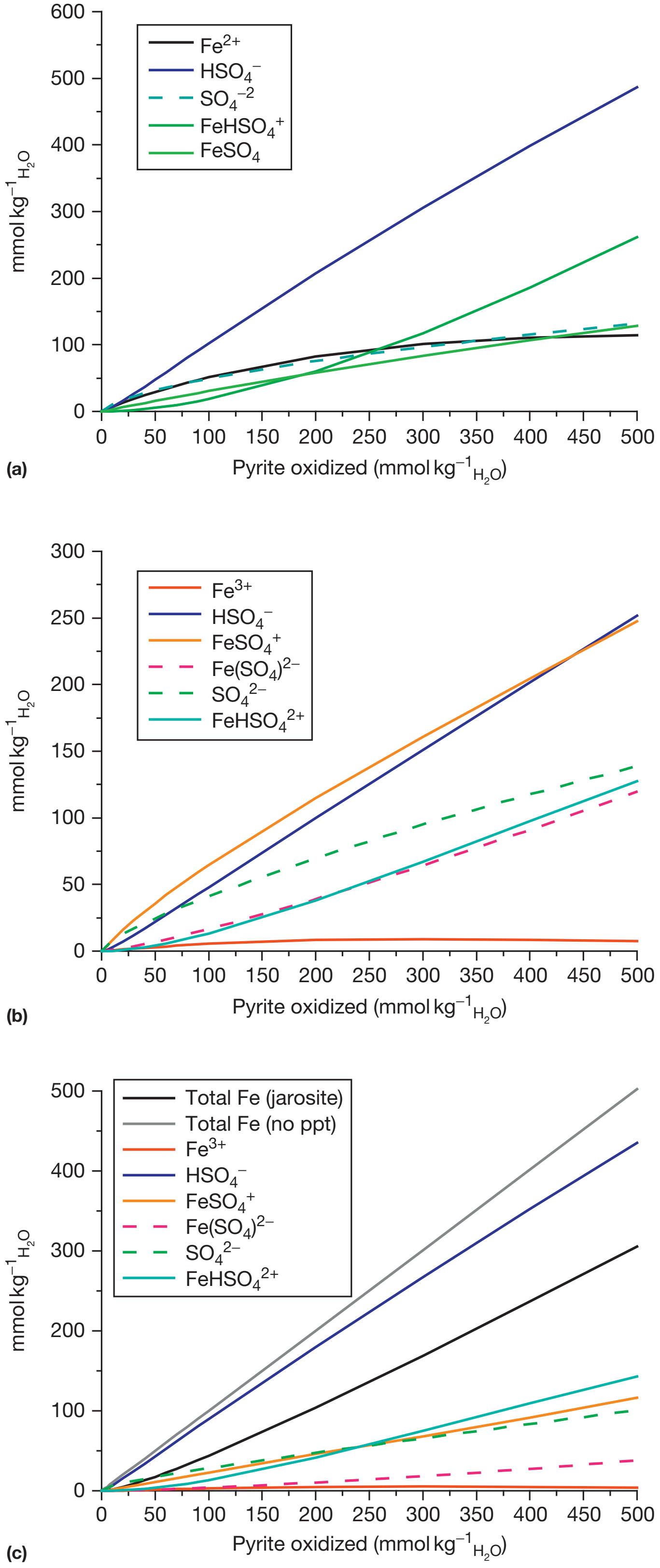

Figure 9 (a) Aqueous speciation for evolution of pyrite oxidation, for example, (i) in Figure 7. (b) Aqueous speciation for evolution of pyrite oxidation, for example, (ii) in Figure 7. (c) Aqueous speciation for evolution of pyrite oxidation, for example, (iv) in Figure 7.

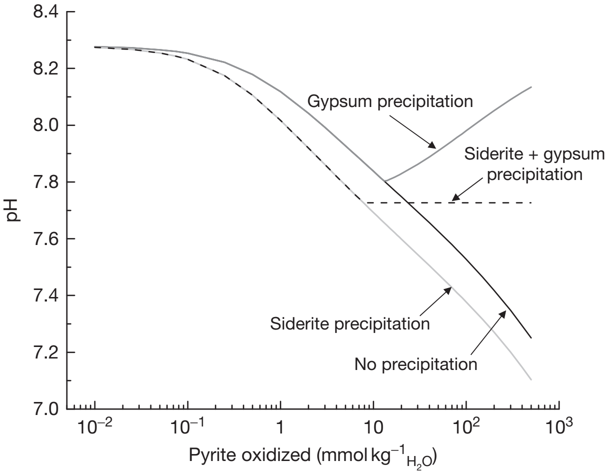

Figure 10 Change in pH as a function of pyrite oxidized in the presence of abundant calcite with lines showing the effects of (i) no secondary mineral precipitation, (ii) precipitation of gypsum only, (iii) precipitation of siderite only, and (iv) precipitation of gypsum and siderite.

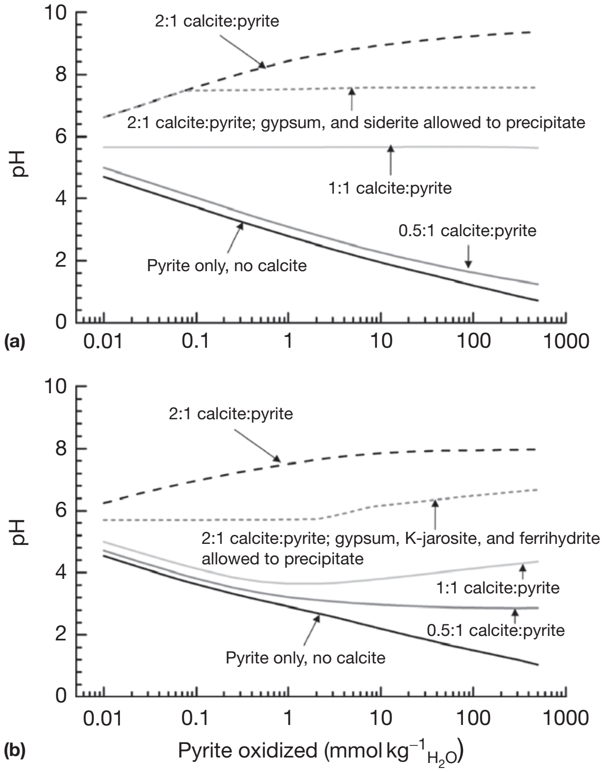

Figure 11 (a) Change in pH as a function of pyrite oxidized and relative to changing calcite/pyrite mole ratios from 0.5 to 2 with no oxidation of dissolved iron. At least a 1:1 mole ratio is required to buffer the pH near neutrality, but, if secondary phases (gypsum and siderite) are allowed to precipitate, a higher ratio of about 2 is required. (b) Change in pH as a function of pyrite oxidized and relative to changing calcite/pyrite mole ratios from 0.5 to 2 with oxidation of dissolved iron. This plot would indicate that mole ratios higher than 2 are needed to adequately neutralize the acidity from pyrite oxidation.

7.2.8.4.5 Seawater–groundwater mixing

Waters not only undergo geochemical reactions, they commonly mix. Seawater intrusion into coastal aquifers is a classic example. Mixing is often enhanced by groundwater withdrawals. When seawater and fresh groundwater mix, and both endmember waters are at saturation with respect to calcite, the resulting mixture will often be undersaturated with respect to calcite and calcite will dissolve if present. The possibility of this scenario and other water mixing effects including mineral precipitation from mixing of waters initially undersaturated was discussed by Runnells (1969). Computations made by Plummer (1975) showed the proportion of mixing over which the undersaturation effect, and consequent dissolution of coastal limestone, was operative. **Figure 12(a)–12(d)** is the example from Plummer (1975) and demonstrates that for a large range of seawater in the mixture, calcite undersaturation can occur, depending on carbon dioxide partial pressure and temperature. These calculations were done over a range of temperatures (5–35 °C), P_{CO_2} (10^{-4} to 1 atm), and pH values. They also were conducted with actual carbonate groundwater compositions and coastal seawater for several locations along the Florida coast.

7.2.8.4.6 Madison regional limestone aquifer

The next example in this set is from the Madison regional aquifer study by Plummer et al. (1990). The Madison Limestone aquifer occurs in Wyoming, Montana, and South Dakota. Plummer et al. (1990) utilized a combination of saturation index constraints, inverse modeling, and carbon and sulfur isotopes to delineate geochemical reaction models for the flow paths. The models indicated that the major reaction is dedolomitization, that is, dolomite dissolution and calcite precipitation driven by anhydrite dissolution, sulfate reduction, and $[Ca^{2+}+Mg^{2+}]/Na^{+}$ cation exchange, with some local halite dissolution.

Dedolomitization is the dissolution of a dolomite driven by gypsum/anhydrite dissolution to form calcite- and a magnesium sulfate-rich groundwater:

$$\mathrm{CaMg(CO_3)_2 + CaSO_4 \rightarrow CaCO_3 + Mg^{2+}_{(aq)} + SO^{2-}_{4(aq)}} \qquad [41]$$

Sulfur isotopes were treated as an isotope dilution problem, and carbon isotopes were treated as Rayleigh distillations (**Chapter 7.9**). Corroboration of the isotopic modeling was achieved by predicting the isotopic compositions of the dolomite and the anhydrite. Actual $\delta^{34}S$ values for anhydrite fit the values assumed in the model calculations. Further consistency was found when the adjusted ^{14}C ages combined with Darcy's law resulted in groundwater flow velocities that agreed within a factor of 5 of those calculated by a digital flow model. **Figure 13** portrays the saturation indices of calcite, dolomite, and gypsum (surrogate for anhydrite) for waters from the Madison aquifer. Calcite reaches saturation quickly and tends to be supersaturated. This supersaturation may reflect the pressure effect on the ion activities and the solubility product constant (pressure corrections were not modeled); it may be caused by pH changes on pumping pressurized water to the surface, it may result from calcite that has some substituted elements displacing the SI values, it may be caused by an inhibition on calcite precipitation kinetics by magnesium, or it may be caused by gypsum dissolving faster than calcite can precipitate.

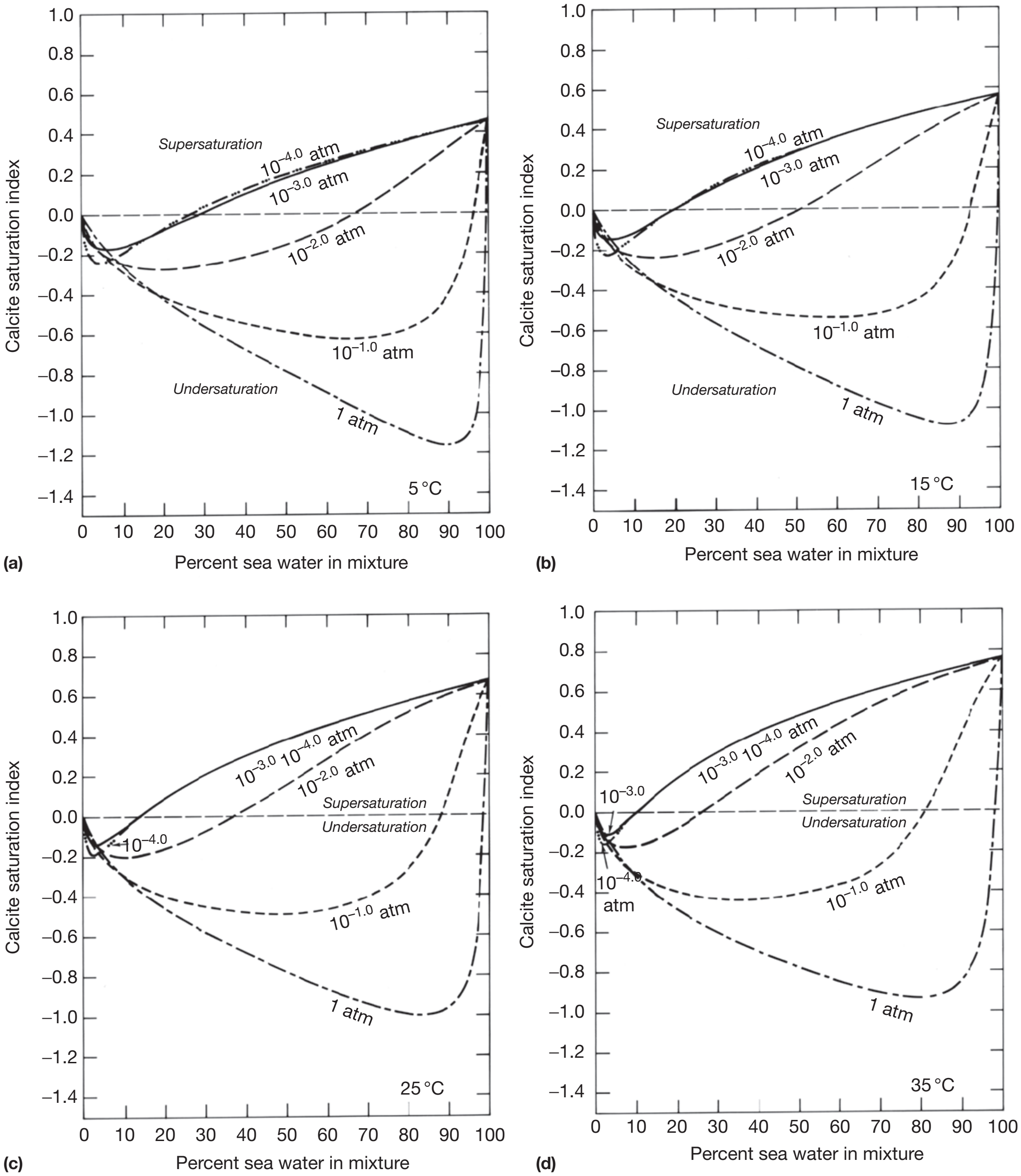

Figure 12 Calcite saturation indices plotted as a function of percent seawater mixing with a carbonate aquifer water with contours representing different levels of P_{CO_2}. Reproduced from Plummer LN (1975) Mixing of sea water with calcium carbonate ground water. *Geological Society of America Memoir* 142: 219–236.

A subset of the mass-balance results for the Madison aquifer study is shown in Table 2 covering the range of parameters encountered from recharge to discharge, although these selected samples are not along the same flow path. The general trend in chemistry is indicated here. Samples near recharge are low in sulfate, and the amount of mass transfer is low. As the water moves downgradient and evolves chemically, it increases in sulfate from anhydrite dissolution. Increased anhydrite dissolution leads to increased dissolution of dolomite and increased calcite precipitation. With increasing age, there is more organic matter (represented by CH_2O in Table 2) available for decomposition, which results in greater amounts of hydrous ferric oxides dissolving (reduction) and pyrite being formed. Cation exchange in Table 2 refers to (Ca + Mg)/Na, that is, exchange of calcium and magnesium for sodium. The measured sulfur isotopic compositions of the H_2S and of the anhydrite match nicely with the model simulation and the stable carbon isotopes.

The basic reaction shown by eqn [41] was modeled using the PHREEQC code, and major ions could be reproduced rather well after accounting for changing P_{CO_2} conditions caused by breakdown of organic matter to CO_2 and

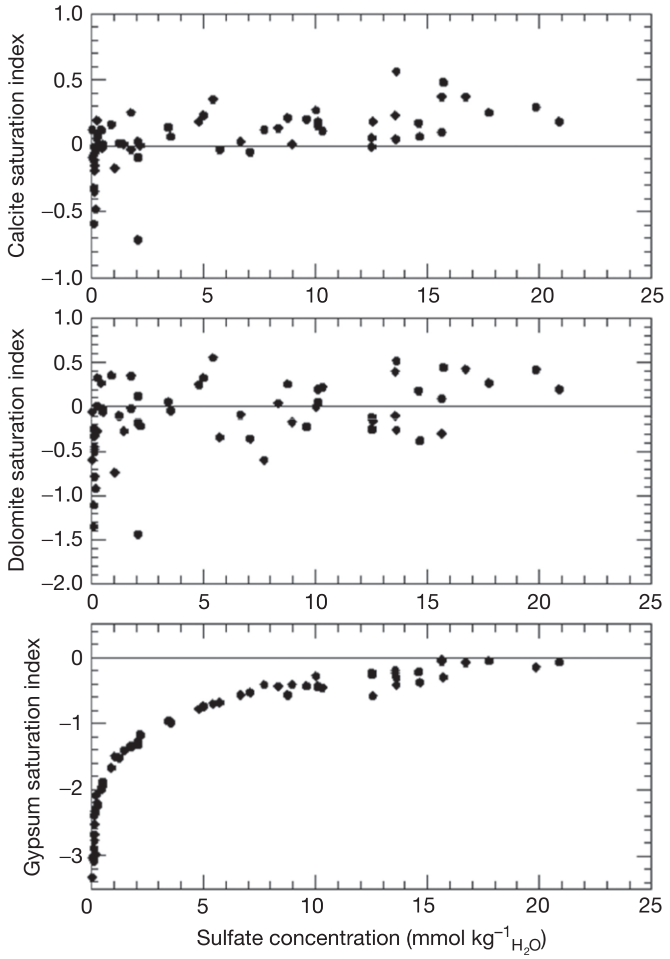

Figure 13 Saturation indices for calcite, dolomite, and gypsum for groundwaters from the Madison Limestone aquifer. Reproduced from Plummer LN, Busby JF, Lee RW, and Hanshaw BB (1990) Geochemical modeling of the Madison aquifer in parts of Montana, Wyoming, and South Dakota. *Water Resources Research* 26: 1981–2014.

Table 2 Selected mass transfer results from Plummer et al. (1990) for the Madison Limestone aquifer, units in millimoles per kilogram water

Well no.	*F6–19*	*F6–17*	*F6–13*	*F7–10*	*F8–25*	*F8–21*	*F3–20*
SO_4	0.18	0.52	2.19	5.73	8.97	13.56	19.86
Dolomite	0.14	0.14	0.60	0.74	1.87	2.90	3.54
Calcite	−0.18	−0.41	−1.62	−2.64	−4.70	−7.15	−5.33
Anhydrite	0.15	0.51	2.27	5.93	9.19	13.56	20.15
CH_2O	0.01	0.02	0.20	0.44	0.71	0.30	0.87
FeOOH	0.00	0.01	0.05	0.12	0.21	0.11	0.09
Pyrite	−0.00	−0.01	−0.05	−0.12	−0.19	−0.06	−0.09
Ion exch.	0.01	0.03	0.04	0.44	0.19	0.14	8.28
NaCl	−0.01	−0.02	0.03	2.83	1.38	0.97	15.31
KCl	0.01	0.02	0.02	0.27	0.28	0.33	2.52
CO_2	−0.07	0.17	−0.21	−0.42	−1.18	−0.40	−0.04
$\delta^{13}C$ (‰) calculated	−8.86	−9.33	−7.79	−9.67	−5.52	−3.59	−2.21
$\Delta^{13}C$ (‰) measured	−7.82	−10.0	−6.80	−9.70	−5.50	−3.50	−2.34
Apparent age (year)	Modern	Modern	Modern	2386	14 461	13 310	22 588

Positive values signify dissolution, negative values precipitation. Samples, although not along the same flow path, are in the general direction of recharge to discharge from left to right.

low-molecular-weight compounds, primarily methane. The range of P_{CO_2} values calculated by Plummer et al. (1990) is shown in **Figure 14(a)**, ranging from slightly less than 10^{-2} to more than 0.1 atm. Calcite saturation indices tend to be supersaturated, so the range for calcite SI values is shown for the range of 0.0–0.5 (**Figure 14(b)**). The range of Ca concentrations relative to sulfate concentrations is shown in **Figure 14 (c)** with the lines representing the modeled values and the data points are the measured values. Lines representing the range in $SI_{calcite}$ for temperatures from 25 to 90 °C had to be shown because of the wide range in groundwater temperatures. These results show that a few simple stoichiometric reactions can account for the major geochemical processes in this regional aquifer.

Mazor et al. (1993) pointed out that some of the samples from the Madison aquifer had high tritium contents when the ^{14}C results indicated dates too old for tritium and suggested that significant mixing of younger and older waters may have occurred. Mixing and dilution trends can have similar chemical appearances to hydrochemical evolution, and caution must be used to distinguish evolutionary trends from mixing trends by age-dating techniques (Bethke and Johnson, 2007; Coplen, 1993; Plummer et al., 1993; Purtschert, 2008).

7.2.8.5 Reactive-Transport Modeling in Streams

Although biologic reactions, mostly dissolved oxygen degradation or nutrient uptake, have been modeled in flowing streams and rivers for a long time, trace-metal reactions have not been modeled until more recently. Bencala (1983) considered solute transport in pool-and-riffle streams using a kinetic term for sorption; Bencala and Walters (1983) introduced transient storage into their modeling of trace-metal transport. One of the most obvious inputs of trace metals to surface waters is from mining and mineral-processing wastes. Techniques for modeling these acid mine water reactions continued to develop during the 1990s from empirical rate constants and partition coefficients to mechanistic sorption models such as surface complexation and equilibrium precipitation of mineral phases (Brown and Hosseinipour, 1991; Kimball et al., 1994, 1995; Runkel et al., 1996a,b, 1999). Reaction–transport models such as these require more accurate stream discharge measurements than can be obtained from current-meter measurements. These are obtained from constant-flow tracer-injection studies along with synoptic sampling, including all possible inflows, so that the transport model can be reliably calibrated. Not only has this approach been used to define sources and sinks of trace metals in mountainous streams but it also has been helpful in predicting remediation scenarios for mine sites (Kimball and Runkel, 2009, 2010; Runkel and Kimball, 2002).

An example of modeling reactive transport of acid mine waters using the OTEQ code is shown in **Figure 15** (Ball et al., 2004) for the drainage released from the Summitville mine in the San Juan Mountains of southwestern Colorado into the Alamosa River. The model was calibrated with tracer-injection and synoptic sampling techniques, including measurements of Fe(II/III), that helped constrain precipitation of

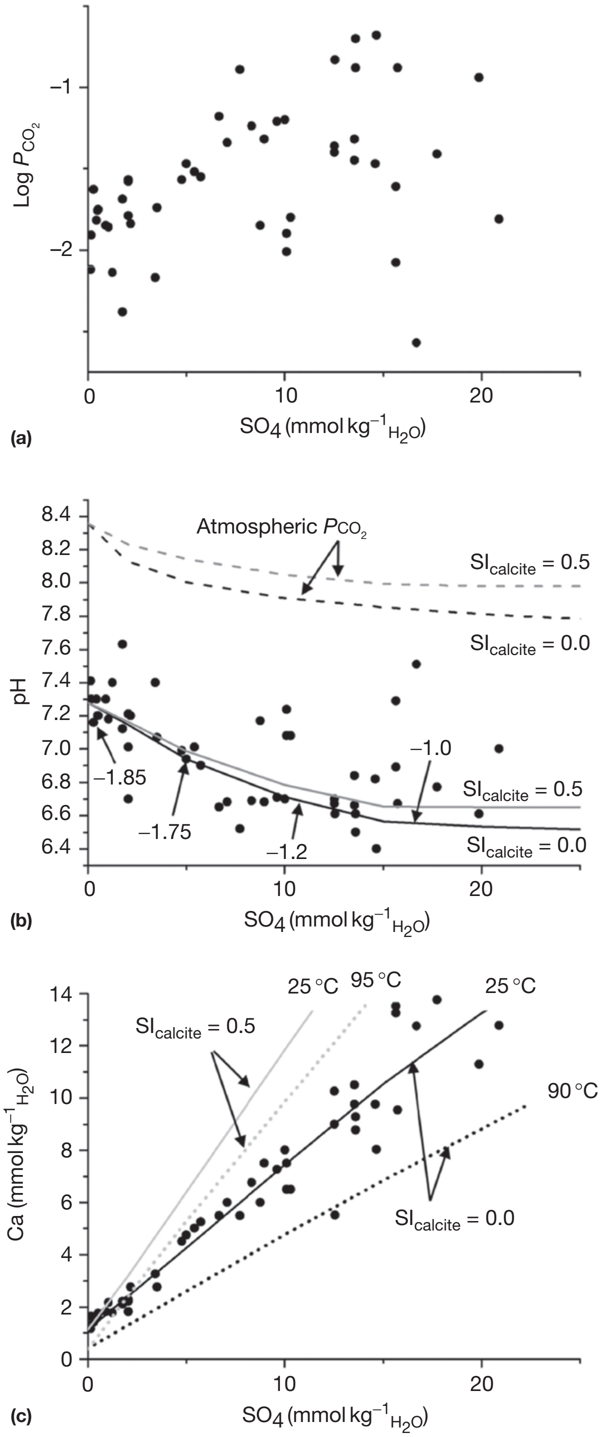

Figure 14 (a) Values of $\log P_{CO_2}$ for Madison Limestone aquifer groundwaters relative to SO_4 concentrations. (Plummer LN, Busby JF, Lee RW, and Hanshaw BB (1990) Geochemical modeling of the Madison aquifer in parts of Montana, Wyoming, and South Dakota. *Water Resources Research* 26: 1981–2014.) (b) The pH values relative to SO_4 concentrations using PHREEQC to simulate dedolomitization and changing the $\log P_{CO_2}$ in accordance with those shown in (a). (c) Change in Ca concentrations relative to SO_4 concentrations.

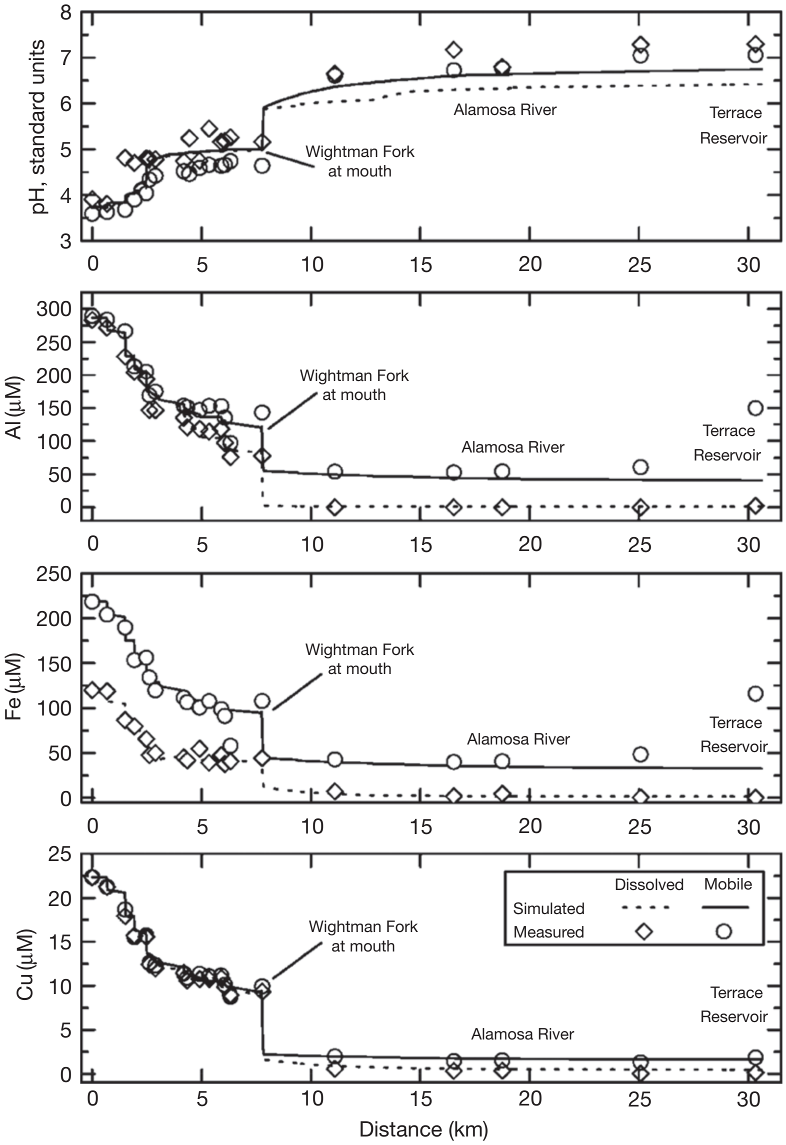

Figure 15 Downstream profiles in the Wightman Fork/Alamosa River system of (a) pH measured and simulated, (b) dissolved aluminum concentrations measured and simulated, (c) dissolved iron concentrations measured and simulated, and (d) copper concentrations measured and simulated. Simulations were obtained with the OTEQ code after calibration on tracer-injection data and Fe(II/III) determinations. Reproduced from Ball JW, Runkel RL, and Nordstrom DK (2004) Evaluating remedial alternatives for the Alamosa River and Wightman Fork, Summitville, Colorado: Application of a reactive-transport model to low- and high-flow synoptic studies. In: Zanetti P (ed.) *The EnviroComp Institute II*, *Environmental Sciences and Environmental Computing*, vol. 2, pp. 1–54 (online publication).

hydrous ferric oxides in the model. Sodium chloride was used as the tracer. Figure 15(a) shows measured pH and simulated pH with reaction. The main in-stream reactive chemistry in this system is the oxidation of iron, the precipitation of hydrous ferric oxides, the precipitation of hydrous aluminum oxides, the adsorption of trace metals, and pH changes (controlled by the oxidation, hydrolysis, and precipitation reactions and by the neutralization of inflows). Simulated and measured dissolved and total aluminum and iron concentrations are shown in Figure 15(b) and 15(c), respectively. Iron and aluminum concentrations decrease rapidly because of precipitation during downstream transport. Figure 15(d) shows the copper concentrations; when adsorption is invoked in the model, the agreement between measured and simulated copper concentrations is within analytical error.

Two papers should be mentioned in the context of reactive-transport modeling in streams. A state-of-the-science workshop of metal's fate and transport in surface waters was summarized by Caruso et al. (2008). This paper is particularly noteworthy because of the overview that includes toxicity modeling, stream modeling, watershed modeling, mercury modeling, site characterization, model limitations and reliability, database needs, and future recommendations for improvements. The need for better testing and evaluation of models and codes was emphasized (especially postauditing); the rate of model and code development outpacing supportive data collection was mentioned, and use of the term 'model validation' was discouraged and 'model evaluation' was felt more appropriate. The other paper (Nordstrom, 2011) reviews many of the results from USGS studies on hydrogeochemical processes affecting metal transport in surface waters from mine wastes and mineralized rock. The importance of geologic, hydrologic, and chemical factors, especially first flush effects, diel variations, iron photoreduction, and reactive-transport modeling, is described.

7.2.8.6 Reactive-Transport Modeling in Groundwater

Much has been published about reactive-transport modeling in groundwaters, and examples have been covered previously (Chapelle, 2003; see **Chapter 7.11**). Recent papers and reviews should also be consulted in this rapidly expanding field (Appelo and Postma, 2005; Bear and Chang, 2009; Bethke, 2008; Brown et al., 2000; Glynn and Brown, 2012; Merkel and Planer-Friedrich, 2008; Postma et al. (2008); Saaltink et al., 2012; Steefel and Maher, 2009; Steefel et al., 2005; Zhu and Anderson, 2002). Special mention should be made of the Glynn and Brown (2012) study because of the detailed evaluation of groundwater geochemical modeling philosophy, including a 15-year perspective on the Pinal Creek study site. An abridged and paraphrased version of their lessons learned is worth repeating here:

1. Constructing, analyzing, and interpreting numerical models, regardless of type, force the modeler to reexamine and revise their conceptual model and perceptions.
2. No model is ever final. Frequent iteration is needed among field observation, field experiments, laboratory experiments, and the periodic assembly and interpretation of the available information through numerical modeling.
3. The combination of inverse modeling and forward or 'predictive' modeling is particularly powerful in helping assess available information. Inverse modeling forces the modeler to constrain the interpretation with basic principles, such as conservation of mass and energy, and with relevant field data and known material properties. Forward modeling allows the modeler to test the model by extrapolating forward in space in time and to do sensitivity analyses that originate with the results from inverse modeling. More importantly, the geochemical modeling at the Pinal Creek site helped identify which reactions and processes were *unreasonable*.
4. The studies conducted at the Pinal Creek site illustrate the fact that nature always keeps surprises in reserve for its observers and interpreters. Humility and frequent testing of assumptions are needed in modeling nature's systems.
5. Given our often limited knowledge of natural systems, it behooves us to model these systems by considering *general* system behavior before interpreting, matching, and predicting *specific* system behavior.
6. Finally, the Pinal Creek project taught us the value of spatial and temporal observations. Systems that have a complex suite of active processes and that exhibit dynamic changes in observed properties require extensive (and often costly) adaptive monitoring programs that have sufficient resolution in both time and space.

7.2.8.7 Geochemical Modeling of Catchments

Attempts to model chemical weathering of catchments have used a variety of approaches and were originally designed to understand acidification processes from the influence of acid rain. The BIRKENES code (Christophersen et al., 1982) was one of the first developed to model catchment stream chemistry. It used cation–anion charge balance, a gibbsite equilibrium solubility control for aluminum concentrations, a Gapon ion exchange for metals sorption, and rates for sulfate adsorption/desorption in a two-reservoir model. The model was calibrated by input and output mass fluxes for the Birkenes catchment in Norway to provide the water and solute flux information and to fit empirical parameters.

The ILWAS code (Integrated Lake-Watershed Acidification Study; Chen et al., 1983; Gherini et al., 1985) also contains a semiempirical model but is much more detailed than the BIRKENES code with respect to its hydrologic and geochemical compartments. Alkalinity was one of the key chemical components in the model. Because the code was originally calibrated on three watersheds receiving acid rain in upstate New York, it was programmed with mineral rate dissolution data, gibbsite solubility equilibrium, and other parameters pertinent to those environments. The considerable quantity of detailed data needed to calibrate the ILWAS code limits its general usefulness.

The MAGIC code (Model of Acidification of Groundwater In Catchments; Cosby et al., 1985a,b) is similar in many respects to the BIRKENES code, but parameters for soil-water and stream-water chemistry are 'lumped' or averaged over the spatial scale that can include many heterogeneities. MAGIC was designed to simulate long-term (annual) averages, whereas BIRKENES was designed to simulate short-term (hours to days) responses. Equilibrium reactions include soil cation-exchange reactions, solubility control by gibbsite, CO_2–H_2O hydrolysis reactions, aqueous speciation of aluminum among sulfate and fluoride complexes, water dissociation, ion balance, and temperature dependence. Activity coefficients appear not to have been used, and the sensitivity of the model to this factor has not been addressed. Wright and Cosby (1987) found good agreement between simulated and measured alkalinities for two manipulated catchments in Norway using the MAGIC code. Organic acids have been included with the code and the simulations of the Norway catchments revisited with improved results (Cosby et al., 1995). An alternative to ILWAS and MAGIC is the code Enhanced Trickle Down (ETD; Nikolaidis et al., 1989, 1991). Geochemical processes include cation exchange, chemical weathering, sulfate adsorption, and sulfate reduction. Comparisons of the three codes, ILWAS, MAGIC, and ETD, were made by Rose et al. (1991a,b). The codes were found to provide similar forecasts on a relative scale but substantial differences with respect to specific concentrations (absolute scale). Codes that contain more detailed consideration of chemistry, especially reaction kinetics, include PROFILE (Sverdrup, 1990; Warfvinge and Sverdrup, 1992) and UNSATCHEM (for the unsaturated zone, Suarez and Simunek (1996)).

An important advance in quantifying weathering rates in catchments was made by Burns et al. (2003) by combining mass-balance considerations with determinations of groundwater residence times. The results showed that plagioclase

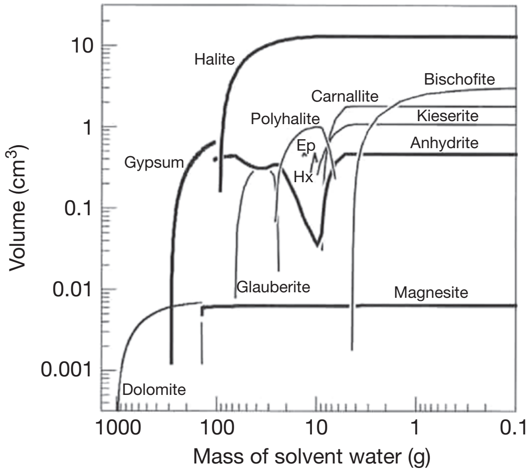

Figure 16 Volumes of minerals precipitated during the equilibrium simulation of seawater evaporation at 25 °C. From Bethke CM (2008) *Geochemical and Biogeochemical Reaction Modeling*, 2nd edn., p. 543. New York: Cambridge University Press. Copyright © 2008. Reprinted with the permission of Cambridge University Press.

weathering was three to four orders of magnitude slower than laboratory rates but very close to the rate calculated by White et al. (2001) based on solid-phase mineralogy and composition.

The main problem with any of these models is that they are often calibrated with data that are too short-term for the long-term processes they are trying to predict on the catchment scale (Drever, 1997b; Hornberger, 2002). And when careful studies of mineralogical changes are obtained, the results integrate information over a long timescale and do not give direct data on water chemistry.

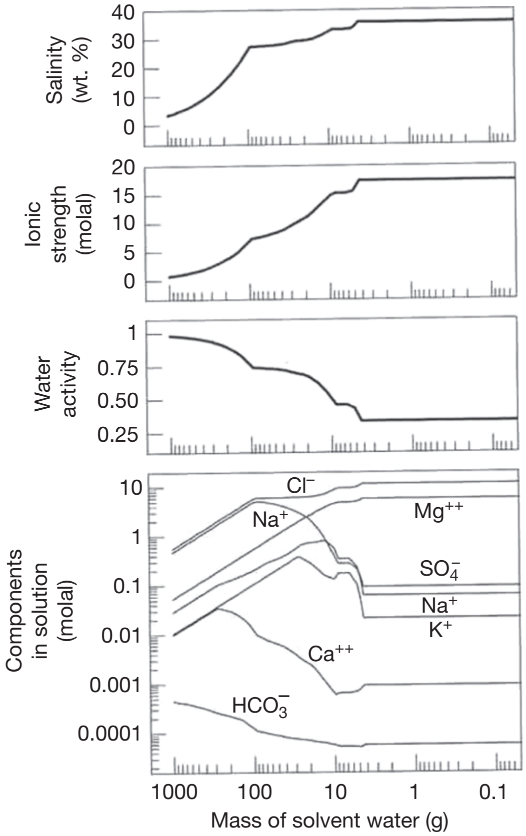

Figure 17 (a–d) Evolution of solute chemistry during the equilibrium simulation of seawater evaporation at 25 °C (Bethke CM (2008) *Geochemical and Biogeochemical Reaction Modeling*, 2nd edn., p. 543. New York: Cambridge University Press. Copyright © 2008. Reprinted with the permission of Cambridge University Press). (a) Salinity, (b) ionic strength, (c) water activity, and (d) solute chemistry.

7.2.8.8 Evaporation of Seawater

Evaporite mineral deposits are important resources for several industrial and agricultural salts and elements. They can occur as marine or nonmarine deposits, and the most common and extensive are the marine deposits formed by evaporation of seawater. Exactly how seawater evaporates to form the mineral sequence found in major evaporate deposits is not fully understood, but a major advance was made by development of the Pitzer model for mixed electrolyte solutions to seawater evaporation (Eugster et al., 1980; Harvie and Weare, 1980; Harvie et al., 1980). Their calculations were reproduced by Bethke (2008), who used the HMW model (Harvie et al., 1984), which includes carbonate species. His results for the sequence of salts formed are reproduced in **Figure 16**, and the change in aqueous ion concentrations is shown in **Figure 17(a)–17(d)**. Seawater evolves from a predominantly NaCl solution to a $MgCl_2$ solution with a sequence of major minerals precipitated that proceeds as follows: dolomite→gypsum→anhydrite→halite. Anhydrite, $CaSO_4$, reacts with the fluid phase to form some glauberite, $Na_2Ca(SO_4)_2$, which disappears on further reaction with anhydrite and the fluid to form polyhalite, $K_2MgCa_2(SO_4)_4 \cdot 2H_2O$. Polyhalite reacts further with the evolving fluid to form kieserite, $MgSO_4 \cdot H_2O$, carnallite, $KMgCl_3 \cdot 6H_2O$, and anhydrite. The enrichment in $MgCl_2$ causes some bischofite, $MgCl_2 \cdot 6H_2O$, to form at the end of evaporation. These reactions all assume equilibrium and that the fluid is always in contact with the precipitating phases so that these back reactions can occur. Another sequence of minor mineral phases can be simulated if the fluid is separated from the precipitating salts (see Bethke, 2008).

7.2.8.9 Reliability of Geochemical Model Simulations

One approach to determine the reliability of geochemical codes is to take well-defined input data and compare the output from several different codes. For comparison of speciation results, Nordstrom et al. (1979) compiled a seawater test case and a river-water test case; that is, seawater and river-water analyses that were used as input to 14 different codes. The results were compared and contrasted, demonstrating that the thermodynamic databases, the number of ion pairs and complexes, the form of the activity coefficients, the assumptions made for redox species, and the assumptions made for equilibrium solubilities of mineral phases were prominent factors in the results. Additional arsenic, selenium, and uranium redox test cases were designed for testing of the WATEQ4F code (Ball and Nordstrom, 1991). Broyd et al. (1985) used a groundwater test case and compared the results from 10 different codes. Such test cases could be expanded to include examples of heterogeneous reactions, mixing with reaction, sorption, temperature dependence, reactive transport, and inverse modeling. The current version of PHREEQC includes 18 examples of code testing. Some of these are true 'tests' in that they can be compared with measurements or independent computations, while others are just examples of the code capability. The EQ3/6 code also shows several examples of code capability in addition to comparative tests. A comparison of PHREEQC and HYDROGEOCHEM codes to simulate transport and reaction of acidic fluids in alluvial material was reported by Brown et al. (2000). This comparison gave similar results, and differences were attributed to different units in model output, different activity coefficient expressions, and different ionic-strength calculations. The equilibrium assumptions used by the codes did not appear to represent well many of the results of a column leaching studies.

In another example, five test cases were computed by PHREEQE and EQ3/6, and the same thermodynamic database was run for each program (INTERA, 1983) to test for any code differences. The five examples were speciation of seawater with major ions, speciation of seawater with complete analysis, dissolution of microcline in dilute HCl, reduction of hematite and calcite by titration with methane, and dedolomitization with gypsum dissolution and increasing temperature. The results were nearly identical for each test case.

Allen et al. (2005) compared simulations of CO_2 solubility at 308 K and 30 MPa using PHREEQC and Geochemist's Workbench but with different databases and assumptions and found considerable differences in predicted solubility. Rosenqvist et al. (2012) found agreement within 20% of the experimental values for CO_2 solubility in water and 1 M NaCl when using the same database for the two codes, PHREEQC and Geochemist's Workbench, at 294 K and 0.3 and 4 MPa. In the latter study, corrections were made to give results in terms of fugacity, which improved the comparisons.

Test cases need to become standard practice when using geochemical codes so that the results will have better credibility. A comparison of code computations with experimental data on activity coefficients and mineral solubilities over a range of conditions also will improve credibility (Nordstrom, 1994).

Bruno et al. (2002) compared the results of blind-prediction modeling for geochemical modeling of several trace elements of concern to radioactive waste disposal for six natural analogue sites. Blind-prediction modeling was an exercise developed in radioactive research on repository analogue sites whereby actual water analyses for major ions were given to different groups of geochemical modelers who were asked to simulate dissolved trace-element concentrations based on assumed solubility equilibria; the results were compared with actual trace-element concentrations determined on the groundwaters but kept secret from the modelers until the modeling was completed. They found that thorium and uranium seem to be controlled by mineral solubilities, whereas strontium, zinc, and REE mobilities seem to be related to the major ion concentrations and complex formation. Other elements, such as nickel, suffer from insufficient thermodynamic data. Sorption reactions were not examined in sufficient detail to draw conclusions.

Another approach to determining model reliability is to perform sensitivity or uncertainty analyses. One of the first examples is the examination of equilibrium aluminum computations for surface waters using the Monte Carlo method of randomizing sources of error in the water analysis and thermodynamic data (Schecher and Driscoll, 1987, 1988). The results showed that uncertainties in the input data did not contribute significantly to computational speciation errors. Nordstrom and Ball (1989) used two different sets of water analyses, groundwater analyses from a granite in Sweden, and surface water analyses from a creek receiving AMD in California. They evaluated uncertainties in the water analyses and uncertainties in the thermodynamic data as possible sources of consistent supersaturation effects for calcite, fluorite, barite, ferric oxyhydroxide, and aluminum hydroxide. Instead of Monte Carlo methods, they used a brute force approach and recomputed the speciation assuming reasonable errors in the input analytical data and in the thermodynamic data. The conclusion was that supersaturation for these minerals could not be accounted for by errors in the water analyses nor in the thermodynamic data. For ferric oxyhydroxide, iron colloids were probably getting through the filter and contributing to the apparent dissolved Fe(III) concentrations and the supersaturation effect. This effect was shown more definitively by Nordstrom (2011). For aluminum hydroxide, the saturation indices did not indicate supersaturation with respect to amorphous aluminum hydroxide, and hence, they were probably reasonable. For the remaining minerals, it was concluded that the supersaturation may have been realistic, because it could not be accounted for by propagation of these errors. Other causes of supersaturation include impure mineral phases (solid substitution or defects), disordered or fine-grained nature, inhibition of precipitation rates, and possible unaccounted-for pressure effects on equilibria.

Criscenti et al. (1996) determined overall uncertainty from geochemical computations by a combination of propagating Monte Carlo-generated analytical and thermodynamic uncertainties through a geochemical code and applying the 'generalized sensitivity analysis' (Spear and Hornberger, 1980) to the output. One of the results of this study is that the aqueous speciation scheme used in many geochemical codes is not necessarily consistent with the speciation scheme used to define standard pH buffers by the National Bureau of Standards. This conclusion raises the possibility that geochemical computations introduce an error when speciating a natural water based on a field pH measurement calibrated with one of these buffers. Cabaniss (1999) investigated methods of uncertainty propagation, comparing the derivative-based method (assumes a linear approximation) with the Monte Carlo technique for solubility equilibria computations of gibbsite, calcite, and jarosite. He found that derivative methods and the assumption of Gaussian uncertainty can misrepresent the propagated uncertainty.

Computational speciation can be compared to analytical speciation for some species. There is always the problem that analytical methods also suffer from operational definitions, interferences, limits of detection, and associated assumptions. Nevertheless, there is no better method of determining accuracy of speciation than by comparing analytical results with computational results (Nordstrom, 1996). In the few instances where this has been done, the comparison ranges from excellent to poor. Examples of studies of this type can be found in Leppard (1983), Batley (1989), Deng et al. (2011), and Nordstrom (1996). Sometimes, comparison of two analytical methods for the same speciation can give spurious results. In **Table 3**, measured and calculated ionic activity coefficients for seawater at 25 °C and 35‰ salinity are compared, after adjusting to a

Table 3 Comparison of measured and calculated ion-activity coefficients in seawater at 25 °C and 35‰ salinity, referenced to $\gamma_{\text{Cl}} = 0.666$

Ion	*Measured*	*Calculated*
H^+	0.590	0.592
Na^+	0.668, 0.670, 0.678	0.674
K^+	0.625	0.619
$NH_4{}^+$	0.616, 0.592	0.624
Mg^{2+}	0.242, 0.22	0.211
Ca^{2+}	0.203, 0.180	0.205
F^-	0.296	0.297
Cl^-	0.666	0.666
OH^-	0.242, 0.254, 0.254	0.263
HS^-	0.681, 0.673, 0.550	0.688
$HCO_3{}^-$	0.576, 0.592, 0.528	0.574
$B(OH)_4{}^-$	0.419, 0.398, 0.351	0.384
$SO_4{}^{2-}$	0.104, 0.112, 0.121, 0.121	0.110
$CO_3{}^{2-}$	0.040, 0.041, 0.035, 0.035	0.041

Source: Millero FJ (2001) *The Physical Chemistry of Natural Waters*, p. 654. New York: Wiley.

reference value of $\gamma_{\text{Cl}} = 0.666$ (Millero, 2001). These values would indicate that for a complex saline solution such as seawater, the activity coefficients can be calculated with a high degree of confidence. Much more effort along these lines is needed to better determine the errors and uncertainties for speciation calculations and to identify reaction equilibria and species for which thermodynamic data need to be measured.

Iron redox speciation was evaluated by comparing the Eh values computed from a speciation code that accepts Fe(II) and Fe(III) concentrations determined analytically with Eh values measured electrometrically with a platinum electrode. An example of this comparison is shown in **Figure 18(a)** (Nordstrom, 2011). For iron concentrations greater than 10^{-6} m, the comparison is generally excellent (usually to within 30 mV), indicating that the analytical data, speciation calculations, and redox measurements are all consistent with equilibrium as predicted by the Nernst equation. This comparison is one of two redox speciation computations that can be tested electrometrically. Deviations from equilibrium are apparent at low iron concentrations, because the electroactivity of iron is low enough that other electron acceptors, such as dissolved oxygen, begin to interfere. When data below detection limits for Fe(III) and the redox potential measurements were eliminated, the agreement improved markedly (**Figure 18(b)**, Nordstrom, 2011). The other redox condition that permits testing with the Nernst equation is sulfide. Berner (1963) showed that the platinum electrode gives Nernstian behavior in anoxic marine sediments in response to dissolved sulfide activities. All other redox species in natural waters are not sufficiently electroactive to establish Nernstian equilibrium.

Deng et al. (2011) demonstrated that if one compares computed free-fluoride ion activities or concentrations (in these examples, with WATEQ4F) with measured values obtained with a fluoride ion-selective electrode, the results are in good agreement down to $\sim 10^{-6}$ m. This agreement between measurement and calculation corroborates the fluoride speciation as calculated by the IA method.

Continued testing of model simulations with experimental and field data is necessary to demonstrate the range of conditions that can be reasonably modeled and what the limitations are. This is the challenge of geochemical modeling.

7.2.9 Final Comments

Numerous models and codes have been developed over the last century for interpreting and portraying low-temperature geochemical processes. They have been applied to a great variety of conditions and processes and have enhanced our ability to understand how low-temperature Earth systems work. However, many of these models have a dangerous sophistication for computing almost any type of possibility without adequately constraining what is probable. Perhaps this affair is a little different from many centuries ago when we had fewer scientific tools and more imagination to play with. The danger in greater model sophistication is the difficulty in testing and refuting it. If we cannot test a model, then we have no means of determining its reliability. And yet, if we do not strive for greater sophistication, then the model lacks representativeness (Oreskes, 2000a).

What we must remember is that modeling is a tool – a useful tool to be sure, but not something that can ever replace the experience gained from directly working on a hydrogeochemical problem for several years. Expert judgment, developed over long time periods and involving many mistakes, along with carefully acquired empirical observations in the field and in the laboratory, will ultimately guide our models from possibility to probability. "… even the most mathematically and computationally sophisticated model will not absolve us of the need for judgment, nor of the need to justify our judgment in human terms" (Oreskes, 2000a). Expert judgment is particularly important in identifying the appropriateness of assumptions in applying a model and constitutes a bigger problem than that of model formulation.

Model reliability is a very important aspect of communicating computational results to managers, risk assessors, stakeholders, politicians, and the public. Unfortunately, sophisticated model computations are not easy to interpret, model results are often nonunique, and modeling is often state-of-the-art science whose reliability has not been adequately tested. Because reliability has often been couched in terms of 'verification' and 'validation' for the convenience of regulatory requirements (Celia et al., 1992; Freedman and Ibaraki, 2003; Huguet, 2001; Jackson, 1988; Jenne and Krupka, 1984; Kirchner et al., 1996; Mattigod, 1995; OECD/NEA, 1994), confusion about the limitations of models and even misunderstandings about how science works have been propagated. Words such as verification and validation might make sense in a regulatory or legal setting but are inappropriate and even incompatible with scientific research and the scientific method (Konikow and Bredehoeft, 1992; Nordstrom, 2012; Oreskes et al., 1994). Validation is a matter of legitimacy and has a different context and meaning than what is sought in science. Evaluation of model capabilities makes scientific sense but not validation (Oreskes, 1998). The question has also been raised as to whether it is really necessary to 'predict' in a temporal sense. Scientific prediction is better described as 'logical' prediction,

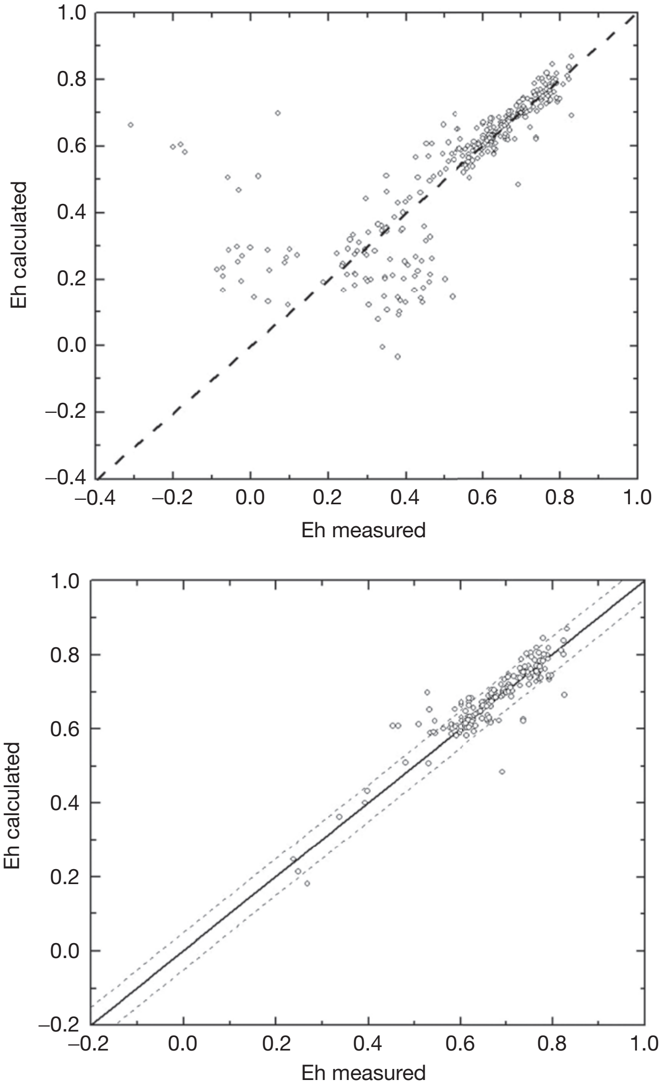

Figure 18 (a) Eh measured with a Pt electrode on-site compared to Eh calculated from Fe(II/III) determinations and speciated with WATEQ4F (Reproduced from Nordstrom DK (2011) Hydrogeochemical processes governing the origin, transport, and fate of major and trace elements from mine wastes and mineralized rock to surface waters. *Applied Geochemistry* 26: 1777–1791). (b) Data from (a) after elimination of data below Fe(III) and Pt electrode detection limits.

not 'temporal' prediction, and hanging regulatory decisions solely on the basis of model predictions may not be wise or necessary (Oreskes, 2004).

Science progresses by testing hypotheses and by its explanatory success. Success is measured by consistency between observations and calculations (which is not proof of validity), logical structure, simplicity combined with wide applicability, and consensus through independent peer review (also not proof of validity). Oreskes (2000a) quoted Richard Feynman, "Doubt is the essence of understanding." Yet doubt is exactly what regulatory agencies are trying to minimize or eliminate. Oreskes (2000a) offered a solution that seems obvious to Earth scientists: our computational prowess has far exceeded our observational data on natural systems. More field data and related empirical observations are needed. Field data will provide the necessary constraints to achieve the legitimacy that is being sought by the public. Sophisticated computations, especially in the hands of the unskilled, have the possibility of achieving any preconceived result unless adequately constrained by empirical data (Nordstrom, 2012).

Future efforts should be directed toward developing standardized test cases for a wide variety of processes against which code performance can be compared and tested: Incorporation of reliable methods of accounting for metal–organic complexing involving humic substances, recognition of artifacts of sample collection in the determination of trace elements in natural waters, more comparisons of analytical versus computed speciation to obtain accuracy estimates of aqueous speciation, development of routine techniques for estimating uncertainties in model calculations, more comparisons of mineral dissolution between lab and field evaluated in terms of mass balances, and more detailed studies of fine-grained mineralogy that are reactive phases in geochemical systems.

Acknowledgments

This paper was accomplished through the support of the National Research Program of the USGS, and it has benefited substantially from the hosts of geochemical modelers who have brought the state of the art to its present status. The authors are grateful for the reviews and editing of Tim Drever, who properly questioned writing misdemeanors and awkward styles.

References

Aagard P and Helgeson HC (1982) Thermodynamic and kinetic constraints on reaction rates among minerals and aqueous solutions: I. Theoretical considerations. *American Journal of Science* 282: 237–285.

Adams JL (1974) *Conceptual Blockbusting: A Guide to Better Ideas*, p. 137. San Francisco: W.H. Freeman and Co.

Alai M, Sutton M, and Carroll S (2005) Evaporative evolution of a Na–Cl–NO_3–K–Ca–SO_4–Si brine at 95°C: Experiments and modeling relevant to Yucca Mountain, Nevada. *Geochemical Transactions* 6: 31–45.

Allen DE, Strazisar BR, Soong Y, and Hedges SW (2005) Modeling carbon dioxide sequestration in saline aquifers: Significance of elevated pressures and salinities. *Fuel Processing Technology* 86: 1569–1580.

Allison JD, Brown DS, and Novo-Gradac KJ (1991) *MINTEQA2/PRODEFA2, A Geochemical Assessment Model for Environmental Systems, Version 3.0 User's Manual*. US Environmental Protection Agency (EPA/600/3-91/021).

Alpers CN and Nordstrom DK (1999) Geochemical modeling of water–rock interactions in mining environments. In: Plumlee GS and Logsdon MJ (eds.) *The Environmental Geochemistry of Mineral Deposits: Part A. Processes, Methods and Health Issues*. *Reviews in Economic Geology*, vol. 6A, pp. 289–324. Littleton, CO: Soc. Econ. Geol.

Alpers CN, Nordstrom DK, and Burchard JM (1992) Compilation and interpretation of water quality and discharge data for acid mine waters at Iron Mountain, Shasta County, California, 1940–91. *US Geol. Surv. Water-Resour. Invest. Report 91-4160*, p. 173.

Andersson JO, Helander T, Höglund L, Shi PF, and Sundman B (2002) Thermo-Calc and DICTRA, Computational tools for materials science. *Calphad* 26: 273–312.

Appelo CAJ and Postma D (2005) *Geochemistry, Groundwater and Pollution*, 2nd edn., p. 649. Rotterdam: A. A. Balkema.

Apps J and Spycher N (2004) Data qualification for thermodynamic data used to support THC calculations. *USDOE report ANL-NBS-HS-000043 REV 00*.

Archer DG and Nordstrom DK (2003) Thermodynamic properties of some arsenic compounds of import to groundwater and other applications. *Journal of Chemical & Engineering Data* (accepted by journal, but censored by NIST).

Arrhenius SA (1889) Über die Reaktionsgeschwindigkeit bei der Inversion von Rohrzucher durch Saüren. (On the reaction rate for the inversion of sucrose by acid). *Zeitschrift für Physikalische Chemie* 4: 226–248.

Atkins P (1998) *Physical Chemistry*, 6th edn., p. 999. New York: W.H. Freeman and Company.

Bain JG, Blowes DW, Robertson WD, and Frind EO (2000) Modelling of sulfide oxidation with reactive transport at a mine drainage site. *Journal of Contaminant Hydrology* 41: 23–47.

Bain JG, Mayer KU, Blowes DW, et al. (2001) Modelling the closure-related geochemical evolution of groundwater at a former uranium mine. *Journal of Contaminant Hydrology* 52: 109–135.

Ball JW, Jenne EA, and Cantrell MW (1981) WATEQ3—A geochemical model with uranium added. *US Geol. Surv. Open-File Report 81–1183*, p. 81.

Ball JW and Nordstrom DK (1989) Final revised analyses of major and trace elements from acid mine waters in the Leviathan Mine Drainage Basin, California and Nevada—October, 1981 to October, 1982. *US Geol. Surv. Water-Resour. Invest. Report 89-4138*, p. 49.

Ball JW and Nordstrom DK (1991) User's manual for WATEQ4F, with revised thermodynamic data base and test cases for calculating speciation of major, trace, and redox elements in natural waters. *US Geol. Surv. Open-File Report 91-183*, p. 189.

Ball JW and Nordstrom DK (1998) Critical evaluation and selection of standard state thermodynamic properties for chromium metal and its aqueous ions, hydrolysis species, oxides, and hydroxides. *Journal of Chemical & Engineering Data* 43: 895–918.

Ball JW, Parks GA, Haas JL, Jr, and Nordstrom DK (1988) A personal computer version of PHAS20, for the simultaneous multiple regression of thermochemical data. *US Geol. Surv. Open-File Report 88-489-A*, p. 119.

Ball JW, Runkel RL, and Nordstrom DK (2004) Evaluating remedial alternatives for the Alamosa River and Wightman Fork, Summitville, Colorado: Application of a reactive-transport model to low- and high-flow synoptic studies. In: Zanetti P (ed.) *The EnviroComp Institute II*, *Environmental Sciences and Environmental Computing*, vol. 2, 1–54 (online publication).

Barnes HL (1967) *Geochemistry of Hydrothermal Ore Deposits*, p. 670. New York: Holt, Rinehart and Winston.

Barnes HL (1997) *Geochemistry of Hydrothermal Ore Deposits*, 3rd edn., p. 972. New York: Wiley.

Baron D and Palmer CD (1996) Solubility of jarosite at 4–35°C. *Geochimica et Cosmochimica Acta* 60: 185–195.

Bassett RL (1997) Chemical modeling on the bare-rock or forested watershed scale. *Hydrological Process* 11: 695–718.

Bassett RL and Melchior DC (1990) Chemical modeling of aqueous systems: An overview. In: Melchior DC and Bassett RL (eds.) *Chemical Modeling of Aqueous Systems II*. *American Chemical Society Symposium Series*, vol. 416, pp. 1–14. Washington, DC: American Chemical Society.

Batley GE (1989) *Trace Element Speciation: Analytical Methods and Problems*, p. 350. Boca Raton, FL: CRC Press.

Bäverman C, Strömberg B, Moreno L, and Neretnieks I (1999) CHEMFRONTS: A coupled geochemical and transport tool. *Journal of Contaminant Hydrology* 36: 333–351.

Bear J and Chang AH-D (2009) *Modeling Groundwater Flow and Contaminant Transport*, p. 834. Heidelberg, Germany: Springer.

Bekins BA, Warren E, and Godsy EM (1998) A comparison of zero-order; first-order; and monod biotransformation models. *Ground Water* 36: 261–268.

Bencala KE (1983) Simulation of solute transport in a mountain pool-and-riffle stream with a kinetic mass transfer model for sorption. *Water Resources Research* 19: 732–738.

Bencala KE and Walters RA (1983) Simulation of solute transport in a mountain pool-and-riffle stream: A transient storage model. *Water Resources Research* 19: 718–724.

Benson SW (1960) *The Foundations of Chemical Kinetics*, p. 703. New York: McGraw-Hill.

Berger AC, Bethke CM, and Krumhansl JL (2000) A process model of natural attenuation in drainage from a historic mining district. *Applied Geochemistry* 15: 655–666.

Berman RG (1988) Internally consistent thermodynamic data for stoichiometric minerals in the system Na_2O–K_2O–CaO–MgO–FeO–Fe_2O_3–Al_2O_3–SiO_2–TiO_2–H_2O–CO_2. *Journal of Petrology* 29: 445–522.

Berner RA (1963) Electrode studies of hydrogen sulfide in marine sediments. *Geochimica et Cosmochimica Acta* 27: 563–575.

Berner RA (1978) Rate control of mineral dissolution under earth surface conditions. *American Journal of Science* 278: 1235–1252.

Berner EK and Berner RA (1996) *Global Environment: Water, Air, and Geochemical Cycles*, p. 376. Upper Saddle River, NJ: Prentice Hall.

Bethke CM (1994) *The Geochemist's Workbench™ Version 2.0: A User's Guide to Rxn, Act2, Tact, React, and Gtplot*. University of Illinois, p. 213.

Bethke CM (2008) *Geochemical and Biogeochemical Reaction Modeling*, 2nd edn., p. 543. New York: Cambridge University Press.

Bethke CM and Johnson TM (2007) Groundwater age and groundwater age dating. *Annual Review of Earth and Planetary Sciences* 36: 121–152.

Bethke CM, Sanford RA, Kirk MF, Jin Q, and Flynn TM (2011) The thermodynamic ladder in geomicrobiology. *American Journal of Science* 311: 183–210.

Bjerrum J (1950) On the tendency of metal ions toward complex formation. *Chemical Reviews* 46: 381–402.

Bormann FH and Likens GE (1967) Nutrient cycling. *Science* 155: 424–429.

Boudart M (1976) Consistency between kinetics and thermodynamics. *The Journal of Physical Chemistry* 80: 2869–2870.

Bowser CJ and Jones BF (1990) Geochemical constraints on ground waters dominated by silicate hydrolysis: An interactive spreadsheet, mass balance approach. *Chemical Geology* 84: 33–35.

Bowser CJ and Jones BF (2002) Mineralogic controls on the composition of natural waters dominated by silicate hydrolysis. *American Journal of Science* 302: 582–662.

Bredehoeft J (2003) From models to performance assessment – The conceptualization problem. *Ground Water* 41: 571–577.

Bredehoeft J (2005) The conceptualization model problem – Surprise. *Hydrogeology Journal* 13: 37–46.

Bricker OP, Jones BF, and Bowser CJ (2003) Mass-balance approach to interpreting weathering reactions in watershed systems. In: Holland HD and Turekian KK (eds.) *Treatise on Geochemistry*, vol. 5, pp. 119–132. Oxford: Elsevier.

Brønsted JN (1922) Studies on solubility: IV. The principle of specific interaction of ions. *Journal of the American Chemical Society* 44: 877–898.

Broshears RE, Runkel RL, Kimball BA, McKnight DM, and Bencala KE (1996) Reactive solute transport in an acidic stream: Experimental pH increase and simulation of controls on pH, aluminum, and iron. *Environmental Science and Technology* 30: 3016–3024.

Brown JG, Bassett RL, and Glynn PD (2000) Reactive transport of metal contaminants in alluvium – Model comparison and column simulation. *Applied Geochemistry* 15: 35–49.

Brown PL, Curti E, and Grambow B (2005) In: Mompean F, Perrone J, and Illemassene M (eds.) *Chemical Thermodynamics of Zirconium*, p. 544. Amsterdam: Elsevier.

Brown LF and Ebinger MH (1998) Modelling precipitation from concentrated solutions with the EQ3/6 chemical speciation code. *Computers & Chemistry* 22: 419–427.

Brown KP and Hosseinipour EZ (1991) New methods for modelling the transport of metals from mineral processing wastes into surface waters. *Journal of Environmental Science and Health A* 26: 157–203.

Broyd TW, Grant MM, and Cross JE (1985) A report on intercomparison studies of computer programs which respectively model: (i) Radionuclide migration (ii) Equilibrium chemistry of groundwater. EUR 10231 EN, Commission of the European Communities, Luxembourg.

Bruno J, Bosbach D, Kulik D, and Navrotsky A (2007) In: Mompean FJ, Illemassene M, and Perrone J (eds.) *Chemical Thermodynamics of Solid Solutions of Interest in Radioactive Waste Management*, p. 266. Amsterdam: Elsevier.

Bruno J, Duro L, and Grivé M (2002) The applicability and limitations of thermodynamic geochemical models to simulate trace element behaviour in natural waters: Lessons learned from natural analogue studies. *Chemical Geology* 190: 371–393.

Bundschuh J and Zilberbrand M (eds.) (2012) *Geochemical Modeling of Groundwater: Vadose and Geothermal Systems*. In: *Multiphysics Modeling*, vol. 5, p. 305. London: CRC Press, Taylor & Francis Group.

Burns DA, Plummer LN, McDonnell JJ, et al. (2003) The geochemical evolution of riparian ground water in a forested piedmont catchment. *Ground Water* 41: 913–925.

Butler JN (1982) *Carbon Dioxide Equilibria and Their Applications*, p. 259. Reading, MA: Addison-Wesley.

Cabaniss SE (1999) Uncertainty propagation in geochemical calculations: Non-linearity in solubility equilibria. *Applied Geochemistry* 14: 255–262.

Campbell K, Nordstrom DK, and Hay M (2011) Kinetic modeling of microbial Fe(II) oxidation, Fe(III) hydrolysis, and mineral precipitation in acid waters. *Goldschmidt 2011, International Geochemistry Conference*, Prague, Czech Republic, 14–19 August (abstract).

Caruso BS, Cox TJ, Runkel RL, et al. (2008) Metals fate and transport modeling in streams and watersheds: State of the science and USEPA workshop review. *Hydrological Processes* 22: 4011–4021.

Celia MA., Gray WG, Hassanizadeh SM, and Carrera J (eds.) (1992) Validation of geo-hydrological models: Part I. *Advances in Water Resources* 15: 1–274.

Chamberlin TC (1897) The method of multiple working hypotheses. *Journal of Geology* 5: 837–848.

Chapelle FH (2003) Geochemistry of groundwater. In: Holland HD and Turekian KK (eds.) *Treatise on Geochemistry*, vol. 5, pp. 425–449. Oxford: Elsevier.

Charlton SR, Macklin CL, and Parkhurst DL (1997) PHREEQCI—A graphical user interface for the geochemical computer program PHREEQC, Vol, p. 9 *US Geol. Surv. Water-Resour. Invest. Report 97-4222*.

Charlton SR and Parkhurst DL (2011) Modules based on the geochemical model PHREEQC for use in scripting and programming languages. *Computers and Geosciences* 37: 1653–1663.

Chase MW, Jr (ed.) (1998) *NIST-JANAF Thermochemical Tables*, 4th edn. *Journal of Physical and Chemical Reference Data*, *Monogr*. 9, Parts I and II. p. 1963.

Chen CW, Gherini SA, and Goldstein RA (1983) The integrated lake-watershed acidification study, vol. 1: Model principles and application procedures. *EPRI Report EA-3221*.

Christophersen N, Seip HM, and Wright RF (1982) A model for streamwater chemistry at Birkenes, Norway. *Water Resources Research* 18: 977–996.

Christov C (2001) Thermodynamic study of the K–Mg–Al–Cl–SO_4–H_2O system at the temperature 298.15 K. *Calphad* 25: 445–454.

Christov C (2003) Thermodynamic study of the co-crystallization of ammonium, sodium and potassium alums and chromium alums. *Calphad* 27: 153–160.

Christov C (2004) Pitzer ion-interaction parameters for Fe(II) and Fe(III) in the quinary $\{Na+K+Mg+Cl+SO_4+H_2O\}$ system at T=298.15 K. *The Journal of Chemical Thermodynamics* 36: 223–235.

Christov C, Dixon A, and Møller N (2007) Thermodynamic modeling of aqueous aluminum chemistry and solid liquid equilibria to high solution concentration and temperature. I. The acidic H–Al–Na–K–Cl–H_2O system from 0° to 100°C. *Journal of Solution Chemistry* 36: 1495–1523.

Christov C and Møller N (2004a) A chemical equilibrium model of solution behavior and solubility in the H–Na–K–Cl–OH–HSO_4–SO_4–H_2O system to high concentration and temperature. *Geochimica et Cosmochimica Acta* 68: 1309–1331.

Christov C and Møller N (2004b) A chemical equilibrium model of solution behavior and solubility in the H–Na–K–Ca–Cl–OH–HSO_4–SO_4–H_2O system to high concentration and temperature. *Geochimica et Cosmochimica Acta* 68: 3717–3739.

Coplen TB (1993) Uses of environmental isotopes. In: Alley WM (ed.) *Regional Ground-Water Quality*, pp. 227–254. New York: Van Nostrand Reinhold.

Cosby BJ, Hornberger GM, Galloway JN, and Wright RF (1985a) Modeling the effects of acid deposition: Assessment of a lumped-parameter model of soil water and streamwater chemistry. *Water Resources Research* 21: 51–63.

Cosby BJ, Hornberger GM, Galloway JN, and Wright RF (1985b) Time scales of catchment acidification. *Environmental Science and Technology* 19: 1144–1149.

Cosby BJ, Wright RF, and Gjessing E (1995) An acidification model (MAGIC) with organic acids evaluated using whole-catchment manipulations in Norway. *Journal of Hydrology* 170: 101–122.

Cox JD, Wagman DD, and Medvedev VA (1989) *CODATA Key Values for Thermodynamics*, p. 271. New York: Hemisphere Publishing Corp.

Criscenti LJ, Laniak GF, and Erikson RL (1996) Propagation of uncertainty through geochemical code calculations. *Geochimica et Cosmochimica Acta* 60: 3551–3568.

Croucher AE and O'Sullivan MJ (2008) Application of the computer code TOUGH2 to the simulation of supercritical conditions in geothermal systems. *Geothermics* 37: 622–634.

Curtis GP (2003) Comparison of approaches for simulating reactive solute transport involving organic degradation reactions by multiple terminal electron acceptors. *Computers and Geosciences* 29: 319–329.

Davis JA and Hayes KF (1986) *Geochemical Processes at Mineral Surfaces*. *American Chemical Society Symposium Series* 323, p. 683. Washington, DC: American Chemical Society.

De Donder Th (1920) *Leçons de Thermodynamique et de Chimie physique*, p. 144. Paris: Gauthier-Villars.

De Wit HA, Groseth T, and Mulder J (2001) Predicting aluminum and soil organic matter solubility using the mechanistic equilibrium model WHAM. *Soil Science Society of America Journal* 65: 1089–1100.

De Wit HA, Kotowski M, and Mulder J (1999) Modeling aluminum and organic matter solubility in the forest floor using WHAM. *Soil Science Society of America Journal* 63: 1141–1148.

Debye P and Hückel E (1923) On the theory of electrolytes. *Physikalische Zeitschrift* 24(185–208): 305–325.

Deng Y, Nordstrom DK, and McCleskey RB (2011) Fluoride geochemistry of thermal waters in Yellowstone National Park: I. Aqueous fluoride speciation. *Geochimica et Cosmochimica Acta* 75: 4476–4489.

Derry GN (1999) *What Science Is and How It Works*, p. 311. New Jersey: Princeton University Press.

Dirkse TP (1986) In: Michalowski T, Akaiwa H, and Izumi F (eds.) *Copper, silver, gold and zinc, cadmium, mercury oxides and hydroxides*. *IUPAC Solubility Data Series*, vol. 23, p. 365. Oxford: Pergamon.

Dobbs JC, Susetyo W, Carreira LA, and Azarraga LV (1989) Competitive binding of protons and metal ions in humic substances by lanthanide ion probe spectroscopy. *Analytical Chemistry* 61: 1519–1524.

Dobson PF, Salah S, Spycher N, and Sonnenthal E (2004) Simulation of water–rock interaction in the Yellowstone geothermal system using TOUGHREACT. *Geothermics* 33: 493–502.

Domenico PA and Schwartz FW (1990) *Physical and Chemical Hydrogeology*, p. 824. New York: Wiley.

Donat JR and Bruland KW (1995) Trace elements in the oceans. In: Salbu B and Steinnes E (eds.) *Trace Elements in Natural Waters*, pp. 247–281. Boca Raton, FL: CRC Press.

Drever JI (1997a) *The Geochemistry of Natural Waters: Surface and Groundwater Environments*, 3rd edn., p. 436. Upper Saddle River, NJ: Prentice Hall.

Drever JI (1997b) Catchment mass balance. In: Saether O and de Cariat P (eds.) *Geochemical Processes, Weathering, and Groundwater Recharge in Catchments*, pp. 241–261. Rotterdam: A. A. Balkema.

Druhan JL, Steefel CI, Molins S, Williams KH, Conrad ME, and DePaolo DJ (2012) Timing the onset of sulfate reduction over multiple subsurface acetate amendments by measurement and modeling of sulfur isotope fractionation. *Environmental Science and Technology* 46: 8895–8902.

Dyrssen D, Jagner D, and Wengelin F (1968) *Computer Calculations of Ionic Equilibria and Titration Procedures*, p. 250. Stockholm: Almqvist and Wiksell.

Dzombak DA and Morel FMM (1990) *Surface Complexation Modelling: Hydrous Ferric Oxide*, p. 393. New York: Wiley.

Eugster HP (1971) The beginnings of experimental petrology. *Science* 173: 481–489.

Eugster HP, Harvie CE, and Weare JH (1980) Mineral equilibria in the six-component seawater system, Na–K–Mg–Ca–SO_4–Cl–H_2O, at 25°C. *Geochimica et Cosmochimica Acta* 44: 1335–1347.

Felmy AR, Girvin DC, and Jenne EA (1984) *MINTEQ – A Computer Program for Calculating Aqueous Geochemical Equilibria*. US Environmental Protection Agency (EPA-600/3-84-032).

Felmy AR, Rai D, and Amonette JE (1990) The solubility of barite and celestite in sodium sulfate: Evaluation of thermodynamic data. *Journal of Solution Chemistry* 19: 175–185.

Freedman VL and Ibaraki M (2003) Coupled reactive mass transport and fluid flow: Issues in model verification. *Advances in Water Resources* 26: 117–127.

Freeze RA and Cherry JA (1979) *Groundwater*, p. 604. Englewood Cliffs, NJ: Prentice Hall.

Gamsjäger H, Bugajski J, Gajda T, Lemire R, and Preis W (2005) In: Mompean FJ, Illemassene M, and Perrone J (eds.) *Chemical Thermodynamics of Nickel*, p. 617. Amsterdam: Elsevier.

Garrels RM (1960) *Mineral Equilibria*, p. 254. New York: Harper and Brothers.

Garrels RM (1967) Genesis of some ground waters from igneous rocks. In: Abelson PH (ed.) *Researches in Geochemistry*, pp. 405–420. New York: Wiley.

Garrels RM and Christ CL (1965) *Solutions, Minerals, and Equilibria*, p. 450. New York: Harper and Row.

Garrels RM and Mackenzie FT (1967) Origin of the chemical composition of some springs and lakes. *Equilibrium Concepts in Natural Water Systems. Adv. Chem. Series* 67, pp. 222–242. Washington, DC: American Chemical Society.

Garrels RM and Thompson ME (1962) A chemical model for seawater at 25°C and one atmosphere total pressure. *American Journal of Science* 260: 57–66.

Garvin D, Parker VB, and White HJ (1987) *CODATA Thermodynamic Tables – Selections for Some Compounds of Calcium and Related Mixtures: A Prototype Set of Tables*, p. 356. Washington, DC: Hemisphere Publishing Corp.

Gerke HH, Molson JW, and Frind EO (1998) Modelling the effect of chemical heterogeneity on acidification and solute leaching in overburden mine spoils. *Journal of Hydrology* 209: 166–185.

Gherini SA, Mok L, Hudson RJM, Davis GF, Chen CW, and Goldstein RA (1985) The ILWAS model: Formulation and application. *Water, Air, and Soil Pollution* 26: 425–459.

Glynn P and Brown J (1996) Reactive transport modelling of acidic metal-contaminated ground water at a site with sparse spatial information. In: Lichtner PC, Steefel CI, and Oelkers EH (eds.) *Reactive Transport in Porous Media. Reviews in Mineralogy and Geochemistry*, vol. 34, pp. 377–438. Washington, DC: Mineralogical Society of America and Geochemical Society.

Glynn P and Brown J (2012) Integrating field observations and inverse and forward modeling: Application at a site with acidic, heavy-metal-contaminated groundwater. In: Bundschuh J and Zilberbrand M (eds.) *Geochemical Modeling of Groundwater, Vadose and Geothermal Systems*, pp. 181–233. Boca Raton, FL: CRC Press.

Glynn P and Plummer LN (2005) Geochemistry and the understanding of ground-water systems. *Hydrogeology Journal* 13: 263–287.

Goldberg ED (1954) Marine geochemistry: 1. Chemical scavengers of the sea. *Journal of Geology* 62: 249–265.

Gottschalk M (1997) Internally consistent thermodynamic data for rock-forming minerals in the system SiO_2–TiO_2–Al_2O_3–Fe_2O_3–CaO–MgO–FeO–K_2O–Na_2O–H_2O–CO_2. *European Journal of Mineralogy* 9: 175–223.

Greenberg JP and Møller N (1989) The prediction of mineral solubilities in natural waters: A chemical equilibrium model for the Na–K–Ca–Cl–SO_4–H_2O system to high concentrations from 0 to 250°C. *Geochimica et Cosmochimica Acta* 53: 2503–2518.

Greenwood H (1989) On models and modeling. *The Canadian Mineralogist* 27: 1–14.

Grenthe I, Fuger J, Konings RJM, et al., (1992) In: Wanner H and Forest I (eds.) *Chemical Thermodynamics of Uranium*, p. 715. Amsterdam: Elsevier.

Grenthe I, Plyasunov AV, and Spahiu K (1997) Estimations of medium effects on thermodynamic data. In: Grenthe I and Puigdomenech I (eds.) *Modelling in Aquatic Chemistry*, pp. 343–444. Paris, France: Organization for Economic Co-operation and Development/Nuclear energy Agency Publications.

Gryzb KR (1995) NOAEM (natural organic anion equilibrium model): A data analysis algorithm for estimating functional properties of dissolved organic matter in aqueous environments: Part I. Ionic component speciation and metal association. *Organic Geochemistry* 23: 379–390.

Guggenheim GA (1935) The specific thermodynamic properties of aqueous solutions of strong electrolytes. *Philosophical Magazine* 19: 588–643.

Guillamont R, Fanghänel T, Fuger J, et al. (2003) In: Mompean FJ, Illemassene M, Domenech-Orti C, and Ben Said K (eds.) *Update on the Chemical Thermodynamics of Uranium, Neptunium, Plutonium, Americium, and Technetium*, p. 919. Amsterdam: Elsevier with CD.

Gurvich LV, Veyts IV, and Alcock CB (1989a) *Thermodynamic Properties of Individual Substances*, vol. 1, p. 468. New York: Hemisphere Publishing Co.

Gurvich LV, Veyts IV, Alcock CB, and Iorish VS (1989b) *Thermodynamic Properties of Individual Substances*, vol. 2, p. 448. Boca Raton, FL: CRC Press.

Gurvich LV, Veyts IV, Alcock CB, and Iorish VS (1993) *Thermodynamic Properties of Individual Substances, Parts 1 and 2*, vol. 3, p. 1120. Boca Raton, FL: CRC Press.

Guthrie JW, Hassan NM, Salam MSA, et al. (2005) Complexation of Ni, Cu, Zn, and Cd by DOC in some metal-impacted freshwater lakes: A comparison of approaches using electrochemical determination of free-metal-ion and labile complexes and a computer speciation model, WHAM V and VI. *Analytica Chimica Acta* 528: 205–218.

Haas JL, Jr (1974) PHAS20, a program for simultaneous multiple regression of a mathematical model to thermochemical data. *Natl. Tech. Info. Service Report AD-780 301*, p. 158.

Haas JL, Jr (1989) TDM, a FORTRAN code for fitting thermodynamic measurements as a function of temperature and pressure, unpublished update for PHAS20.

Haas JL Jr. and Fisher JR (1976) Simultaneous evaluation and correlation of thermodynamic data. *American Journal of Science* 276: 525–545.

Harned HS and Owen BB (1958) *The Physical Chemistry of Electrolyte Solutions*, 3rd edn., p. 354. New York: Reinhold.

Harvie CE, Eugster HP, and Weare JH (1982) Mineral equilibria in the six-component seawater system, Na–K–Mg–Ca–SO_4–Cl–H_2O at 25°C: II. Composition of the saturated solutions. *Geochimica et Cosmochimica Acta* 46: 1603–1618.

Harvie CE, Greenberg JP, and Weare JH (1987) A chemical equilibrium algorithm for highly non-ideal multiphase systems: Free energy minimization. *Geochimica et Cosmochimica Acta* 51: 1045–1057.

Harvie CE, Møller N, and Weare JH (1984) The prediction of mineral solubilities in natural waters: The Na–K–Mg–Ca–H–Cl–SO_4–OH–HCO_3–CO_3–CO_2–H_2O system to high ionic strengths at 25°C. *Geochimica et Cosmochimica Acta* 48: 723–751.

Harvie CE and Weare JH (1980) The prediction of mineral solubilities in natural waters: The Na–K–Mg–Ca–Cl–SO_4–H_2O system from zero to high concentration at 25°C. *Geochimica et Cosmochimica Acta* 44: 981–997.

Harvie CE, Weare JH, Hardie LA, and Eugster HP (1980) Evaporation of seawater: Calculated mineral sequences. *Science* 208: 498–500.

Helgeson HC (1964) *Complexing and Hydrothermal Ore Deposition*, p. 128. New York: Pergamon.

Helgeson HC (1967) Thermodynamics of complex dissociation in aqueous solution at elevated temperatures. *The Journal of Physical Chemistry* 71: 3121–3136.

Helgeson HC (1968) Evaluation of irreversible reactions in geochemical processes involving minerals and aqueous solutions: I. Thermodynamic relations. *Geochimica et Cosmochimica Acta* 32: 853–877.

Helgeson HC (1969) Thermodynamics of hydrothermal systems at elevated temperatures and pressures. *American Journal of Science* 167: 729–804.

Helgeson HC (1971) Kinetics of mass transfer among silicates and aqueous solutions. *Geochimica et Cosmochimica Acta* 35: 421–469.

Helgeson HC, Brown TH, Nigrini A, and Jones TA (1970) Calculation of mass transfer in geochemical processes involving aqueous solution. *Geochimica et Cosmochimica Acta* 34: 569–592.

Helgeson HC, Delany JM, Nesbitt HW, and Bird DW (1978) Summary and critique of the thermodynamic properties of rock-forming minerals. *American Journal of Science* 278-A: 1–229.

Helgeson HC, Garrels RM, and Mackenzie FT (1969) Evaluation of irreversible reactions in geochemical processes involving minerals and aqueous solutions: II. Applications. *Geochimica et Cosmochimica Acta* 33: 455–481.

Helgeson HC and Kirkham DH (1974a) Theoretical prediction of the thermodynamic behavior of aqueous electrolytes at high pressures and temperatures: I. Summary of the thermodynamic/electrostatic properties of the solvent. *American Journal of Science* 274: 1089–1198.

Helgeson HC and Kirkham DH (1974b) Theoretical prediction of the thermodynamic behavior of aqueous electrolytes at high pressures and temperatures: II. Debye-Hückel parameters for activity coefficients and relative partial molal properties. *American Journal of Science* 274: 1199–1261.

Helgeson HC and Kirkham DH (1976) Theoretical prediction of the thermodynamic behavior of aqueous electrolytes at high pressures and temperatures: III. Equation of state for aqueous species at infinite dilution. *American Journal of Science* 276: 97–240.

Helgeson HC, Kirkham DH, and Flowers GC (1981) Theoretical prediction of the thermodynamic behavior of aqueous electrolytes at high pressures and temperatures: IV. Calculation of activity coefficients and relative partial molal properties to 600°C and 5 kb. *American Journal of Science* 281: 1249–1516.

Helgeson HC and Murphy WM (1983) Calculation of mass transfer as a function of time and surface area in geochemical processes: I. Computational approach. *Mathematical Geology* 15: 109–130.

Helgeson HC, Murphy WM, and Aagard P (1984) Thermodynamic and kinetic constraints on reaction rates among minerals and aqueous solutions: II. Rate constants, effective surface area, and the hydrolysis of feldspar. *Geochimica et Cosmochimica Acta* 48: 2405–2432.

Hem JD (1959) *Study and Interpretation of the Chemical Characteristics of Natural Water*. US Geol. Surv. Water-Supply Paper 1473, p. 269.

Hem JD (1961) *Calculation and Use of Ion Activity*. US Geol. Surv. Water-Supply Paper 1535-C.

Hem JD and Cropper WH (1959) *Survey of Ferrous-ferric Chemical Equilibria and Redox Potentials*. US Geol. Survey Water-Supply Paper 1459-145A.

Hitchon B, Perkins EH, and Gunter WD (1996) *Introduction of Ground Water Geochemistry and SOLMINEQ.GW*. Alberta: Geoscience Publishing Ltd.

Hochella MF Jr. and White AF (eds.) (1990) *Mineral–Water Interface Geochemistry*. In: *Reviews in Mineralogy*, vol. 23, p. 603. Washington, DC: Mineralogical Society of America.

Högfeldt E (1982) *Stability Constants of Metal-Ion Complexes. Part A: Inorganic Ligands. IUPAC Chemical Data Series* 21, p. 310. Oxford: Pergamon Press.

Holland TJB and Powell R (1998) An internally consistent thermodynamic data set for phases of petrological interest. *Journal of Metamorphic Geology* 16: 309–343.

Hornberger GM (2002) Impacts of acidic atmospheric deposition on the chemical composition of stream water and soil water. In: Beck MB (ed.) *Environmental Foresight and Models: A Manifesto*, pp. 131–145. New York: Elsevier.

Huber C, Filella M, and Town RM (2002) Computer modelling of trace metal ion speciation: Practical implementation of a linear continuous function for complexation by natural organic matter. *Computers and Geosciences* 28: 587–596.

Hückel E (1925) Zur Theorie konzentrierterer wässeriger Lösungen starker Elektrolyte (On the theory of strong electrolytes in concentrated aqueous solutions). *Physikalische Zeitschrift* 26: 93–147.

Huguet JM (2001) Testing and validation of numerical models of groundwater flow, solute transport and chemical reactions in fractured granites: A quantitative study of the hydrogeological and hydrochemical impact produced. ENRESA Tech. Publ. 06/2001, p. 253.

Hummel W, Anderegg G, Puigdomenech I, Rao L, and Tochiyama O (2005) In: Mompean FJ, Perrone J, and Illemassene M (eds.) *Chemical Thermodynamics of Compounds and Complexes of U, Np, Pu, Am, Tc, Se, Ni and Zr with Selected Organic Ligands*, p. 919. Amsterdam: Elsevier with CD.

Hummel W, Berner U, Curti E, Pearson FJ, and Thoenen T (2002) Nagra/PSI Chemical Thermodynamic Data Base 01/01, p. 565.

Hunter KS, Wang Y, and Van Cappellen P (1998) Kinetic modeling of microbially-driven redox chemistry of subsurface environments: Coupling transport, microbial metabolism and geochemistry. *Journal of Hydrology* 209: 53–80.

Ingri N, Kakolowicz W, Sillén LG, and Warnqvist B (1967) HALTAFALL, a general program for calculating the composition of equilibrium mixtures. *Talanta* 14: 1261–1286.

Ingri N and Sillén LG (1962) High-speed computers as a supplement to graphical methods: II. Some computer programs for studies of complex formation equilibria. *Acta Chemica Scandinavica* 16: 173–191.

INTERA (1983) Geochemical models suitable for performance assessment of nuclear waste storage: Comparison of PHREEQE and EQ3/EQ6. INTERA Environmental Consultants Inc., ONWI-473, p. 114.

Jackson KJ (1988) Verification and validation studies of the addition of Pitzer's equations to the EQ3/6 brine model. UCRL-53841, p. 26.

Jansen B, Mulder J, and Verstraten JM (2003) Organic complexation of Al and Fe in acidic soil solutions: Comparison of diffusive gradients in thin films analyses with Models V and VI predictions. *Analytica Chimica Acta* 498: 105–117.

Jansen B, Mulder J, and Verstraten JM (2005) Modeling aluminum solubility in intrazonal podzols using WHAM-S/Model V. *Journal of Plant Nutrition and Soil Science* 168: 325–333.

Jenne EA (ed.) (1979) *Chemical Modeling in Aqueous Systems. American Chemical Society Symposium Series 93*, p. 914. Washington, DC: American Chemical Society.

Jenne EA and Krupka KM (1984) Validation of geochemical models. *USNRC Report PNL-SA-12442*, p. 9.

Jin Q and Bethke CM (2005) Predicting the rate of microbial respiration. *Geochimica et Cosmochimica Acta* 69: 1133–1143.

Jin Q and Bethke CM (2007) The thermodynamics and kinetics of microbial respiration. *American Journal of Science* 307: 643–677.

Johnson DB (2001) Importance of microbial ecology in the development of new mineral technologies. *Hydrometallurgy* 59: 147–157.

Johnson KA and Goody RS (2011) The original Michaelis constant: Translation of the 1913 Michaelis-Menten paper. *Biochemistry* 50: 8264–8269.

Johnson JW, Nitao JJ, and Morris JP (2005) Reactive transport modeling of cap-rock integrity during natural and engineered CO_2 storage. In: Thomas D and Benson S (eds.) *Carbon Dioxide Capture for Storage in Deep Geologic Formations–Results from the CO_2 Capture Project, Vol. 2: Geologic Storage of Carbon Dioxide with Monitoring and Verification*, pp. 787–813. Amsterdam: Elsevier.

Johnson JW, Oelkers EH, and Helgeson HC (1992) SUPCRT92: A software package for calculating the standard molal thermodynamic properties of minerals, gases, aqueous species, and reactions from 1 to 5,000 bars and 0° to 1,000°C. *Computers and Geosciences* 18: 899–947.

Judson HF (1980) *The Search for Solutions*, p. 211. New York: Holt, Rinehart and Winston.

Kharaka YK and Barnes I (1973) SOLMNEQ: Solution-mineral equilibrium computations. *Natl. Tech. Info. Serv. Report PB214-899*, p. 82.

Kharaka YK, Gunter WD, Aggarwal PK, Perkins EH, and Debraal JD (1988) SOLMINEQ.88: A computer program for geochemical modeling of water–rock. interactions. *US Geol. Surv. Water-Resour. Invest. Report 88-4227*, p. 420

Kimball BA, Broshears RE, Bencala KE, and McKnight DM (1994) Coupling of hydrologic transport and chemical reactions in a stream affected by acid mine drainage. *Environmental Science and Technology* 28: 2065–2073.

Kimball BA, Callender E, and Axtmann EV (1995) Effects of colloids on metal transport in a river receiving acid mine drainage, Upper Arkansas River, Colorado, USA. *Applied Geochemistry* 10: 285–306.

Kimball BA and Runkel RL (2009) Spatially detailed quantification of metal loading for decision making: Metal mass loading to American Fork and Mary Ellen Gulch, Utah. *Mine Water and the Environment* 28: 274–290.

Kimball BA and Runkel RL (2010) Evaluating remediation alternatives for mine drainage, Little Cottonwood Cree, Utah, USA. *Environmental Earth Sciences* 60: 1021–1036.

Kimball BA, Runkel RL, and Walton-Day K (2003) Use of field-scale experiments and reactive transport modeling to evaluate remediation alternatives in streams affected by acid mine drainage. In: Jambor JL, Blowes DW, and Ritchie AIM (eds.) *Environmental Aspects of Mine Wastes. Mineral. Assoc. Canada Short Course Ser.*, vol. 31, pp. 261–282. Ottawa: Mineralogical Association of Canada.

Kimball BA, Runkel RL, Wanty RB, and Verplanck PL (2010) Reactive solute-transport simulation of pre-mining metal concentrations in mine-impacted catchments: Redwell Basin, Colorado, USA. *Chemical Geology* 269: 124–136.

Kipp KL, Jr (1987) HST3D—A computer code for simulation of heat and solute transport in three-dimensional ground-water flow systems. *US Geol. Surv. Water-Resour. Invest. Report 86-4095*, p. 517.

Kipp KL, Jr (1998) Guide to the revised heat and solute transport simulator: HST3D. *US Geol. Surv. water-Resour. Report 97-4157*, p. 149.

Kirchner JW, Hooper RP, Kendall C, Neal C, and Leavesley G (1996) Testing and validating environmental models. *The Science of the Total Environment* 183: 33–47.

Konikow LF and Bredehoeft JD (1992) Ground-water models cannot be validated. *Advances in Water Resources* 15: 75–83.

Krauskopf KB (1951) The solubility of gold. *Economic Geology* 46: 858–870.

Krauskopf KB (1955) Sedimentary deposits of rare metals. *Econ. Geol. Fiftieth Anniv. Part I*, pp. 411–463.

Krauskopf KB (1956) Factors controlling the concentrations of thirteen rare metals in sea water. *Geochimica et Cosmochimica Acta* 9: 1–32.

Krauskopf KB (1967) *Introduction to Geochemistry*, p. 721. New York: McGraw-Hill.

Kulik DA (2009) Thermodynamic concepts in modeling sorption at the mineral-water interface. In: Oelkers EH and Schott J (eds.) *Thermodynamics and Kinetics of Water–Rock Interaction. Reviews in Mineralogy and Geochemistry*, vol. 70, pp. 125–180. Washington, DC: Mineralogical Society of America Geochemical Society.

Laidler KJ (1987) *Chemical Kinetics*, 3rd edn., p. 531. New York: Harper and Row.

Laidler KJ and Meiser JH (1982) Physical Chemistry, p. 920. Menlo Park, CA: Benjamin/Cummings.

Lambert I and Clever HL (1992) Einaga H, Hala J, Komatsu Y, Lorimer JW, Vorob'ev AF, and Mustafin DI (eds.) *Alkaline Earth Hydroxides in Water and Aqueous Solutions. IUPAC Solubility Data Series*, vol. 52, p. 365. Oxford, Pergamon.

Langmuir D (1971) The geochemistry of some carbonate ground waters in central Pennsylvania. *Geochimica et Cosmochimica Acta* 35: 1023–1045.

Langmuir D (1997) *Aqueous Environmental Geochemistry*, p. 600. Upper Saddle River, NJ: Prentice Hall.

Lasaga AC (1984) Chemical kinetics of water–rock interactions. *Journal of Geophysical Research* 89: 4009–4025.

Latimer WM (1952) *The Oxidation State of the Elements and Their Potentials in Aqueous Solution*, p. 392. New York: Prentice Hall.

Lemire RJ, Fuger J, Nitsche H, et al. (2001) *Chemical Thermodynamics of Neptunium and Plutonium*, p. 836. Amsterdam: Elsevier.

Leppard GG (1983) *Trace Element Speciation in Surface Waters and Its Ecological Implications*. *NATO Conf. Series*, vol. 6, p. 320. New York: Plenum.

Lewis GN and Randall M (1921) The activity coefficient of strong electrolytes. *Journal of the American Chemical Society* 43: 1112–1153.

Lewis GN and Randall M (1923) *Thermodynamics and the Free Energy of Chemical Substances*, p. 653. New York: McGraw-Hill.

Li L, Gawande N, Kowalsky MB, Steefel CI, and Hubbard SS (2011) Physicochemical heterogeneity controls on uranium bioreduction rates at the field scale. *Environmental Science and Technology* 45: 9959–9966.

Lichtner PC (1996) Continuum formulation of multicomponent-multiphase reactive transport. In: Lichtner PC, Steefel CI, and Oelkers EH (eds.) *Reactive Transport in Porous Media*. *Reviews in Mineralogy*, vol. 34, pp. 1–81. Washington, DC: Mineralogical Society of America.

Lichtner PC (2001) FLOTRAN users manual. *Los Alamos National Laboratory Report LA-UR-01-2349*, Los Alamos, NM.

Lichtner PC, Steefel CI, and Oelkers EH (eds.) (1996) *Reactive Transport in Porous Media*. In: *Reviews in Mineralogy*, vol. 34, p. 438. Washington, DC: Mineralogical Society of America.

Lide DR and Kehiaian HV (1994) *CRC Handbook of Thermophysical and Thermochemical Data*, p. 518. Boca Raton, FL: CRC Press.

Likens GE, Bormann FH, Pierce RS, Eaton JS, and Johnson NM (1977) *Biogeochemistry of a Forested Ecosystem*, p. 146. New York: Springer.

Lobo VMM and Quaresma JL (1989) *Handbook of Electrolyte Solutions*. Parts A & B, p. 2320. Amsterdam: Elsevier.

Loeppert RH, Schwab AP, and Goldberg S (1995) *Chemical Equilibrium and Reaction Models*, p. 422. Spec. Publ. 42. Madison, WI: Soil Science Society of America.

Lofts S and Tipping E (2011) Assessing WHAM/Model VII against field measurements of free metal ion concentrations: Model performance and the role of uncertainty in parameters and inputs. *Environmental Chemistry* 8: 501–516.

Lofts S, Woof C, Tipping E, Clarke N, and Mulder J (2001) Modelling pH buffering and aluminium solubility in European forest soils. *European Journal of Soil Science* 52: 189–204.

Lukas HL, Fries SG, and Sundman B (2007) *Computational Thermodynamics: The Calphad Method*, p. 324. Cambridge: Cambridge University Press.

Mangold DC and Tsang C-F (1991) A summary of subsurface hydrological and hydrochemical models. *Reviews of Geophysics* 29: 51–79.

Marion GM (2001) Carbonate mineral solubility at low temperatures in the Na–K–Mg–Ca–H–Cl–SO_4–OH–HCO_3–CO_3–CO_2–H_2O system. *Geochimica et Cosmochimica Acta* 65: 1883–1896.

Marion GM (2002) A molal-based model for strong acid chemistry at low temperatures ($<$200 to 298 K). *Geochimica et Cosmochimica Acta* 66: 2499–2516.

Marion GM (2007) Adapting molar data (without density) for molal models. *Computers and Geosciences* 33: 829–834.

Marion GM, Catling DC, Crowley JK, and Kargel JS (2011) Modeling hot spring chemistries with applications to martian silica formation. *Icarus* 212: 629–642.

Marion GM, Catling DC, and Kargel JS (2003) Modeling aqueous ferrous iron chemistry at low temperatures with application to Mars. *Geochimica et Cosmochimica Acta* 67: 4251–4266.

Marion GM, Catling DC, and Kargel JS (2006) Modeling gas hydrate equilibria in electrolyte solutions. *Calphad* 30: 248–259.

Marion GM, Crowley JK, Thomson BJ, et al. (2009) Modeling aluminum-silicon chemistries and application to Australian acidic playa lakes as analogues for Mars. *Geochimica et Cosmochimica Acta* 73: 3493–3511.

Marion GM and Farren RE (1999) Mineral solubilities in the Na–K–Mg–Ca–Cl–SO_4–H_2O system: A re-evaluation of the sulfate chemistry in the Spencer–Møller–Weare model. *Geochimica et Cosmochimica Acta* 63: 1305–1318.

Marion GM and Grant SA (1994) FREZCHEM: A chemical thermodynamic model for aqueous solutions at subzero temperatures. *CRREL Spec. Rept. 94–18*. Hanover, NH: USACRREL.

Marion GM and Kargel JS (2008) *Cold Aqueous Planetary Geochemistry with FREZCHEM: From Modeling to the Search for Life at the Limits*, p. 251. Heidelberg: Springer.

Marion GM, Kargel JS, and Catling DC (2008) Modeling ferrous-ferric iron chemistry with application to Martian surface geochemistry. *Geochimica et Cosmochimica Acta* 72: 242–266.

Marion GM, Kargel JS, Catling DC, and Jakubowski SD (2005) Effects of pressure on aqueous chemical equilibria at subzero temperatures with applications to Europa. *Geochimica et Cosmochimica Acta* 69: 259–274.

Marion GM, Mironenko MV, and Roberts MW (2010) FREZCHEM: A geochemical model for cold aqueous solutions. *Computers and Geosciences* 36: 10–15.

Martell AE and Smith RM (1974–1976) *Critical Stability Constants, Vol. 1: Amino Acids, Vol. 2: Amines, Vol. 3: Other Organic Ligands, Vol. 4: Inorganic Compounds*, p. 1636. New York: Plenum.

Mattigod SV (1995) Validation of geochemical equilibrium models. In: Loeppert RH, Schwab AB, and Goldberg S (eds.) *Chemical Equilibrium and Reaction Models*, pp. 201–218. Spec. Publ. 42. Madison, WI: Soil Science Society of America.

Mayer KU, Benner SG, and Blowes DW (1999) The reactive transport model MIN3P: Application to acid-mine drainage generation and treatment—Nickel Rim mine site, Sudbury, Ontario. In: Goldsack D, Bezlie N, Yearwood P, and Hall G (eds.) *Proceedings of Sudbury '99 Mining and Environment II*. Sudbury, pp. 145–154.

Mayer KU, Blowes DW, and Frind EO (2003) Advances in reactive-transport modelling of contaminant release and attenuation from mine-waste deposits. In: Jambor JL, Blowes DW, and Ritchie AIM (eds.) *Mineralogical Association of Canada Short Course Series* 31, pp. 283–302. Ottawa: Mineralogical Association of Canada.

Mazor E, Drever JI, Finlay J, Huntoon PW, and Lundy DA (1993) Hydrochemical implications of groundwater mixing: An example from the Southern Laramie Basin, Wyoming. *Water Resources Research* 29: 193–205.

McCleskey RB, Nordstrom DK, Ryan JN, and Ball JW (2012) A new method of calculating electrical conductivity with applications to natural waters. *Geochimica et Cosmochimica Acta* 77: 369–382.

Melchior DC and Bassett RL (eds.) (1990) *Chemical Modeling of Aqueous Systems: II*. In: *American Chemical Society Symposium Series* 416, p. 556. Washington, DC: American Chemical Society.

Merkel BJ and Planer-Friedrich B (2008) In: Nordstrom DK (ed.) *Groundwater Geochemistry–A Practical Guide to Modeling of Natural and Contaminated Aquatic Systems*, p. 230. Berlin: Springer.

Michaelis L and Menten ML (1913) Die Kinetik der Invertinwirkung. *Biochemische Zeitschrift* 49: 333–369 [transl. Goody, R.S. and Johnson, K.A., The kinetics of invertase action, supplement to Johnson and Goody (2011)].

Millero FJ (2001) *The Physical Chemistry of Natural Waters*, p. 654. New York: Wiley.

Millero FJ and Pierrot D (1998) A chemical model for natural waters. *Aquatic Geochemistry* 4: 153–199.

Millero FJ and Roy R (1997) A chemical model for the carbonate system in natural waters. *Croatica Chemica Acta* 70: 1–38.

Millero FJ and Schreiber DR (1982) Use of the ion pairing model to estimate activity coefficients of the ionic components of natural waters. *American Journal of Science* 282: 1508–1540.

Molchanov S, Gendel Y, Ioslvich I, and Lahav O (2007) Improved experimental and computational methodology for determining the kinetic equation and the extant kinetic constants of Fe(II) oxidation by *Acidithiobacillus ferrooxidans*. *Applied and Environmental Microbiology* 73: 1742–1752.

Møller N (1988) The prediction of mineral solubilities in natural waters: A chemical equilibrium model for the Na–Ca–Cl–SO_4–H_2O system, to high temperature and concentration. *Geochimica et Cosmochimica Acta* 52: 821–837.

Møller N, Greenberg JP, and Weare JH (1998) Computer modeling for geothermal systems: Predicting carbonate and silica scale formation, CO_2 breakout and H_2S exchange. *Transport Porous Media* 33: 173–204.

Monnin C (1990) The influence of pressure on the activity coefficients of the solutes and on the solubility of minerals in the system Na–Ca–Cl–SO_4–H_2O to 200°C and 1 kbar, and to high NaCl concentration. *Geochimica et Cosmochimica Acta* 52: 821–834.

Monnin C and Ramboz C (1996) The anhydrite saturation index of the ponded brines and the sediment pore waters of the Red Sea deeps. *Chemical Geology* 127: 141–159.

Monod J (1949) The growth of bacterial cultures. *Annual Review of Microbiology* 3: 371–394.

Moore J, Adams M, Allis R, Lutz S, and Rauzi S (2005) Mineralogical and geochemical consequences of the long-term presence of CO_2 in natural reservoirs. *Chemical Geology* 217: 365–385.

Morel FMM and Hering JG (1993) *Principles and Applications of Aquatic Chemistry*, p. 588. New York: Wiley.

Morel FMM and Morgan JJ (1972) A numerical method for computing equilibria in aqueous systems. *Environmental Science and Technology* 6: 58–67.

Murphy WM and Helgeson HC (1987) Thermodynamic and kinetic constraints on reaction rates among minerals and aqueous solutions: III. Activated complexes and the pH dependence of the rates of feldspar, pyroxene, wollastonite, and olivine hydrolysis. *Geochimica et Cosmochimica Acta* 51: 3137–3153.

Murphy WM, Oelkers EH, and Lichtner PC (1989) Surface reaction versus diffusion control of mineral dissolution and growth rates in geochemical processes. *Chemical Geology* 78: 357–380.

Nemati M, Harrison STL, Hansford GS, and Webb C (1998) Biological oxidation of ferrous sulphate by Thiobacillus ferrooxidans: A review on the kinetic aspects. *Biochemical Engineering Journal* 1: 171–190.

Nieto JM, Sarmiento AM, Olias M, et al. (2007) Acid mine drainage in the Tinto and Odiel rivers (Iberian Pyrite Belt, SW Spain) and bioavailability of the transported metals to the Huelva Estuary. *Environmental International* 33: 445–455.

Nikolaidis NP, Muller PK, Schnoor JL, and Hu HL (1991) Modeling the hydrogeochemical response of a stream to acid deposition using the enhanced trickle-down model. *Research Journal of the Water Pollution Control Federation* 63: 220–227.

Nikolaidis NP, Schnoor JL, and Geogakakos KP (1989) Modeling of long-term lake alkalinity responses to acid deposition. *Journal of the Water Pollution Control Federation* 61: 188–199.

Nondorf L, Gutierrez M, and Plymate TG (2011) Modeling carbon sequestration geochemical reactions for a proposed site in Springfield, Missouri. *Environmental Geosciences* 18: 91–99.

Nordstrom DK (1977) *Hydrogeochemical and Microbiological Factors Affecting the Heavy Metal Chemistry of an Acid Mine Drainage System*. PhD Dissertation, Stanford University, p. 210.

Nordstrom DK (1985) The rate of ferrous iron oxidation in a stream receiving acid mine effluent. *Selected Papers Hydrol. Sci. 1985, U.S. Geol. Survey Water-Supply Paper 2270*, pp. 113–119.

Nordstrom DK (1994) On the evaluation and application of geochemical models, Appendix 2. In: *Proc. 5th CEC Natural Analogue Working Group and Alligator Rivers Analogue Project*, Toledo, Spain, 5–19 October, 1992. EUR 15176 EN, pp. 375–385.

Nordstrom DK (1996) Trace metal speciation in natural waters: Computational vs. analytical. *Water, Air, and Soil Pollution* 90: 257–267.

Nordstrom DK (1999) Some fundamentals of aqueous geochemistry. In: Plumlee GS and Logsdon MJ (eds.) *The Environmental Geochemistry of Mineral Deposits, Part A. Processes, Techniques, and Health Issues. Reviews in Economic Geology*, vol. 6A, pp. 117–123. Littleton, CO: Society of Economic Geologists.

Nordstrom DK (2000) Advances in the hydrogeochemistry and microbiology of acid mine waters. *International Geology Review* 42: 499–515.

Nordstrom DK (2003) Effects of microbiological and geochemical interactions in mine drainage. In: Jambor JL, Blowes DW, and Ritchie AIM (eds.) *Environmental Aspects of Mine Wastes. MAC Short Course Series* 31, pp. 227–238. Ottawa: Mineralogical Association of Canada.

Nordstrom DK (2009) Pitfalls and limitations of mineral equilibrium assumptions for geochemical modeling of water–rock interactions at mine sites. *8th Int. Conf. Acid Rock Drainage*, Skellefteå, Sweden, 23–26 June, pp. 362–372.

Nordstrom DK (2011) Hydrogeochemical processes governing the origin, transport, and fate of major and trace elements from mine wastes and mineralized rock to surface waters. *Applied Geochemistry* 26: 1777–1791.

Nordstrom DK (2012) Models, validation, and applied geochemistry: Issues in science, philosophy, and communication. *Applied Geochemistry* 27: 1899–1919.

Nordstrom DK and Archer DG (2003) Arsenic thermodynamic data and environmental geochemistry. In: Welch AH and Stollenwerk KG (eds.) *Arsenic in Ground Water*, pp. 1–25. Boston, MA: Kluwer.

Nordstrom DK and Ball JW (1989) Mineral saturation states in natural waters and their sensitivity to thermodynamic and analytic errors. *Sciences Geologiques Bulletin* 42: 269–280.

Nordstrom DK and Munoz JL (1994) *Geochemical Thermodynamics*, 2nd edn., p. 493. Caldwell, NJ: The Blackburn Press.

Nordstrom DK, Plummer LN, Langmuir D, et al. (1990) Revised chemical equilibrium data for major water-mineral reactions and their limitations. In: Melchior DC and Bassett RL (eds.) *Chemical Modeling of Aqueous Systems II. American Chemical Society Symposium Series* 416, pp. 398–413. Washington, DC: American Chemical Society.

Nordstrom DK, Plummer LN, Wigley TML, et al. (1979) A comparison of computerized chemical models for equilibrium calculations in aqueous systems. *Chemical Modeling of Aqueous Systems. American Chemical Society Symposium Series* 93, pp. 857–892. Washington, DC: American Chemical Society.

OECD/NEA (1994) *In situ* experiments at the Stripa Mine. In: *Proc. 4th Int. NEA/SKB Symp.*, Stockholm, Sweden, 14–16 October, 1992, p. 468.

OECD/NEA (2012) Thermodynamic sorption modelling in support of radioactive waste disposal safety cases. NEA Sorption Project Phase III, p. 152.

Oelkers EH, Bénézeth P, and Pokrovski GB (2009) Thermodynamic databases for water–rock interactions. In: Oelkers EH and Schott J (eds.) *Thermodynamics and Kinetics of Water–Rock Interaction. Reviews in Mineralogy and Geochemistry*, vol. 70, pp. 1–46. Washington, DC: Mineralogical Society of America, Geochemical Society.

Oelkers EH, Helgeson HC, Shock EL, Sverjensky DA, Johnson JW, and Pokrovskii VA (1995) Summary of the apparent partial molal Gibbs free energies of formation of aqueous species, minerals, and gases at pressures 1 to 5000 bars and temperatures 25 to 1000°C. *Journal of Physical and Chemical Reference Data* 24: 1401–1506.

Oelkers EH and Schott J (2009) *Thermodynamics and Kinetics of Water–Rock Interaction. Reviews in Mineralogy and Geochemistry*, vol. 70, p. 569. Washington, DC: Mineralogical Society of America, Geochemical Society.

Ojumu TV, Petersen J, Searby GE, and Hansford GS (2006) A review of rate equations proposed for microbial ferrous-iron oxidation with a view to application to heap bioleaching. *Hydrometallurgy* 83: 21–28.

Olin Å, Noläng B, Osadchii EG, Öhman L-O, and Rosé E (2005) In: Mompean FJ, Perrone J, and Illemassene M (eds.) *Chemical Thermodynamics of Selenium*, p. 851. Amsterdam: Elsevier with CD.

Oreskes N (1998) Evaluation (not validation) of quantitative models. *Environmental Health Perspectives* 106: 1453–1460.

Oreskes N (2000a) Why believe a computer? Models, measures, and meaning in the natural world. In: Schneiderman J (ed.) *The Earth Around Us*, pp. 70–82. New York: W. H. Freeman.

Oreskes N (2000b) Why predict? Historical perspectives on prediction in earth science. In: Sarawitz D, Pielke RA Jr., and Byerly R Jr. (eds.) *Prediction: Science, Decision Making, and the Future of Nature*, pp. 23–40. Washington, DC: Island Press.

Oreskes N, Shrader-Frechette K, and Belitz K (1994) Verification, validation, and confirmation of numerical models in the earth sciences. *Science* 263: 641–646.

Oreskes N (2004) Science and public policy: what's proof got to do with it? *Environmental Science & Policy* 7: 369–383.

Pačes T (1983) Rate constants of dissolution derived from the measurements of mass balance in hydrological catchments. *Geochimica et Cosmochimica Acta* 47: 1855–1863.

Pačes T (1984) Mass-balance approach to the understanding of geochemical processes in aqueous systems. In: Eriksson E (ed.) *Hydrochemical Balances of Freshwater Systems. Proc. Uppsala Symp.*, IAHS Publ. No. 150. Washington, DC: International Association of Hydrological Sciences, pp. 223–235.

Palandri JL and Kharaka YK (2004) A compilation of rate parameters of water-mineral interaction kinetics for application to geochemical modeling. *US Geol. Survey Open-File Report 2004-1068*, p. 64.

Pantelis G, Ritchie AIM, and Stepnyants YA (2002) A conceptual model for the oxidation and transport processes in sulphidic waste rock dumps. *Applied Mathematical Modelling* 26: 751–770.

Park AJ and Ortoleva PJ (2003) WRIS.TEQ: Multi-mineralic water–rock interaction, mass-transfer and textural dynamics simulator. *Computers and Geosciences* 29: 277–290.

Parkhurst DL (1997) Geochemical mole-balancing with uncertain data. *Water Resources Research* 33: 1957–1970.

Parkhurst DL and Appelo CAJ (1999) User's guide to PHREEQC (version 2)—A computer program for speciation, batch-reaction, one-dimensional transport, and inverse geochemical calculations. *US Geol. Surv. Water-Resour. Invest. Report 99-4259*, p. 312.

Parkhurst DL, Kipp KL, and Charlton, SR (2010) PHAST Version 2—A program for simulating ground-water flow, solute transport, and multicomponent geochemical reactions. *US Geol. Surv. Tech. Meth. 6-A35*, p. 235.

Parkhurst DL, Kipp KL, Engesgaard P, and Charlton SR (2004) PHAST—A program for simulating ground-water flow, solute transport, and multicomponent geochemical reactions. *US Geol. Surv. Tech. Meth. 6-A8*, p. 154.

Parkhurst DL and Plummer LN (1993) Geochemical models. In: Alley WM (ed.) *Regional Ground-water Quality*, pp. 199–226. New York: Van Nostrand Reinhold.

Parkhurst DL, Plummer LN, and Thorstenson DC (1980) PHREEQE – A computer program for geochemical calculations. *US Geol. Surv. Water-Resour. Invest. Report 80-96*, p. 195.

Parkhurst DL, Plummer LN, and Thorstenson DC (1982) BALANCE—A computer program for calculating mass transfer for geochemical reactions in ground water. *US Geol. Surv. Water-Resour. Invest. Report 82-14*, p. 29.

Parkhurst DL, Thorstenson DC, and Kipp KL (2001) Calculating carbon-isotope compositions in an unsaturated zone with seasonally varying CO_2 production. In: Wang Y (ed.) *Hydrogeology and the Environment*, pp. 220–224. Wuhan, China: China Environmental Science Press.

Parry WT, Forster CB, Evans JP, Bowen BB, and Chan MA (2007) Geochemistry of CO_2 sequestration in the Jurassic Navajo Sandstone, Colorado Plateau, Utah. *Environmental Geosciences* 14: 91–109.

Perdue EM and Lytle CR (1983) Distribution model for binding of protons and metal ions by humic substances. *Environmental Science and Technology* 17: 654–660.

Perdue EM, Reuter JH, and Parrish RS (1984) A statistical model of proton binding by humus. *Geochimica et Cosmochimica Acta* 48: 1257–1263.

Perkins EH, Kharaka YK, Gunter WD, and Debraal JD (1990) Geochemical modeling of water–rock interactions using SOLMINEQ.88. In: Melchior C and Bassett RL (eds.)

Chemical Modeling of Aqueous Systems II D. Symposium Series 416, pp. 117–127. Washington, DC: American Chemical Society.

Perrin DD (1979) *Organic Ligands. Stability Constants of Metal-Ion Complexes. Part B. IUPAC Chemical Data Series No. 22*, p. 1263. Oxford: Pergamon Press.

Perrin DD (1982) *Ionisation Constants of Inorganic Acids and Bases. IUPAC Chemical Data Series No. 29*, p. 180. Oxford: Pergamon Press.

Pirt SJ (1982) Maintenance energy: A general model for energy-limited and energy-sufficient growth. *Archives of Microbiology* 133: 300–302.

Pitzer KS (1973) Thermodynamics of electrolytes: I. Theoretical basis and general equations. *The Journal of Physical Chemistry* 77: 268–277.

Pitzer KS (1979) Theory: Ion interaction approach. In: Pytkowicz RM (ed.) *Activity Coefficients in Electrolyte Solutions* 1, pp. 157–208. Boca Raton, FL: CRC Press.

Pitzer KS (1991a) Ion interaction approach: Theory and data correlation. In: Pitzer KS (ed.) *Activity Coefficients in Electrolyte Solution*, 2nd edn., pp. 75–153. Boca Raton, FL: CRC Press.

Pitzer KS (ed.) (1991a) *Activity Coefficients in Electrolyte Solutions*, 2nd edn., p. 542. Boca Raton, FL: CRC Press.

Pitzer KS and Brewer L (1961) *Thermodynamics*, p. 723. New York: McGraw-Hill.

Plummer LN (1975) Mixing of sea water with calcium carbonate ground water. *Geological Society of America. Memoir* 142: 219–236.

Plummer LN (1977) Defining reactions and mass transfer in part of the Floridan aquifer. *Water Resources Research* 13: 801–812.

Plummer LN (1984) Geochemical modeling: A comparison of forward and inverse methods. In: Hitchon B and Wallick EI (eds.) *Practical Applications of Ground Water Geochemistry. First Canadian/American Conf Hydrogeol*, pp. 149–177. Worthington, OH: National Well Water Association.

Plummer LN and Back W (1980) The mass balance approach: Applications to interpreting chemical evolution of hydrologic systems. *American Journal of Science* 280: 130–142.

Plummer LN, Busby JF, Lee RW, and Hanshaw BB (1990) Geochemical modeling of the Madison aquifer in parts of Montana, Wyoming, and South Dakota. *Water Resources Research* 26: 1981–2014.

Plummer LN, Michel RL, Thurman EM, and Glynn PD (1993) Environmental tracers for age dating young ground water. In: Alley WM (ed.) *Regional Ground-Water Quality*, pp. 255–294. New York: Van Nostrand Reinhold.

Plummer LN and Parkhurst DL (1990) Application of the Pitzer equations to the PHREEQE geochemical model. In: Melchior DC and Bassett RL (eds.) *Chemical Modeling of Aqueous Systems II. American Chemical Society Symposium Series* 416, pp. 128–137. Washington, DC: American Chemical Society.

Plummer LN, Parkhurst DL, Fleming GW, and Dunkle SA (1988) A computer program incorporating Pitzer's equations for calculation of geochemical reactions in Brines. *US Geol. Surv. Water-Resour. Invest. Report 88-4153*, p. 310.

Plummer LN, Parkhurst DL, and Thorstenson DC (1983) Development of reaction models for groundwater systems. *Geochimica et Cosmochimica Acta* 47: 665–685.

Plummer LN, Prestemon EC, and Parkhurst DL (1991) An interactive code (NETPATH) for modeling net geochemical reactions along a flow path. *US Geol. Surv. Water-Resour. Invest. Report 91-4078*, p. 227.

Popper KR (1934) *Logik der Forschung (The Logic of Scientific Discovery)*. Berlin: Springer.

Posner AM (1964) Titration curves of humic acid. In: *Proc. 8th Int. Congr. Soil Sci.*, Part II, Bucharest, Romania.

Postma D, Kjøller C, Andersen MS, Condesso MT, and Gaus I (2008) Geochemical modelling of processes controlling baseline compositions of groundwater. In: Edmunds WM and Shand P (eds.) *Natural Groundwater Quality*, p. 469. Oxford: Blackwell.

Pruess K (1991) TOUGH2 – A general purpose numerical simulator for multiphase fluid and heat flow. *Lawrence Berkeley National Laboratory Report LBL-29400*.

Pruess K (2004) The TOUGH codes – A family of simulation tools for multiphase flow and transport processes in permeable media. *Vadose Zone Journal* 3: 738–746.

Ptacek CJ and Blowes D (2000) Predicting sulfate-mineral solubility in concentrated waters. In: Jambor JL, Alpers CN, and Nordstrom DK (eds.) *Sulfate Minerals: Crystallography, Geochemistry, and Environmental Significance. Reviews in Mineralogy and Geochemistry*, vol. 40, pp. 513–540. Washington, DC: Mineralogical Society of America and Geochemical Society.

Ptacek CJ and Blowes DW (2003) Geochemistry of concentrated water at mine-waste sites. In: Jambor JL, Blowes DW, and Ritchie AIM (eds.) *Mineralogical Association of Canada Short Course Series 31*, pp. 283–302. Ottawa: Mineralogical Association of Canada.

Purtschert R (2008) Timescales and tracers. In: Edmunds WM and Shand P (eds.) *Natural Groundwater Quality*, pp. 91–130. Oxford: Blackwell.

Pytkowicz RM (ed.) (1979) *Activity Coefficients in Electrolyte Solutions*, vols. 1 and 2, pp. 228 and 330. Boca Raton, FL: CRC Press.

Rand M, Fuger J, Grenthe I, Neck V, and Rai D (2009) In: Illemassene M, Perrone J, and Mompean FJ (eds.) *Chemical Thermodynamics of Thorium*, p. 942. Amsterdam: Elsevier with CD.

Rard JA, Rand MH, Anderegg G, and Wanner H (1999) In: Sandino MCA and Östhols E (eds.) *Chemical Thermodynamics of Technetium*, p. 568. Amsterdam: Elsevier.

Ritchie AIM (2003) Oxidation and gas transport in piles of sulfidic material. In: Jambor JL, Blowes DW, and Ritchie AIM (eds.) *Environmental Aspects of Mine Wastes*. Mineralogical Association of Canada Short Course Series 31, pp. 73–94.

Robie RA and Hemingway BS (1995) Thermodynamic properties of minerals and related substances at 298.15 K and 1 bar (10^5 Pascals) pressure and at higher temperatures. *US Geol. Surv. Bull. 2131*, p. 461.

Robinson RA and Stokes RH (1959) *Electrolyte Solutions*, 2nd edn., p. 571. Butterworth, London: Academic Press.

Rose KA, Cook RB, Brenkert AL, Gardner RH, and Hettelingh JP (1991a) Systematic comparison of ILWAS, MAGIC, and ETD watershed acidification models: 1. Mapping among model inputs and deterministic results. *Water Resources Research* 27: 2577–2589.

Rose KA, Cook RB, Brenkert AL, Gardner RH, and Hettelingh JP (1991b) Systematic comparison of ILWAS, MAGIC, and ETD watershed acidification models: 2. Monte Carlo analysis under regional variability. *Water Resources Research* 27: 2591–2603.

Rosenqvist J, Kilpatrick AD, and Yardley BWD (2012) Solubility of carbon dioxide in aqueous fluids and mineral suspensions at 294 K and subcritical pressures. *Applied Geochemistry* 27: 1610–1614.

Rossini FD, Wagman DD, Evans WH, Levine S, and Jaffe I (1952) Selected Values of Chemical Thermodynamic Properties. *National Bureau of Standards Circular* 500, p. 1268.

Rubin J (1983) Transport of reacting solutes in porous media: Relation between mathematical nature of problem formulation and chemical nature of reactions. *Water Resources Research* 19: 1231–1252.

Rubin J (1990) Solute transport with multisegment, equilibrium-controlled reactions: A feed forward simulation method. *Water Resources Research* 26: 2029–2055.

Runkel RL (1998) One-dimensional transport with inflow and storage (OTIS): A solute transport model for streams and rivers. *US Geol. Surv. Water-Resour. Invest. Report. 98-4018.*

Runkel RL (2010) One-dimensional transport with equilibrium chemistry (OTEQ) – A reactive transport model for streams and rivers. *US Geol. Surv. Tech. Methods*, Book 6, ch. B6, p. 101.

Runkel RL, Bencala KE, Broshears RE, and Chapra SC (1996a) Reactive solute transport in streams: 1. Development of an equilibrium-based model. *Water Resources Research* 32: 409–418.

Runkel RL and Kimball BA (2002) Evaluating remedial alternatives for an acid mine drainage stream: Application of a reactive transport model. *Environmental Science and Technology* 36: 1093–1101.

Runkel RL, Kimball BA, McKnight DM, and Bencala KE (1999) Reactive solute transport in streams: A surface complexation approach for trace metal sorption. *Water Resources Research* 35: 3829–3840.

Runkel RL, Kimball BA, Walton-Day K, and Verplanck PL (2007) A simulation-based approach for estimating premining water quality: Red Mountain Creek, Colorado. *Applied Geochemistry* 22: 1899–1918.

Runkel RL, Kimball BA, Walton-Day K, Verplanck PL, and Broshears RE (2012) Evaluating remedial alternatives for an acid mine drainage stream: A model post audit. *Environmental Science and Technology* 46: 340–347.

Runkel RL, McKnight DM, and Bencala KE (1996b) Reactive solute transport in streams: 2. Simulation of a pH modification experiment. *Water Resources Research* 32: 419–430.

Runnells DD (1969) Diagenesis, chemical sediments, and the mixing of natural waters. *Journal of Sedimentary Petrology* 39: 1188–1201.

Saaltink MW, Batlle F, Ayora C, Carrera J, and Olivella S (2004) RETRASO, a code for modeling reactive transport in saturated and unsaturated porous media. *Geologica Acta* 2: 235–251.

Saaltink MW, Yakirevich A, Carrera J, and Ayora C (2012) Fluid flow, solute and heat transport equations. In: Bundschuh J and Zilberbrand M (eds.) *Geochemical Modeling of Groundwater, Vadose and Geothermal Systems*, pp. 83–126. Boca Raton, FL: CRC Press/Balkema.

Salvage KM and Yeh G-T (1998) Development and application of a numerical model of kinetic and equilibrium microbiological and geochemical reactions (BIOKEMOD). *Journal of Hydrology* 209: 27–52.

Santana-Casiano JM, González-Dávila M, and Millero FJ (2006) The role of Fe(II) species on the oxidation of Fe(II) in natural waters in the presences of O_2 and H_2O_2. *Marine Chemistry* 99: 70–82.

Scatchard G (1936) Concentrated solutions of electrolytes. *Chemical Reviews* 19: 309–327.

Scharer JM, Nicholson RV, Halbert B, and Snodgrass WJ (1994) A computer program to assess acid generation in pyritic tailings. In: Alpers CN and Blowes DW (eds.) *Environmental Geochemistry of Sulfide Oxidation*. *American Chemical Society Symposium Series* 550, pp. 132–152. Washington, DC: American Chemical Society.

Scharlin P (1996) *Carbon Dioxide in Water and Aqueous Electrolyte Solutions*. *IUPAC Solubility Data Series*, vol. 62, p. 383. UK: Oxford University Press.

Schecher WD and Driscoll CT (1987) An evaluation of uncertainty associated with aluminum equilibrium calculations. *Water Resources Research* 23: 525–534.

Schecher WD and Driscoll CT (1988) An evaluation of the equilibrium calculations within acidification models: The effect of uncertainty in measured chemical components. *Water Resources Research* 24: 533–540.

Serjeant EP and Dempsey B (1979) *Ionisation Constants of Organic Acids in Aqueous Solution*. *IUPAC Chemical Data Series* 23, p. 989. Oxford: Pergamon Press.

Servos JW (1990) Physical Chemistry from Ostwald to Pauling: The Making of a Science in America, p. 402. New York: Princeton University Press.

Sherman DM (2009) Surface complexation modeling: Mineral fluid equilibria at the molecular scale. In: Oelkers EH and Schott J (eds.) *Thermodynamics and Kinetics of Water–Rock Interaction*. *Reviews in Mineralogy and Geochemistry*, vol. 70, pp. 181–206. Washington, DC: Mineralogical Society of America, Geochemical Society.

Shock EL and Helgeson HC (1988) Calculation of the thermodynamic and transport properties of aqueous species at high pressures and temperatures: Correlation algorithms for ionic species and equation of state predictions to 5 kb and 1000°C. *Geochimica et Cosmochimica Acta* 52: 2009–2036.

Shock EL and Helgeson HC (1990) Calculation of the thermodynamic and transport properties of aqueous species at high pressures and temperatures: Standard partial molal properties of organic species. *Geochimica et Cosmochimica Acta* 54: 915–946.

Shock EL, Helgeson HC, and Sverjensky DA (1989) Calculation of the thermodynamic and transport properties of aqueous species at high pressures and temperatures: Standard partial moral properties of inorganic neutral species. *Geochimica et Cosmochimica Acta* 53: 2157–2183.

Sillén LG (1961) The physical chemistry of seawater. In: Sears M (ed.) *The Sea* pp. 549–581. Am. Assoc. Adv. Sci. Publ. 67.

Sillén LG (1962) High-speed computers as a supplement to graphical methods: I. The functional behavior of the error square sum. *Acta Chemica Scandinavica* 16: 159–172.

Sillén LG and Martell AE (1964) *Stability Constants of Metal-ion Complexes*, p. 754. Spec. Publ. 17. London: Chemical Society.

Sillén LG and Martell AE (1971) *Stability Constants of Metal-ion Complexes*. Suppl. No. 1, 865 pp. Spec. Publ. 25. London: Chemical Society.

Silva RJ, Bidoglio G, Rand MH, Robouch PB, Wanner H, and Puigdomenech I (1995) *Chemical Thermodynamics of Americium*, p. 392. Amsterdam: Elsevier.

Silverman MP and Lundgren DG (1959) Studies on the chemoautotrophic iron bacterium Ferrobacillus ferrooxidans. I. An improved medium and a harvesting procedure for securing high cell yields. *Journal of Bacteriology* 77: 642–647.

Singer PC and Stumm W (1970) Acid mine drainage: The rate determining step. *Science* 167: 1121–1123.

Smith WR and Missen RW (1982) *Chemical Reaction Equilibrium Analysis*, p. 364. New York: Wiley.

Spear RC and Hornberger GM (1980) Eutrophication in Peel Inlet: II. Identification of critical uncertainties via Generalized Sensitivity Analysis. *Water Research* 14: 43–59.

Spencer RJ, Møller N, and Weare JH (1990) The prediction of mineral solubilities in natural waters: A chemical equilibrium model for the $Na–K–Ca–Mg–Cl–SO_4–H_2O$ system at temperatures below 25°C. *Geochimica et Cosmochimica Acta* 54: 575–590.

Steefel CI (2007) *CrunchFlow User's Manual*. Berkeley: Lawrence Berkeley National Laboratory.

Steefel CI, DePaolo DJ, and Lichtner PC (2005) Reactive transport modeling: An essential tool and a new research approach for the Earth sciences. *Earth and Planetary Science Letters* 240: 539–558.

Steefel CI and Lasaga AC (1994) A coupled model for transport of multiple chemical species and kinetic precipitation/dissolution reactions with application to reactive flow in single phase hydrothermal systems. *American Journal of Science* 294: 529–592.

Steefel CI and Lichtner PC (1998) Multicomponent reactive transport in discrete fractures: I. Controls on reaction front geometry. *Journal of Hydrology* 209: 186–199.

Steefel CI and Maher K (2009) Fluid-rock interaction: A reactive transport approach. In: Oelkers EH and Schott J (eds.) *Thermodynamics and Kinetics of Water–Rock Interaction*. *Reviews in Mineralogy and Geochemistry* 70, pp. 485–532. Mineralogical Society of America, Geochemical Society.

Steefel CI and Van Cappellen P (1998) Reactive transport modeling of natural systems. *Journal of Hydrology* 209: 1–7.

Steefel CI and Yabusaki SB (1996) OS3D/GIMRT, Software for multicomponent-multidimensional reactive transport. User Manual and Programmer's Guide, PNL-11166, Richland.

Stockdale A, Tipping E, Hamilton-Taylor J, and Lofts S (2011) Trace metals in the open oceans: Speciation modeling based on humic-type ligands. *Environmental Chemistry* 8: 304–319.

Stockdale A, Tipping E, Lofts S, Ormerod SJ, Clements WH, and Blust R (2010) Toxicity of proton-metal mixtures in the field: Linking stream macroinvertebrates species diversity to chemical speciation and bioavailability. *Aquatic Toxicology* 100: 112–119.

Stone AT and Morgan JJ (1990) Kinetics of chemical transformations in the environment. In: Stumm W (ed.) *Aquatic Chemical Kinetics*, pp. 1–41. New York: Wiley.

Stumm W (1987) *Aquatic Surface Chemistry*, p. 519. New York: Wiley.

Stumm W and Morgan JJ (1996) *Aquatic Chemistry*, 3rd edn., p. 1022. New York: Wiley.

Suarez DL and Simunek J (1996) Solute transport modelling under variably saturated water-flow conditions. In: Lichtner PC, Steefel CI, and Oelkers EH (eds.) *Reactive Transport in Porous Media*. *Reviews in Mineralogy,* pp. 229–268. Washington, DC: Mineralogical Society of America.

Sverdrup HU (1990) *The Kinetics of Base Cation Release due to Chemical Weathering*, p. 246. Lund, Sweden: Lund University Press.

Tanger JC and Helgeson HC (1988) Calculation of the thermodynamics and transport properties of aqueous species at high pressures and temperatures: Revised equations of state for the standard partial molal properties of ions and electrolytes. *American Journal of Science* 288: 19–98.

Tebes-Stevens C, Valocchi AJ, VanBriesen JM, and Rittmann BE (1998) Multicomponent transport with coupled geochemical and microbiological reactions: Model description and example simulations. *Journal of Hydrology* 209: 8–26.

Thoenen T, Berner U, Curti E, Hummel W, and Pearson FJ (2004) Development and application of the Nagra/PSI chemical thermodynamic data base 01/01. In: Gieré R and Stille P (eds.) *Energy, Waste, and the Environment: A Geochemical Perspective*, pp. 561–577. Special Publications 236. London: Geological Society.

Thorstenson DC and Parkhurst DL (2002) Calculation of individual isotope equilibrium constants for implementation in geochemical models. *US Geol*. *Survey Water-Resour*. *Invest*. *Report 02-4172*, p. 129.

Thullner M, Regnier P, and Van Cappellen P (2007) Modeling microbially induced carbon degradation in redox-stratified subsurface environments: Concepts and open questions. *Geomicrobiology Journal* 24: 139–155.

Tipping E (1994) WHAM—A chemical equilibrium model and computer code for waters, sediments and soils incorporating a discrete site/electrostatic model of ion-binding by humic substances. *Computers and Geosciences* 20: 973–1023.

Tipping E (1998) Modelling the properties and behavior of dissolved organic matter in soils. *Mitteilungen der Deutschen Bodenkundlichen Gesellschaft* 87: 237–252.

Tipping E (2002) *Cation Binding by Humic Substances*, p. 434. UK: Cambridge University Press.

Tipping E (2007) Modelling the interactions of Hg(II) and methylmercury with humic substances using WHAM/Model VI. *Applied Geochemistry* 22: 1624–1635.

Tipping E and Carter HT (2011) Aluminum speciation in streams and lakes of the UK Acid Waters Monitoring Network, modeled with WHAM. *The Science of the Total Environment* 409: 1550–1558.

Tipping E, Lofts S, and Sonke JE (2011) Humic ion-binding model VII: A revised parameterisation of cation-binding by humic substances. *Environmental Chemistry* 8: 225–235.

Tipping E, Rey-Castro C, Bryan SE, and Hamilton-Taylor J (2002) Al(III) and Fe(III) binding by humic substances in freshwaters, and implications for trace metal speciation. *Geochimica et Cosmochimica Acta* 66: 3211–3224.

Tosca NJ, Smirnov A, and McLennan SM (2007) Application of the Pitzer ion interaction model to isopiestic data for the $Fe_2(SO_4)_3–SO_4–H_2O$ system at 298.15 and 323.15 K. *Geochimica et Cosmochimica Acta* 71: 2680–2698.

Truesdell AH and Jones BF (1974) WATEQ, a computer program for calculating chemical equilibria of natural waters. *Journal of Research of the US Geological Survey* 2: 233–248.

USEPA (1998, 1999) MINTEQA2/PRODEFA2., a geochemical assessment model for environmental systems. User manual supplement for version 4.0. http://epa.gov/ceampubl/mmedia/minteq/supplei.pdf, p. 76.

Van der Lee J (1998) Thermodynamic and mathematical concepts of CHESS. Technical Report LHM/RD/98/39, CIG, E´ cole des Mines de Paris, Fontainebleau.